BIOSORPTION OF TOXIC HEAVY METALS BY FUNGAL BIOMASS

Lam Kim-hung

M. PHIL.

THE HONG KONG POLYTECHNIC UNIVERSITY

1998

Declaration

I hearby declare that this thesis summarizes my own work carried out since my registration for the Degree of Master of Philosophy in October, 1995; and it has not been previously included in a thesis, dissertation or report submitted to this or any other institution for a degree, diploma or other qualification.

Kim - hung, Lam

December, 1997

Acknowledgements

This thesis is based on the research work carried out in the Department of Applied Biology and Chemical Technology, Hong Kong Polytechnic University, during the period from October, 1995 to December, 1997 under the supervision of Dr. W. Lo and Dr. C. P. Lau.

The author wishes to express his sincere gratitude to all acadmic and technical staff of Hong Kong Polytechnic University who have helped in various ways during the course of this study. I would like to thank

Dr. W. Lo for his supervision, valuable suggestions, as well as guidance, and for critical reading of this manuscript;

Dr. C. P. Lau for his supervision and encouragement;

Dr. K. P. Ho for his provision of help and academic suggestions;

Professor F. T. Chau and Mr. Alex Leung for the provision of the programming software, Matlab version 4.0; and

Miss Coty, W. C. Tsui and all the technical staffs.

Finally I would like to thank the Research Committee of the Hong Kong Polytechnic University for funding this project (grant no. 0350-532).

Abstract

Research in recent years has established that metal biosorption using microbial biomass can be developed into potentially cost-effective process for removing metals or recovering valuable metals from industrial effluents. Of particular interest are abundant fungal biomass types produced as a waste byproduct of large-scale industrial processes which can be very inexpensive sources of metal biosorbent. Different fungal strains have been selected for studying their ability to remove lead and copper ions from aqueous solution. Batch biosorption experiments were conducted to examine the kinetic and equilibrium of lead and copper biosorption.

The biosorption kinetic data shows that both lead and copper biosorption may be divided into two phases: (i) a fast biosorption phase with most of the metal ions taken up from solution within the first 15 minutes, and; (ii) a much slower second phase which continued even after 24 h.

For equilibrium studies of lead biosorption, the Langmuir isotherm fit the equilibrium data better than the Freundlich isotherm. *Aspergillus niger* and *Mucor rouxii* exhibited exceptionally high lead biosorption capacities, up to 50 % of the fungal biomass dry weight employed. These two fungal strains may be applied to develop potentially cost-effective biosorbents for removing lead from effluents.

For equilibrium studies of copper biosorption, the Freundlich isotherm generally fit the equilibrium data better than the Langmuir isotherm. *Aspergillus nidulans, Mucor rouxii, Cladosporium cladosporioides and Phycomyces blakeleeanus* (+) exhibited moderate copper biosorption capacities (about 1-1.5% of the fungal biomass dry weight employed).

Based on these kinetic and equilibrium data, *Mucor rouxii* has been selected for further studies. The pH was found to have significant effect on lead and copper biosorption. The *Mucor rouxii* biomass exhibited the highest removal efficiency at pH 6.0 for lead and at pH 5.0 for copper. The effects of chemical treatments on copper biosorption of *Mucor rouxii* were studied. It was found that while alkaline treatment significantly increased copper biosorption capacity by 100%, acid, heat and formaldehyde treatments reduced copper biosorption capacity. The substitution of mycological peptone with bacto peptone in the growth medium caused the morphological change of the fungal biomass from filamentous form to yeast-like form. However, no improvement of the lead or copper biosorption capacities was observed.

The biomass was also found to adsorb a variety of different metal cations. At pH 5.0, the biosorption capacities for metals decreased in the following order: Pb^{2+} > Zn^{2+} > Mg^{2+} > Cr^{3+} > Cd^{2-} > Ag^{+} > Ni^{2+} > Cu^{2+} > Co^{2-} > Na^{+}. A linear correlation between biosorption capacity and ionic radius of the metal ions was not observed.

However, the metal biosorption capacity correlated much better with Z^2/r where Z is the ionic charge and r the ionic radius.

Equilibrium batch studies of metal biosorption had been extended to binary metal system (Pb^{2+} + Cu^{2+}). Scatchard plots of lead biosorption at different initial copper concentrations strongly indicated the presence of multiple lead binding sites on the cell surfaces. Three-dimensional biosorption isotherm surfaces had been used to evaluate the performance of the binary metal biosorption system. The biosorption of lead decreased when copper was present. Three biosorption mathematical models (i.e. competitive, noncompetitive and modified multi-component models) were evaluated for their predictive ability of metal biosorption for the binary metal system. The modified multi-component model had the smallest sum of square residue which indicated a greater match with the experimental data.

Table of Contents

List of Figures (page number)

List of Tables (page number)

Chapter 1. Introduction

1.1. Motivation and research objectives

Metals are some of the most common pollutants produced by the industrial sector. In Hong Kong, heavy metals discharged into the environment from textile, printed circuit boards and electroplating industries constitute one of the major causes of water pollution. It is estimated that 2 tonnes of heavy metals are discharged daily into Hong Kong waters before the enactment of the Water Control Ordinance. The effluents of the electroplating factories and the printed circuit board factories are usually acidic and contain high concentrations of copper, nickel, chromium, tin and lead. For a typical printed circuit board factory, it is estimated that the amount of copper lost to environment is 55 kg/month. Discharge of heavy metals into open water poses serious environmental and human health hazards (Panchanadikar *et al.*, 1994) because of their toxicity, their tendency to bioaccumulate, and their abundance and persistence in the environment. Thus it is imperative that metals are removed before being discharged into the sewage system or into the aquatic environment.

Current technologies for metal removal such as chemical precipitation, electrochemical treatment and ion exchange provide only partially effective treatment and are costly to implement and use, especially when the metal concentration is low (around 1-100 mg/L). The use of ion exchange resins solely for purifying wastewaters is, in most cases, inappropriate because of the high cost of the materials.

Certain types of microorganisms can passively bind and accumulate metals even when metabolically inactive or dead (Muraleedharan *et al.*, 1991). The microorganisms can chemically attract and remove metal cations from the aqueous solution. The sorption of dissolved heavy metal cations based on the chemical activity of microbial biomass, alive or dead, is known as biosorption (Volesky, 1990). The biosorption depends not only on the chemical composition of the cell or its components such as the

cell wall but also on external physico-chemical factors and the solution chemistry of the metal. The mechanism of metal uptake can be due to physical sorption, ion exchange, complexation with cell surface groups (Muraleedharan and Venkobachar, 1990) or bioaccumulation. In the past decade, many different metal biosorbent materials of three main biomass types (algae, fungi and bacteria) have been studied for their ability to remove and recover metals (Lewis and Kiff, 1988; Guven and Akyuz, 1995; Volesky and Holan, 1995). Biosorption using microbial biomass can be developed into potentially cost-effective process for removing metals or recovering valuable metals from industrial effluents. Fungal biomass may be better suited for this purpose than other biomass types because abundant biomass types produced as a waste byproduct of large-scale industrial processes (e.g., fermentation, activated sludge waste-water treatment) can be very inexpensive sources of metal biosorbent. The conversion of the biomass waste into metal biosorbent does not only drastically reduce the production cost of biosorbent but also the disposal cost of the biomass waste.

The overall objective of the proposed work is to develop an inexpensive and effective biosorption process for removing and recovering heavy metals from aqueous wastes and for remediating metal-contaminated sites using fungal-based biosorbents. Different fungal strains have to be screened first for selecting biomass which can remove metals effectively from aqueous environment. For practical reasons, the screening process will be limited to two metals, lead and copper. Lead are most important considering the environmental impact of mobilized metal. Copper is not toxic to the extent of lead and , but its extensive use in electroplating and printed circuit board industries has caused high level of copper in the sediment of Victoria Harbour. Based on the batch kinetic and equilibrium data of lead and copper biosorption. a fungal species have been selected for further studies.

Next, the factors affecting metal biosorption must be studied. These factors include metal concentration in solution, biomass concentration. solution pH. the metabolic state of the biomass and treatment methods. Review of literature indicates

that experimental data and theoretical analysis are needed on the performance of biosorbent systems with multimetal aqueous mixture. Most research work on biosorption has been limited to studies on single metals. To assess the full potential of biosorption, experimental data and theoretical analysis are needed on the performance of biosorbent systems with multimetal aqueous mixture. The studies of toxic metal biosorption are then extended to binary metal systems. For practical reasons, the studies are limited to two metals, lead and copper, in aqueous binary mixtures. In order to simulate mathematically the metal biosorption process in binary mixtures, isotherm models are developed to describe the equilibrium of the binary metal system.

To summarize, the specific goals for this project period are to:

(i) screen a series of selected fungal strains by batch biosorption experiments for effective lead and copper removal at different metal and biomass concentrations;

(ii) investigate the effect of solution pH on lead and copper biosorption by selected fungal biomass;

(iii) examine the effect of different biomass treatment methods and growth medium composition on copper biosorption;

(iv) measure and compare the biosorption capacities of zinc, nickel, cobalt, magnesium, cadmium. chromium and sodium ions;

(v) evaluate and simulate mathematically the capacity of the selected fungal biomass for binding binary metal solutions for process scale-up and performance prediction.

1.2 Methodology

Examination of the proposed solid-liquid biosorption system has been based on two types of investigations: (i) equilibrium batch biosorption tests and (ii) biosorption kinetic studies. Data on the equilibria of these processes can be obtained from experimental biosorption equilibrium isotherms determined from batch biosorption experiments. An isotherm which is steep from the origin at low residual metal

concentrations, indicating a high affinity of the biosorbent for the metal ions, is highly desirable. Such a biosorbent would be performing well at very low concentrations of the metal ions in the solution and would help ensure low metal concentrations in the effluent stream. The maximum biosorption uptake value (capacity) determined from the isotherm is another important feature of the biosorbent, characterizing its performance at high residual metal concentration. In addition to equilibrium studies, kinetics of the biosorption has also been determined in order to establish the rate of metal uptake and release. Rapid uptake would provide a short solution-biosorbent contact time and would be desirable for continuous operation.

The biosorption depends not only on the chemical composition of the cell or its components such as the cell wall but also on external physico-chemical factors and the solution chemistry of the metal. Therefore factors affecting metal biosorption must be studied. These factors include metal concentration in solution, biomass concentration, solution pH, the metabolic state of the biomass, biomass treatment methods, growth medium composition and the presence of competing cations. For scale-up and performance prediction purposes, mathematical models must be developed to describe the equilibrium of binary metal biosorption.

Chapter 2. Background

2.1. Biosorption

Microorganisms such as algae, fungi and bacteria; and their derivatives such as extracellular polymers produced by bacteria as well as chitosan, a component present in crabs, shrimps and fungi, may also adsorb metal ions. The uptake of heavy metals by biomass can take place by an active mode (dependent on the metabolic activity) known as bioaccumulation or by a passive mode (sorption and/or complexation). These metal uptake phenomenon are termed as biosorption.

Volesky and Holan (1995) defined biosorption as the sorption and/or complexation of dissolved metals based on the chemical activity of microbial biomass. Another definition is given by Muraleedharan *et al.* (1991) who described biosorption as a process in which solids of natural origin such as microorganisms, alive or dead, or derivatives, are employed for sequestation of heavy metals from an aqueous environment.

The biosorption phenomenon can be applied to develop novel environmental technology for removing and recovering heavy metals from waste effluents and remediating metal contaminated sites.

2.2. Mechanisms of biosorption

The understanding of the biosorption mechanisms is essential to develop microbial processes for removing and recovering of metals from aqueous effluents. Biosorption mechanisms can be examined and analysed by both instrumental and chemical methods. However, up to now the mechanisms of biosorption are not well understood.

Metal ions in aqueous environments can be removed by the cells through several ways. These include endocellular, exocellular and pericellular processes (Figure 1). For

Mode of metal uptake by living microorganisms

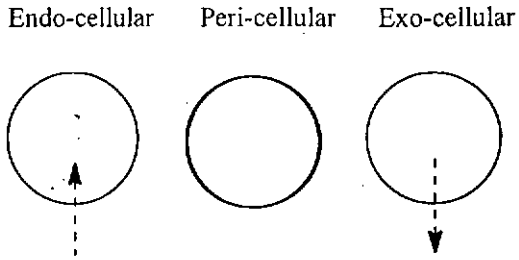

Examples of microorganisms	magnetotactic bacteria	*Saccharomyces*	sulfate reducing bacteria
Processes	magnetite synthesis	Uranium accumulation	sulfide biogenesis
Potential applications	Selective biosynthesis of pure materials	Accumulation of strategic metals in process/waste streams	Metal removal from mine drainage

Figure 1. Examples of microbial processes for metal removal from solution and its potential applications (Olson, 1987).

living cells, three modes can occur but for the nonliving cells, pericellular process may be the sole and major uptake way. The endocellular modes can occur in the living cells with an efficient energy-dependent transport system to accumulate the essential metals against the large concentration gradient. Enzymatic alterations of metals, for example, oxidation, reduction, dealkalation of organometals, and metal complexation or sequestration, and transport to cells can occur during the endocellular process. The exocellular process of metal removal can be achieved by precipitation with the metabolic products of cells. The pericellular process can occur in both the living and nonliving cells. The uptake was due to the interactions between the metal cations and the functional groups present on the cell wall surface (Olson, 1987).

Volesky and Holan (1995) suggested that metals biosorption based on several mechanisms that quantitatively and qualitatively differ according to the species used, the origin of the biomass, and its processing. Metal sequestration follows complex mechanisms. The mechanisms may include bioaccumlation, ion-exchange, chelation, adsorption by physical forces, as well as ion entrapment in inner- and intrafibrillar capillaries and spaces of the structural polysaccharides network as a result of the concentration gradient and diffusion through cell walls and membranes (Volesky and Holan, 1995).

A lot of extensive studies comparing the biosorption capacity of dead fungal cells with that of living cells had been administered. The biosorption capacity of dead cells may be greater, equivalent to or less than that of living cells (Kapoor and Viraraghavan, 1995). Pons and Fuste (1993) reported that uranium uptake by immobilized *Pseudomonas* species EPS 5028 cells was 47% higher after heat treatment. Siegel (1986) reported that the heat treatment on mycelium of *Penicillium* species would decrease the percentage of lead uptake at equilibrium. The conficting reports may be due to the difference in the biomass types, the metals employed in their studies or different research methodologies.

Gadd *et al.* (1988) reported that *Saccharomyces cerevisiae* showed a rapid wall binding with copper in the absence of glucose. For *Rhizopus arrhizus*, the improvement of copper removal is very small even in the presence of glucose implying that a large proportion of copper removal was due to passive wall binding rather than intracellular uptake mechanism (Gadd *et al.*, 1988).

The higher copper uptake by live and freeze-dried aerobically *grown S. cerevisiae* than by anaerobically grown cells may be due to the presence of an active copper-binding protein metallothionein (Kapoor and Viraraghavan, 1995). Treen-sears *et al.* (1984a) observed that growth, uptake capacity and biosorptive yield were enhanced by the addition of mineral salts to the growth media. Growth media may vary the cell wall composition which would affect metal uptake.

Many extracellular fungal products can complex or precipitate heavy metals. Citric acid, for example, can be an efficient metal-ion chelator, and oxalic acid can interact with metal ions to form insoluble oxalate crystals around cell walls and in the external medium. The H_2S production by yeasts can precipitate metals as insoluble sulfides in and around cell walls. Many fungi and yeasts can release Fe-binding molecules called siderophores for forming Fe^{3+} chelates which can subsequently be taken into the cell (Gadd, 1990).

Gadd (1990) suggested that metabolism-independent biosorption is the dominant mechanism of uptake even in living cells. For nonliving biomass, metabolism-independent metal binding to cell walls and external surfaces is the dominant mechanism. The uptake may involve adsorption processes such as ionic, chemical and physical adsorption. A variety of different functional groups present on cell surfaces, such as carboxyl, amine, hydroxyl, phosphate and sulfhydryl groups is responsible for metal chelation. Beveridge and Murray (1980) suggested that metal ions can be adsorbed by complexing with negatively charged reaction sites on the cell surfaces. The importance of different functional groups cannot be determined easily (Strandberg *et al.*, 1981). When the fungal cell wall is first in contact with the metal ions in solution, the

metal can deposit on the surface or within the cell wall structure before interacting with the cytoplasmic materials or other cellular parts. In some cases, for living cells, intracellular uptake may take place due to the increased permeability as a result of cell wall rupture and subsequent exposure of the metal-binding sites (Gadd, 1990).

Yakubu and Dudency (1996) proposed a model to describe the ion-exchange of uranium with proton at the cell wall surface of *Aspergillus niger*. The data fit the model quite well. This may suggest that ion-exchange may be one of the principal mechanisms for metal sequestering during the rapid initial uptake phase. Treen-Sears (1984b) employed *Rhizopus arrhizus* beads to carry out the column biosorption studies of uranium, he observed that the H^+ eluted was twice the amount of uranium. He sugested that ion-exchange took place in the process (Treen-Sears *et al.*, 1984 b).

Since the cell walls of different microorganisms can vary considerably in their overall composition, there must be differences in uptake capacities among different species. The microbial cell walls are rich in polysaccharides and glycoproteins such as glucans (β 1-6 and 1-3 linked D-glucose residues), chitin (β 1-4 linked N-acetyl-D-glucosoamine), chitosan (β 1-4 linked D-glucosoamine), mannans (β 1-4 linked mannose) and phosphomannans (phosphorylated mannans) (Modak and Natarajan. 1995). These polymers are composed of a large number of different functional groups. Fungal cell wall consists of amino- or nonamino-polysaccharides up to 90 % of the dry mass, which form a multilaminate architecture (Farkas, 1979). Fungal cell wall contains chitin and chitosan. The fungal cell wall can be regarded in general as a two-phase system containing chitin skeleton framework embedded in a matrix of amorphous polysaccharide (Muzzarelli, 1972; Farkas, 1979). Figure 2a is a model showing the major molecules present in the fungal cell wall (Stegel, 1990). Figure 2b is a model showing the composition of the fungal cell wall of *Achlya ambisexualis* (Volesky, 1990). Tsezos (1983) reported that chitin and chitosan, components of the cell wall, can sequester metal ions. Fourest and Roux (1992) suggested that chitin and chitosan are

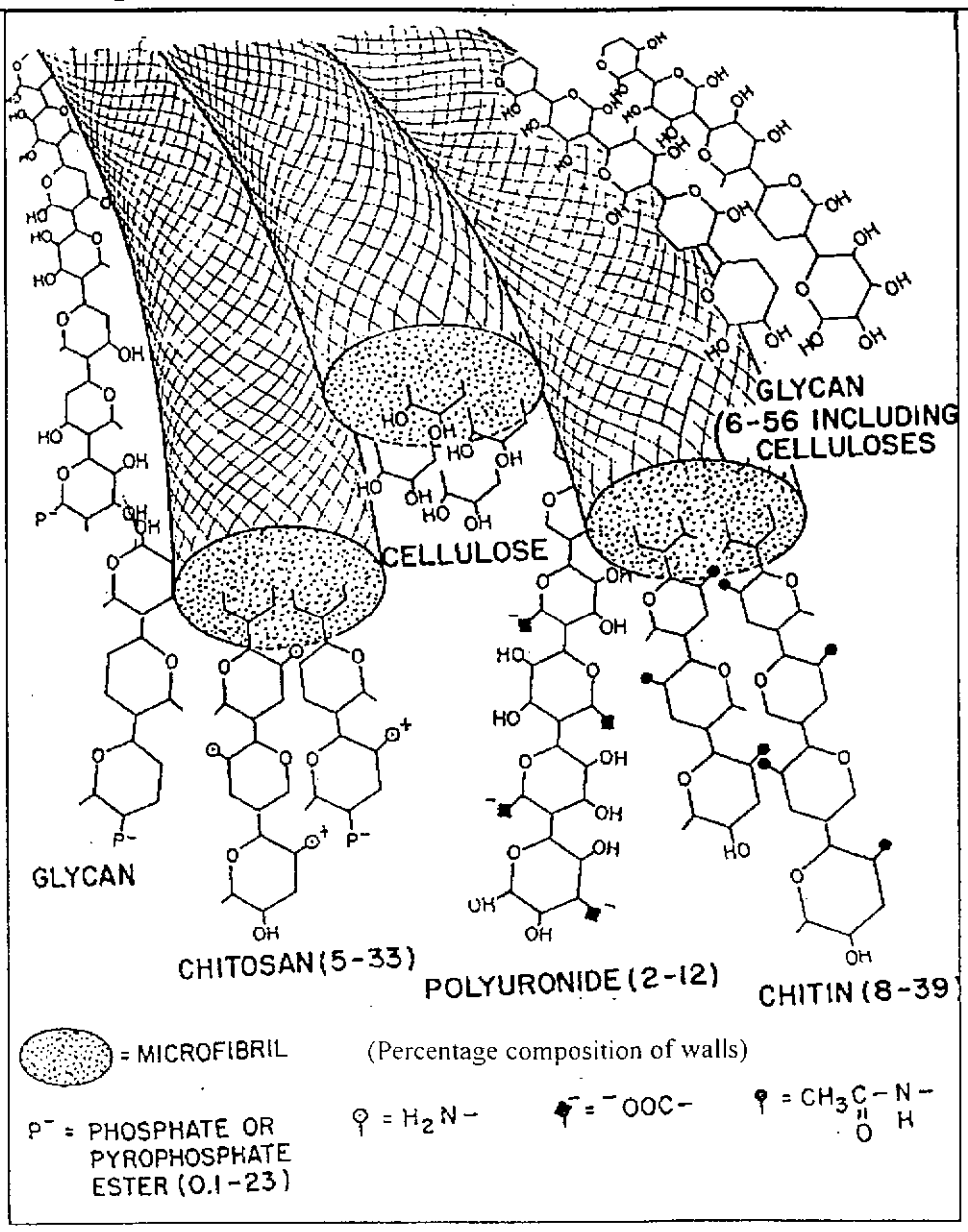

Figure 2.a. Major fungal polysaccharides active in biosorption (Stegel et al., 1990).

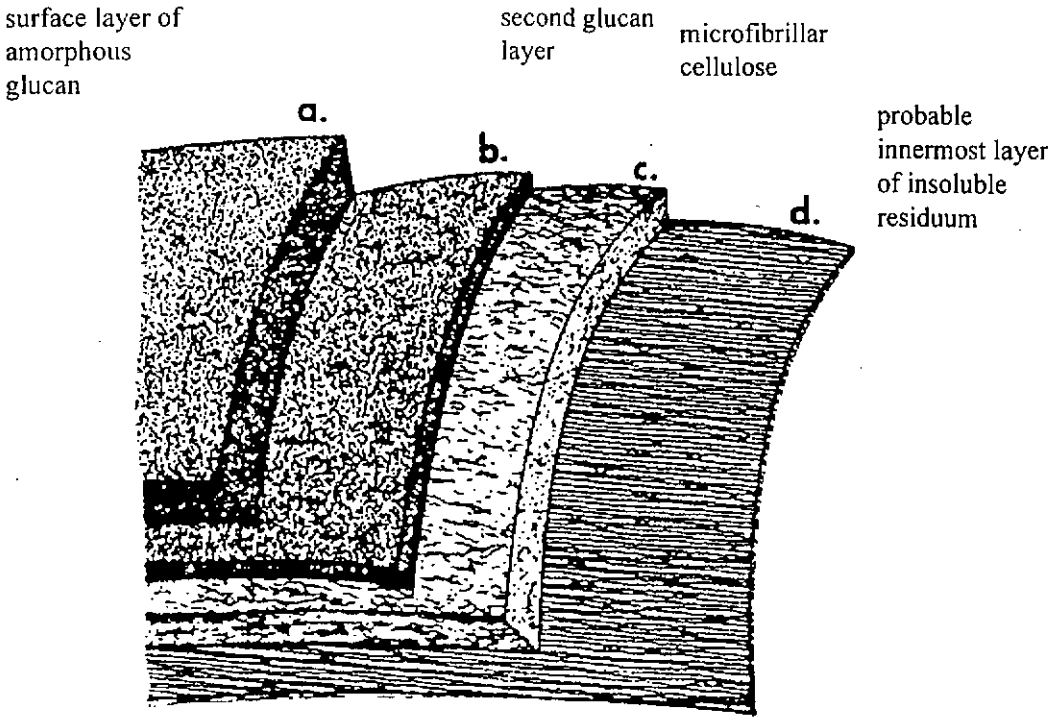

Figure 2.b. A proposed model of laminated wall layers in the hyphal wall of *Achlya ambisexualis* (Volesky, 1990).

important sites for metal chelation and, therefore, important to its uptake. Chitin and chitosan contents of the fungal cell wall can change during growth of the mycelia (Blumenthal and Roseman, 1957; Aronson, and Machlis, 1959; Bartnicki-Garcia and Nickerson, 1962; Farkas, 1980) and this may account for the variations in uptake capacity of different metals at different cell age (Kapoor, 1995).

Uranium has been shown to be deposited throughout the cell wall of non-living *Rhizopus arrhizus* cells exposed to uranium solutions. Mass spectroscopy and near infra-red spectroscopy have indicated that the amine nitrogen of the chitin is the primary site for complexation of uranium in the cell wall (Tsezos and Volesky, 1981, 1982a and 1982b). Tsezos and Volesky (1981, 1982a and 1982b) had carried out quite a large amount of work on radionuclides, U and Th. Tsezos and Volesky (1982a) proposed the processes for U uptake based on the experimental evidences made by the studies. These studies employed electron microscopy, X-ray energy dispersion analysis, electron paramagnetic resonance and infrared spectroscopy. They postulated a three step process as follows:

1. The first process is complex formation between the dissolved uranium ionic species and the chitin present in the cell wall of *Rhizopus arrhizus*. Uranium coordinates to the amino nitrogen of the chitin crystallates and is retained within the cell wall of the mycelium.
2. The second process is the adsorption of additional uranium by the chitin network which is closed to that complexed by chitin nitrogen.
3. The third process is the hydrolysis of the uranium-chitin complex that was formed by the first process and the precipitation of the hydrolysis product on the cell wall upon which the chitin nitrogen that was believed will reengage further uranium until the accumulation of hydrolysis product inhibits the cycle.

Tsezos and Volesky (1982b) observed that the thorium biosorption mechansim is different. These processes are listed as shown:

1. The first process involves a coordinated complex formed between thorium and nitrogen of the cell wall chitin. (There is a great discrepancy between the biosorption capacity of pure chitin (8 mg/g biomass) and that of *Rhizopus arrhizus* (larger than 170 mg/g biomass); thus other processes are suggested to be involved other than complexation by chitin.)
2. The second process involved the adsorption of hydrolyzed thorium ions by the outer layers of the *R. arrhizus* cell wall.

Tsezos and Volesky (1982a, 1983b) suggested that uranium forms a complex with the chitin nitrogen and a free radical (hydroxyl group) was postulated to participate in the uranyl ion coordination to nitrogen. The presence of Cu^{2+} and Fe^{2+} reduced the uranium uptake probably due to the existence of competition for the nitrogen sites of the chitin crystalline network.

Muraleedharan and Venkobachar (1990) reported that the biosorption capacity of copper by a macro-fungus (wood-rotting fungus) *Ganoderma lucidum* was only reduced by 5% when the biosorbent was devoid of chitin. This in turn suggested that chitin was not playing a major role for copper biosorption in the case studied. The electron paramagnetic resonance spectroscopy indicated that there was an unidentified free radical in the cell wall matrix. The authors concluded that this cell wall matrix, which encompassed and trapped the free radical, open up on metal uptake. The opened cell wall matrix interacted with the metal and resulted in the uptake of the metal. The metal - protein interactions is well known (Spiro, 1980). However, they also showed that proteins did not play a significant role in the case for copper uptake of *G. lucidum*. The more recent data suggested that the structural polysaccharides of *G. lucidum* were the main sites of interaction. The biosorption site is believed to be the oxygen dominated and the majority of the metal taken up was exchanged with calcium and the hydrogen present on the cell wall (Muraleedharan *et al.*, 1994).

Even after the chemical modification of the carboxyl groups of copper-tolerant and copper-sensitive strains of *Mucor rouxii*, there is still 70-75 % Cu (II) bound of that

obtained by the native untreated cells. Jorge *et al.* (1996) suggested that carboxyl groups might not be fully responsible for Cu (II) binding. He claimed that other groups such as amino, hydroxyl, phosphoryl, oxalate, sulfate, and sulfonate might also be involved in copper binding.

Siegel (1990) reported that biosorption of UO_2^- ion by various purified cell wall polymers is in the following order: chitin > cellulose phosphate > carboxymethyl cellulose > cellulose. The difference between the highest and the lowest is only 20 %. It was further shown that metal ion-uncharged molecule interactions also took an important role in the contribution of biosorption process, which had been overlooked in the past (Kapoor, 1995).

Tobin *et al.* (1984) investigated biosorption of 17 metal species by heat-killed *Rhizopus arrhizus* at pH of 4.0. He claimed that a linear relationship was observed between maximum metal biosorption capacity of biomass and ionic radii of various cations. Higher uptake capacity was observed for larger cations except Cr^{3+} and alkali metal cations. The failure of adsorbing alkali metal cations may be due to the inability of these cations to form complex with the ligand groups of the fungal cell wall (Kuyucak and Volesky, 1988).

Tobin *et al.* (1984) suggested that the complex solution chemistry complicated the exact mechanism determination. Differences in affinities between different elements and their ionic species may exist for various ligands encountered in biological systems.

The metal biosorption mechanism of fungal biosorbent has been studied largely in relation to chitin, chitosan (derivative obtained by deacetylation of chitin) and cellulose. The role of other cell wall components, such as glycans, proteins, lipids,polyuronides and melanin may also play an important part for biosorption and further studies are needed (Kapoor, 1995).

2.3. Metal biosorption kinetics

Biosorption, involved a fast sorption reaction mechanisms based predominantly on chemisorption, is similar to conventional sorption processes (Volesky and Holan, 1995). The kinetics of such reactions is so fast that the measurements of metal uptake rates may be a challenging problem with the use of specially designed equipment (Tsezos and Volesky, 1982a, 1982b; Tsezos, 1981). Volesky and Holan (1995) suggested that in many biosorption systems, most of the metal biosorption occurred in a matter of 5 - 15 minutes after solid-liquid contact (Kuyucak and Volesky, 1989a, 1989b), followed in some cases by residual and much slower additional metal deposition, perhaps indicating a different secondary metal-binding mechanism.

Gadd (1986) and Blackwell *et al.* (1995) suggested that fungal metal uptake step was a biphasic process involve a metabolism-independent and metabolism-dependent step. The initial step was rapid and lasted for a few minutes. This step was independent of temperature and any energy-dependent metabolism. The uptake step was the binding process, involved both living cells and nonliving cells, might be due to ion-exchange, adsorption, complexation, precipitation and crystallization with the multilaminate and microfrillar cell wall structure. The second step was a slow step, bioaccumulation, affected by temperature and any metabolism and only occurred in living cells.

Copper uptake by living *S. cerevisiae* yeast cells was biphasic, consisting of an initial rapid surface binding of copper ions, followed by a second, slower, intracellular uptake of copper. The initial rapid uptake phase was completed in 5 seconds and the second slower phase lasted for 150 minutes (Kapoor and Viraraghavan, 1995).

Intracellular uptake process, in which metal ions are transported through the cell membrane into the cells, is metabolism-dependent and requires energy (for example, glucose). Therefore, this process can be inhibited by temperature. However, high concentration of metal ions was employed in the metal uptake studies, the energy-

dependent intracellular uptake process may be difficult to be detected and may not be a significant contribution of total uptake (Gadd, 1990).

Tsezos and Volesky (1982a) reported that uranium biosorption by *Rhizopus arrhizus* involved 3 steps. The fast process is the coordination of uranium to the cell wall chitin amine N and adsorbed to the chitin structure. Then a slower rate of precipitation reaction of $UO_2(OH)_2$ within the chitin microcrystalline cell wall structure occurred. Strandberg *et al.* (1981) claimed that additional uranium would crystalized on already bound molecules present on the cell wall of *Saccharomyces cerevisiae*. Similar multiple uptake mechanisms, in the absence of metabolism and intracellular bioaccumulation process, were also observed by Gadd *et al.* (1988).

2.4. Factors affecting biosorption

For living and nonliving biomass, different physical and chemical factors can affect the biosorption processes. The metal uptake depends on several factors. These include pH of the metal solution, temperature, contact time and the presence of cations and anions other than the target cations and anions (Modak and Natarajan, 1995; Kapoor and Viraraghavan, 1995).

2.4.1. Effects of solution pH

For nonliving cell, the biosorption process can regard as the adsorption or ion exchange process (Margaret *et al.*, 1984). The change in pH can alter both the metal uptake ability and capacity. Solution chemistry can also be affected by the change in solution pH. Many researchers have investigated the pH effects of the aqueous solution on metal uptake (Aksu and Kutsal, 1991; Fourest and Roux, 1992; Fris and Keith, 1986; Kuyucak and Volesky, 1988: Luef *et al.*, 1991). A general experimental trend (Modak and Natarajan. 1995), observed for different metals and biomass, is that metal uptake is not significant at low pH (pH 1 - 2). At very low pH, the solution would have a high concentration of hydronium ions to compete with the metal cations for the active sites on the biosorbents. As a consequence, metal uptake is low. Besides, the solution

chemistry of different metals is strongly affected by its pH value (Doyle *et al.*, 1980; Garnham *et al.*, 1993). The metal uptake increases as pH is increased until it reaches a maximum at an optimal pH (pH 3 - 5). As the pH is increased beyond the optimum value, the metal uptake decreases.

Kuyucak and Volesky (1988b) claimed that the optimum pH for all metals biosorption was between 4 and 5 except for gold. For uranium biosorption by *Rhizopus* and *Aspergillus* species, (Tsezos and Volesky, 1981), the optimum removal was reached in the pH range of 4 - 5, and removals was reduced heavily at a pH of 2.5. Uranium removal by *Penicillium* species was more or less the same in the pH range of 2.5 - 9.5 (Galun *et al.*, 1983b).

Uranium uptake decreased as pH was lowered from 4 to 2. Tsezos (1983b) suggested that the decrease was due to an increased hydronium ions concentration. The metal cations probably encountered increased competition from the increased hydronium ion population before they reached the binding sites. As a result, the metal uptake decreased.

Zhou and Kiff (1991) suggested that the cell wall ligands were bound closely with the H^+ at low pH with a subsequent increase in repulsion against the positively charged metal ions. As pH were increased, more ligands with negative charge would be exposed for positively charged metal ions (Harris and Ramelow, 1990; Zhou and Kiff, 1991). Harris and Ramelow (1990) revealed that the metal biosorption capacity was lowest at its isoelectric pH. Above the isoelectric pH, the ligands on the cell wall would carry a net negative charge, which enhanced their metal uptake capability. Below the isoelectric pH, on the other hand, ligands would become positively charged which resulted in a subsequent attraction of metallic ions with positive charge and adsorption onto the cell surface. At higher pH, the solution chemistry becomes important. As pH was increased beyond its optimum values (pH 5 to 7), the metal uptake decreased. The decrease may be due to the reduced solubility and the precipitation of base metals (Harris and Ramelow, 1990; Zhou and Kiff, 1991). However, for radionuclides (Tsezos

and Keller, 1983; Pons and Fuste, 1983) and precious metals such as silver and gold, (Balakrishnan *et al.*, 1984; Byerley *et al.*, 1989) good uptake is still possible at alkaline pH (pH 8 to 10).

2.4.2. Effects of temperature

Temperature can affect cell metabolism. However, the biosorption of metal by nonliving cell is metabolism-independent and, therefore, is not significantly affected by temperature. Many investigators reported that metal uptake by several biomass types was not significantly affected by increasing the temperature from 4 to 45^{0}C (Modak and Natarajan, 1995). Examples of these studies include copper uptake by fungal biomass such as *Rhizopus arrhizus, Cladosporium resinae and Penicillium italicum* (de Rome and Gadd, 1987), zinc (Failla *et al.*, 1976) and uranium uptake respectively by *Candida utilis* and immobilized *Pseudomonas* species EPS 5028 (Pons and Fuste, 1993).

Kuyucak and Volesky (1988) reported that cobalt uptake by *Ascophyllum noddsum* (algae) was not significant for temperature changes from 23 to 40^{0}C. However, the cobalt uptake capacity increased much when temperature changed from 4 to 23^{0}C. A significant negative temperature effect was observed at 80^{0}C or over.

The initial biosorption rate was found to be temperature-dependent (Sag and Tulin, 1996). At solution pH 2.0, biomass loading of 1 g/L *Rhizopus arrhizus* and initial metal ions concentration of 150 mg/L, the initial biosorption rates of chromium (VI) and iron (III) were doubled with a 10^{0}C increase.

2.4.3. Effects of cations

Most research work on biosorption has been limited to studies on single metal ion species in aqueous solutions. The presence of other cations significantly affected metal uptake by nonliving biomass. (Kuyucak and Volesky, 1988a: Tobin *et al.*, 1988; Niu *et al.*, 1993; Jang *et al.*, 1995; Chong and Volesky, 1995; Sag and Kutsal, 1996; Rose, 1996).

Previous studies (Kuyucak *et al.*, 1988; Tobin *et al.*, 1988; Niu *et al.*, 1993; Jang *et al.*, 1995; Chong and Volesky, 1995; Sag and Kutsal, 1996; Rose, 1996) have reported that the presence of other cations reduced metal uptake by biomass. However, the positive effect of the other cations on metal uptake had also been reported. There is an increase in Cu^{2+} uptake by *Aureobasidium pullulans* in the presence of Hg^{2+} (Gadd and Mowll, 1985). Gadd and Mowll (1985) suggested that the increase may be due to the increased permeability of the cell wall. Kuyucak and Volesky (1988a) reported that Co^{2+} uptake by *Ascophyllum nodosum* was increased in the presence of potassium ions. The lead uptake by *Penicillium chrysogenum* was increased with the presence of cadmium ions (Niu *et al.*, 1993).

2.4.4. Effects of anions

Different anions have different effects on the uptake of metal cations. Uranium uptake in seawater by several microorganisms was lowered in the presence of carbonate anions. These phenomena can be explained by the formation of a stable complex which weakened the interaction between the biomass and uranium (Modak and Natarajan, 1995). The addition of complexing ligands or the reduction of pH to a value less than 2 reversed metal binding which further showed that ion - exchange or complexation may be the dominant mechanism governing uranium uptake of fungal biomass. The stability of uranyl complexes was in the following descending order: $EDTA^{2-} > CH_3CO_2^- > C_2O_4^{2-} > SCN^- > SO_4^{2-} > NO^{3-} \geq Cl^-$ (Margaret *et al.*, 1984). The presence of anions in solution was also found to inhibit the uptake of La^{3+}, Cd^{2+}, Pb^{2+}, UO_2^{2+} and Ag^+ by *Rhizopus arrhizus* biomass (Tobin *et al.*, 1987). The effects ranged from total inhibition of Cd^{2+} and Pb^{2+} uptake at equimolar concentrations of EDTA to no change in La^{3+} or UO_2^{2+} uptake at 12-fold molar excesses of Cl^- or CO_3^{2-} (Tobin *et al.*, 1987). Kuyucak and Volesky (1989) reported that Co^{2+} uptake by *Ascophyllum nodosum* was reduced in the presence of various anions such as SO_4^{2-}, PO_4^{3-}, CO_3^{2-} and NO_3^-. Among these anions, NO_3^- proved to be the strongest inhibitor for cobalt uptake regardless of the solution pH and the initial concentration (Kuyucak and Volesky, 1989a). Zhou and Kiff

(1991) discovered that the biosorption of copper by *Rhizopus arrhizus* was inhibited by a variety of anions present in the following order : EDTA >> SO_4^{2-} >> Cl^- . Inhibition by anions may be due to their interactions with metal ions and cell surfaces. At low copper concentration and high anion concentration nearly all the copper ions will be complexed to form metal-ligand complexes which may be non-adsorbing or weakly adsorbing, resulting in a decrease in copper uptake (Zhou and Kiff, 1991).

2.5. Biosorption as a metal removal technology

The different metals used in many industrial application processes, especially mining, mineral-processing and industrial electroplating generated a large quantities of aqueous effluents bearing high level of heavy metals. The development of the process for removing heavy metals from these point sources was needed. The process developed must be effective and inexpensive.

2.5.1. Comparison between the conventional technology and biosorption technology

Many industrial processes, especially mining and mineral-processing generated a large quantities of aqueous effluents bearing high levels of heavy metals. Many different physico-chemical processes can be employed to remove heavy metals from the aqueous effluents. These processes include precipitation, coagulation, ion exchange, membrane processes (reverse osmosis, electrodialysis, ultrafiltration) and adsorption (Beszedits, 1983). Conventional precipitation and coagulation become less effective and expensive when metal concentrations are in the range of 1 to 100 mg/L (Kapoor, 1995). Besides, a large volume of sludge is produced, creating a solid waste management problem. Membrane processes operations are costly, complicated and not efficient. Heavy metals removal employing activated carbon adsorption process is expensive. The different technologies for metal removal are compared in Table 1 (Volesky 1990; Kapoor, 1995).

2.5.2. Technological considerations for biosorbents

From the engineering point of view, a steep adsorption isotherm with a high saturation plateau is a desirable characteristic for the biosorbents. The uranium biosorption by some industrial fungal species (*Rhizopus arrhizus* and *Penicillium chrysogenum*) can provide a steeper isotherm with a higher saturation than that of conventional ion-exchanger, ionex IRA-400 and industrial activated sludge (Volesky, 1987).

Microbial biomass can be applied to develop excellent and inexpensive biosorbents for metal removal and recovery. Volesky (1987) suggested that at least four board areas of applications for new biosorbent (biological originated materials) can be considered:

1. detoxification of metal-bearing wastewaters,
2. decontamination of radioactive wastewaters,
3. recovery of metals from ore processing solutions,
4. concentration/recovery of strategic/rare metals from seawater.

The employment of living organisms in environmental technology is usually not feasible in all situations. Firstly, industrial effluents usually contain a high content of heavy or toxic metals at vary pH conditions. The microorgansims usually cannot growth and maintain in such an environment. Besides, regeneration using different varieties of regenerants without killing the cell to recover the heavy or toxic metals after the biosorption processes is not possible. The worst of all, continuous supply of organic nutrients is needed to keep the microorganisms alive.

There are actually several advantages of the using nonliving organisms over living ones (Modak and Natarajan, 1995) in developing metal removal technology :

1. There is no need to supply costly nutrients for the nonliving biomass.

Table 1. Comparison among different technologies of metal removal and recovery (Volesky, 1990; Kapoor, 1995)

Technology	Properties of each technology					
	Concentration dependence	Regeneration	pH adjustment	Selectivity	Effluent concentration (mg/L)	Sludge generation
Biosorption	required	yes	Required	yes	< 1	no
Precipitation	not required	no	Not required	no	2 - 5	yes
Ion exchange	required	yes	Some	yes	< 1	no
Membrane	not required	no	Some	no	1 - 5	-
Evaporation	required	-	Required	no	1 - 5	-
Adsorption with activated carbon	required	yes	Some	no	1 - 5	No

2. The nonliving biomass is growth-independent; therefore, physiological constraints of the cell can be eliminated. Hence, a wider range of operating conditions such as pH, temperature and metal concentrations are feasible.
3. Besides, the biomass which is produced by the fermentation industries as wastes can be employed for such a process. These industries can continuously supply such a cheap source of biomass.
4. Recovery of valuable metals by different regenerants or by incineration can be possible.

New biosorbent developed must be regenerated for multiple reuse. Besides, they must be highly selective, efficient and cheap (Volesky, 1987). Besides, the small particle size and low strength of cells can cause difficulties in separating the biomass from the treated effluent. Therefore, there is a need for immobilizating and pelletizating the biomass for the industrial process applications. Foam biomass support particles, sand, paper or textile-making fibers and polymers have been applied for biomass immobilization in the metal removal process (Tobin *et al.*, 1993; Zhou and Kiff, 1991; Huang and Morehart. 1990; Tsezos and Deutschmann, 1990).

For application purposes, the high rates of metal biosorption are very advantageous. Because of the fast kinetics of the biosorption reactions, the overall sorption rate is more often controlled by mass transfer of the sorbed solute (metal) to the active reaction site. While the intraparticle diffusion normally appears to be the overall rate-controlling step, the particle external film diffusion also plays a role, which depends on the hydraulic flow regime (turbulence and/or back-mixing) in the reactor system (Volesky and Holan. 1995).

2.5.3. Sources of biomass

Fungi and yeasts can grow easily. Their properties can be controlled both genetically and morphologically. Different fungal strains are widely used in a variety of large-scale industrial fermentation processes which result in high yields of biomass. For

example, *Rhizopus arrhizus* is used for lipase production (Fourest and Roux, 1992) and *Penicillium chrysogenum* is used for penicillin production (Niu *et al.*, 1993). *Aspergillus* strains are utilized in the industrial production of citric acid and enzymes like amylases, glucose isomerase and lipase, while *Saccharomyces cerevisiae* is applied in the food and beverage industries. The abundant biomass types produced as a waste byproduct of these fermentation processes can be very inexpensive sources of metal biosorbent. The conversion of the biomass waste into useful metal biosorbent does not only drastically reduce the production cost of biosorbent but also the disposal cost of the biomass waste.

2.6. Models to describe physiochemical mechanisms of heavy metal removal

2.6.1. Adsorption theory

Adsorption of molecules can be represented as a adsorption equilibrium reaction

$$B + M \Leftrightarrow B \bullet M$$

where B represent the adsorbate (biosorbent), M the adsorbent (metal), and B • M the adsorbed compounds. Adsorbates can attach to the substrate surface by various forces such as hydrogen bonds, dipole-dipole interactions, and van der Waals forces (Snoeyink, 1990). Adsorbates are held on the surface in 2 ways: physisorption and chemisorption. In physisorption (an abbreviation of 'physical adsorption'), there is a van der Waals interaction (for example, a dispersion of a dipole interaction) between the adsorbate and the substrate. Van de Waals interactions are long range but weak in nature, and the energy released when a particle is physisorbed is of the same order of magnitude as the enthalpy of condensation. In chemisorption (an abbreviation of 'chemical adsorption') the particles stick to the surface by forming a chemical (usually covalent) bond, and tend to find sites that maximize their coordination number with the substrate. The enthalpy of chemisorption is very much greater than for physisorption (Atkins, 1990).

Adsorption involves the interphase accumulation of concentration of substances at a surface or interface. The process can occur at an interface between any two phases,

such as, liquid-liquid, gas-liquid, gas-solid, or liquid-solid interfaces. The material being concentrated or adsorbed is the adsorbate, and the adsorbing phase is termed the adsorbent (Weber and Walter, 1972). Giles *et al.* (1960) conducted a comprehensive study of true solution adsorption isotherms - plots of bound or adsorbed solute concentration q_e against the free solute concentration in solution (equilibrium concentration of solute) C_e at a fixed temperature. Classifications systems, invented by Giles *et al.* (1960), divides all isotherms into the 4 major types according to the initial slope, and sub-groups are described by each class, based on the shape of the upper parts of the curves. The four main classes are named the S, L (i.e."Langmuir" type), H ("high affinity") and C ("constant partition") isotherms. The general shape of the 4 basic isotherms types are shown in Figure 3. The sigmoidal relationship between q_e and C_e is characteristic of the S curve, the initial direction of curvature shows that adsorption becomes easier as concentration rises. The L curve with the initial curvature shows that as more sites in the substrate are filled it becomes increasing difficult for a bombarding solute molecule to find a vacant site available. Example, such as systems with highly polar solute (i.e. phenol) and substrate (i.e. alumina) give this type of curve. The H curve is a special case of the L curve, in which the solute has such high affinity that in dilute solutions it is completely adsorbed, or at least there is no measurable amount remaining in solution. The initial part of the isotherm is therefore vertical. The adsorbed species are often large units, i.e., ionic micelles or polymeric molecules, but sometimes they are apparently single ions which exchange with others of much lower affinity for the surface, e.g. sulphonated dye ions which exchange with chloride ions on alumina,and cyanide dye cations adsorbed by ion-ion attraction on silver halides. In most extreme form, the curve is a horizontal line running into the vertical axis. This was found for chemisorption of fatty acids on *Ranny nickel*. The C curve is characterised by the constant partition of solute between solution and substrate, right up to the maximum possible adsorption, where an abrupt change to a horizontal plateau occurs. It is important to note that the lowest part of the L curve is sometimes virtually linear, and some intermediate between S and L types may be found. The equilibrium of a solute (metal ion) distributed between the liquid and solid phases can be described by various

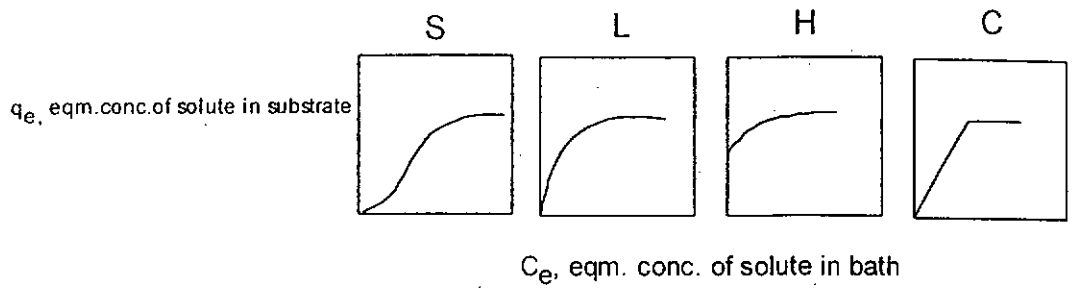

Figure 3. System of isotherm classification.

models. Two most widely accepted adsorption isotherm models for single solute systems are *Langmuir* and *Freundlich* isotherms. Batch equilibrium experiments may be conducted to derive these classical isotherms for evaluating and comparing the potential of different biosorption systems.

2.6.1. Adsorption Models

2.6.1.1. *Langmuir isotherm.*

The *Langmuir* model is valid for single-layer adsorption. The derivation of the *Langmuir* adsorption isotherm involves several implicit assumptions: (i) all the sites of the solid have the same activity for adsorption; (ii) there is no interaction between the adsorbed molecules; (iii) all the adsorption occurs by the same mechanism, and all the adsorbent complex have the same structure. The derivation of this equation is based on the adsorption and desorption of the adsorbate on the surface. The final form of the equation may be written as:

$$q = \frac{K C_e q_{max}}{(1 + K C_e)}$$

$$\text{where} \quad K = K_0 \exp(-\frac{\Delta H}{RT})$$

and q and C_e are the equilibrium surface and solution concentrations respectively. The constant q_{max} represents the theoretical maximum uptake of solute per unit mass of adsorbent that can be achieved as C_e is increased, and K is a constant which is related to the energy of adsorption and increases as the strength of the adsorption bond increases. K_0 is a constant containing the entropy term, ΔH is the heat of adsorption, R is the universal gas constant and T is the absolute temperature. In order to determine the value of K and q_{max}, the above equation may be transformed into the following form:

$$\frac{C_e}{q_e} = \frac{1}{K q_{max}} + \frac{C_e}{q_{max}}$$

or

$$\frac{1}{q_e} = \frac{1}{q_{max} K C_e} + \frac{1}{q_{max}}$$

The value of q may be determined by measuring the concentration of the metal ion in the aqueous phase before and after contacting with the biomass. A plot of C_e/q (or $1/q_e$) against C_e (or $1/C_e$) would give a straight line with slope of $1/q_{max}$ ($1/Kq_{max}$) and intercept of $1/Kq_{max}$ (or $1/q_{max}$) if the data fit the isotherm. The value of q_{max} measures the theoretical maximum metal biosorption capacity of the biomass. The value of K measures the affinity of metal ions adsorbed to the biomass.

For very small amounts of adsorption, when $KC_e << 1$, the specific adsorption is proportional to the final concentration of adsorbate in solution, yielding a linear adsorption relationship

$$q_e = Q^0 K C_e$$

For large amounts of adsorption, where $KC_e >> 1$

$$q_e \approx Q^0$$

2.6.1.2. *Freundlich isotherm.*

This model is a semiempirical equation attributed to *Freundlich* (*Freundlich*, 1926). Similar to *Langmuir* model, it is valid for monolayer adsorption. This model was developed for heterogenous surface in which the energy term, K, in *Langmuir* equation varies as a function of surface coverage, q_e, strictly due to variations in heat of adsorption (Adamson, 1967). This classical equation is also widely employed, particularly in the low to intermediate concentration range. It is expressed as

$$q_e = k C_e^{\frac{1}{n}}$$

where q is the amount of solute uptake per unit mass of adsorbent, k ($\propto RTnKe^{\Delta H/RT}$) and n are *Frenndlich* constants. If adsorption is favourable, then $n > 1$. n is a constant

representing the mutual interaction of adsorbed species. Experimental values of n are usually greater than unity and this means that the forces between the adsorbed molecules are repulsive (Sag and Kutsal, 1995).

The *Freundlich* isotherm may be rearranged as follows :

$$\ln q_e = \ln k + \frac{1}{n} \ln C_e$$

The intercept (ln k) for $C_e = 1$ ($\ln C_e = 0$) is related primarily to the capacity of the adsorbent for the adsorbate, and the slope 1/n is a function of the strength of adsorption. For fixed value of k and C_e, the smaller the value of 1/n, the stronger the adsorption bond is. As 1/n becomes very small, the capacity tends to be independent of C_e, and the isotherm plot approaches the horizontal; the value of q_e then essential constant, and the isotherm is called irreversible. If the value of 1/n is large, the adsorption bond is weak, and the value of q_e changes markedly with small changes in C_e. However, the *Freundlich* isotherm cannot apply to all values of C_e. As C_e increases, q_e increases only until the adsorbent approach saturation. At saturation, q_e is a constant, independent of further increases in C_e, and the *Freundlich* isotherm no longer applies.

The *Freundlich* equation generally agrees quite well with the *Langmuir* equation and the experimental data over moderate ranges of concentration, C_e. Unlike *Langmuir* equation, it does not reduce to a linear adsorption expression at very low concentrations. It does not agree well with the *Langmuir* equation at very high concentrations, since the value of n would reach some limit when the surface is fully covered.

Both models can describe many biosorption data but not necessarily give a meaningful physical interpretation in biosorption. Table 2 is a summary of isotherm applications for description of the biosorption data.

2.6.1.3. BET isotherms

Brunauer, Emmett, Teller (BET) model represents isotherm reflecting apparent multilayer adsorption. Similar to *Langmuir* model, it is limited by the assumption of uniform energies of adsorption on the surface. Graphically the most common BET isotherm is represented in Figure 4.

The saturation concentration of the solute in the solution at a given temperature is represented by C_s. The BET isotherm can be reduced to *Langmuir* isotherm when the limit of adsorption is a monolayer.

The *Langmuir* equation is based on the assumptions that maximum adsorption corresponds to a saturated monolayer of solute molecules on the adsorbent surface, where the energy of adsorption is constant and no transmigration of adsorbate in the plane of surface. While, the BET model assumes that a number of layers of adsorbate molecules form at the surface and that the *Langmuir* equation applies to each layer. Another assumption of the BET model is that a given layer need not complete formation prior to initiation of subsequent layers; the equilibrium condition will therefore involve several types of surfaces in the sense of number of layers of molecules on each surface site. For adsorption from solution with the additional assumption that layers beyond the first have equal energies of adsorption, the BET equation takes the simplified form

$$q_e = \frac{BC_eQ^0}{(C_s - C_e)[1 + (B + (B-1)(C_e / C_s)]}$$

in which C_s is the saturation concentration of the solute, C_e is the measured concentration in solution at equilibriumm Q^0 is the number of moles of solute adsorbed per unit weight of adsorbent in forming a complete monolayer on the surface, q_e is the number of moles of solute adsorbed per unit weight at concentration C_e, and B is a constant expressive of the energy of interaction with the surface. The equation may be rearranged and linearized in the following form

$$\frac{C_e}{(C_s - C_e)q_e} = \frac{1}{BQ^0} + (\frac{B-1}{BQ^0})(\frac{C_e}{C_s})$$

Table 2. Applications of several types of models for metal uptake by microorganisms

Isotherm	Metal	Biomass type	Reference
Langmuir	Cu	*Aspergillus oryzae*	Huang *et al.*, 1991
	Cd	*Saccharomyces cerevisiae*	Volesky *et al.*, 1993
Freundlich	Ag	*Aspergillus niger*	Mullen *et al.*, 1992
	Cu	*Aspergillus niger*	Mullen *et al.*, 1992
	La	*Aspergillus niger*	Mullen *et al.*, 1992
Langmuir & Freundlich	Th	*Aspergillus terrcus*	Tsezos and Volesky, 1981
	U	*Aspergillus terrcus*	Tsezos and Volesky, 1981
	Th	*Rhizopus arrhizus*	Tsezos and Volesky, 1981
BET	Cu	*Rhizopus arrhizus*	Rome and Gadd, 1987
Scatchard	Cu	*Aureobasidium pullulans*	Geoffrey *et al.*, 1985
	Cu	*Saccharomyces cerevisiae*	Huang *et al.*, 1990

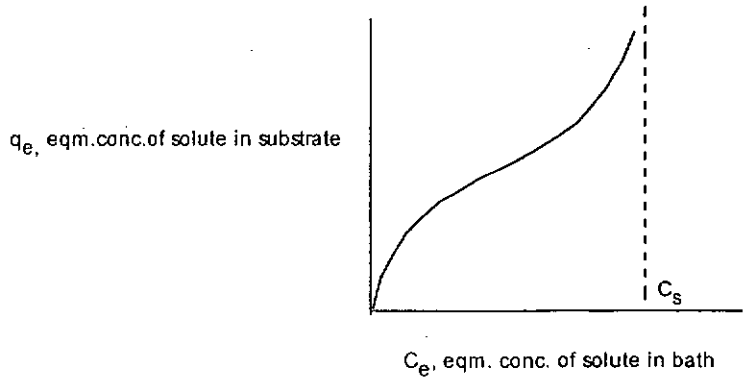

Figure 4. Typical isotherm for BET adsorption pattern

A plot of the term $C_e/(C_s-C_e)q_e$ against C_e/C_s gives a straight line of slope $(B - 1)/BQ^0$ and intercept $1/BQ^0$ for data which accord with the BET model.

There is no similar "total capacity" for adsorption which follows the BET type II pattern (Figure 4) as q_e tends asymptotically toward infinity as C_e approaches C_s. Often the value of Q^0 is found to correspond closely to the inflection point of the q_e versus C_e plot.

2.6.3. *Scatchard* Plot

Scatchard plots have been shown to describe the equilibrium data (Huang *et al.*, 1990). The model was developed for describing the attractions of protein for small molecules and ions (Hirs and Timashelt, 1978; Kapoor and Viraraghavan, 1995). The interaction product (MX) between the metal ions (M) and the binding sites (X) on the cell surface can be described by the following equations :

$$M + X \Leftrightarrow MX \quad \text{.....} \quad (1)$$

$$K = \frac{[MX]}{[M]_e[X]} \quad \text{.....} \quad (2)$$

where $[M]_e$ is the equilibrium metal ions concentration, [X] is the concentration of free ligand, and X_0 is the concentration of potential binding sites.

By the relationships $[X] = X_0 - [MX]$, a plot equation with bound ligand concentration divided by free-ligand concentration versus the concentration of bound ligand will give the typical *Scatchard* plot as follows :

$$\frac{[MX]}{[M]_e} = K([X_0] - [MX]) \quad \text{.....} \quad (3)$$

The plot of $[MX]/[M]_e$ against [MX] gives a slope of –K. The intercept of the *Scatchard* plot in this form is KX_0, and together with the value of X_0 obtained from the abscissa intercept, it provides another way of determining K. This will become important for the interpretation of nonlinear *Scatchard* plots.

Chapter 3. Materials and Methods

3.1. Instrumentation

The agar slants inoculated with fungal spores were incubated in a low temperature incubator (Shel Lab model 2020 operated at 25°C). The fungal biomass was cultivated in a controlled environment orbital shaker (New Brunswick Scientific Psycrotherm 3,430,926, USA) and the batch biosorption experiments were carried out in both Labline and Sanyo controlled temperature orbital shakers. Chemical solutions and equipment were sterilized by autoclave (Tokyo Hirayama, model HA-30 and Sakura Finetechnical, model ASV-3022) at 121°C at 1.1 kgf/cm^2. The centrifuges used were Beckman J2-M1 and J2-21 model. For samples less than 2.5 mL, Sigma 113 batch-top centrifuge was used. The metal concentration of the samples was determined by atomic absorption spectrophotometers (Varian Tectron 1200 and Perkin-Elmer Analyst 100 with a model HGA-800 graphite furnace). The specific and sensitive wavelengths for the determination of different metals in the supernatent are described in Perkin-Elmer technical manual part number, 0303-0152 (Perkin-Elmer Corporation, 1994). For lead determination, 283.3 nm was used, while for copper, 324.7 nm was used. The wavelengths used for other elements are listed in Table 3.

3.2. Materials and chemicals

The deionized-distilled (dd) water utilized in this research was prepared by deionization and distillation processes with Fisons 'Fi-streem' Tank. Metal stock solution was prepared by dissolving exact quantities of BDH A. R. grade nitrate salts of the corresponding metals in dd water. For the atomic absorption spectrophotometer calibration, spectro grade metal nitrate standards were used. The standards were also prepared by digesting one gram of the corresponding metals in minimal amount of 70% A. R. grade nitric acid and then diluted to 1.00 litre with dd water. Glasswares and

plasticware were washed in detergent, rinsed, soaked twice for a minimum of 24 h. in 10% HNO_3, and rinsed four times with dd water.

The fungal strains were maintained routinely on Potato Dextrose Agar (PDA, Oxoid CM139) plates. The Oxoid L 40 mycological peptone and the bacto peptone (Difco) were used for preparing the PYG (Peptone, Yeast Extract and Glucose) liquid medium.

3.3. Fungal and yeast strains

Ten different strains of fungi and yeast were used in these experiments (Table 4). These strains are from subdivision *Zygomycotina, Deuteromycotina, Basidiomycotina and Ascomycotina* of Division *Eumycota.* Of all these strains, *Aspergillus niger, Aspergillus nidulans, Penicillium chrysogenum, Rhizopus stolonifer* (-), and *Saccharomyces cerevisiae* were obtained from our own culture stock. The strains of *Mucor rouxii* ATCC 24905, *Rhizopus oryzae* ATCC 46242, and *Cladosporium cladosporioides* ATCC 20251 were obtained from the American Type Culture Collection (ATCC). The strains of *Absidia coerula* NRRL 1310 and *Agaricus bisporus* NRRL 2335 were obtained from the Northern Utilization Research and Development Division, US Department of Agriculture, Peoria, ILLinois, USA. *Aspergillus* and *Mucor* species were selected because they both contain chitin and chitosan which provide prominent metal adsorption ability (Volesky, 1990). The wall of *A. niger* is in the chitin-glucan group, and that of *M. rouxii* is in the chitosan-chitin group. Species from other subdivision were also been chosen for comparing with the *Aspergillus* and *Mucor* species.

Table 3. Wavelengths slected for atomic absorption spectrophotometric measurement of several selected metals

Metals	Ag	Cd	Co	Cr	Mg	Na	Ni	Zn
Wavelength (nm)	328.1	228.8	240.7	357.9	285.2	589.0	352.4	213.9

Table 4. Fungal and yeast strains selected for biosorption experiments

Subdivision (of Division *Eumycota*)	Fungal and yeast strains
Zygomycotina	*Absidia coerulea, Mucor rouxii, Phycomyces blakeleeanus* (+), *Rhizopus oryzae, Rhizopus stolonifer* (-)
Deuteromyctina	*Aspergillus niger, Aspergillus nidulans, Aspergillus terricola, Cladosporium cladosporioides, Penicillium chrysogenum, Penicillium notatum*
Basidiomycotina	*Agaricus bisporus*
Ascomycotina	*Saccharomyces cerevisiae* (yeast)

3.4. Preparation of Biomass

The fungi were maintained routinely on 2% potato dextrose agar (PDA, Oxoid) plates. To produce the biomass for biosorption experiments, the seed cultures were prepared by loop-inoculating and incubating the fungi in 100 mL liquid PYG medium at pH 4.5 and temperature 25°C on an orbital shaker at 200 rpm. The PYG medium contained 0.4% D-glucose, 0.3% mycological peptone and 1% yeast extract. After 24 h cultivation, 10 mL of the seed culture was then transferred to inoculate 100 mL PYG broth. The cultures were grown at pH 4.5 and temperature 25°C on orbital shaker at 200 rpm for one week. The fungal biomass was then harvested by filtration, washed with dd water, resuspended, and washed again. The biomass was freeze-dried with a Heto FD8 freeze dryer at 0°C and at reduced pressure over 2 days. The product was finally ground in a mortar and pestle.

3.5. Metal biosorption kinetic and equilibrium studies

3.5.1. Lead biosorption experiments

A batch equilibration method was used in investigating different fungal species for their metals biosorption capacities. For lead biosorption study, the batch biosorption experiments were carried out using constant initial lead concentrations and varied biomass concentrations. A series of 500 mL Nalgene polypropylene bottles were prepared with known volume of serial dilutions of standardized lead nitrate solution and pH of the solution was adjusted to 5.0 by 0.1 M of nitric acid and 0.1 M sodium hydroxide. The freeze-dried biomass in dd water was homogenized by Janke-kunkel IKA-Labortechnik Ultra-turrax T25 homogenizer at a speed of 24,000 rpm for 5 min. and the pH of the biomass aliquot was also adjusted to 5.0 by 0.1 M of nitric acid and 0.1 M sodium hydroxide. Different known volume of the homogenized biomass suspension and dd water were added to the bottles, resulting in initial lead concentrations of 100 ppm in 200 mL total solution volume, unless specified otherwise.

The biomass concentration ranged from about 0.05 g/L to about 1.5 g/L. The mixture was then incubated at 25°C on orbital shaker operated at 200 rpm for a minimum of 72 h. Samples were taken out at different time intervals, transferred to micro-centrifuge tubes and centrifuged to remove the suspended fungal biomass. The metal concentration of the supernatant was then determined by atomic absorption spectrophotometers (Varian Tectron model 1200, Perkin-Elmer Analyst 100 with a model HGA-800 graphite furnace) at wavelength 283.3 nm. The biosorption experiments were duplicated.

3.5.2. Copper biosorption experiments

The batch copper biosorption experiments were carried out using constant biomass at different initial copper concentrations. A series of 500 mL Nalgene polypropylene bottles were prepared with a fixed known volume (25 mL) of different concentrations of standardized copper (II) nitrate solution and pH of the solution was adjusted to 5.0 by 0.1 M of nitric acid and 0.1 M sodium hydroxide. The freeze-dried biomass in dd water was homogenized by Janke-kunkel IKA-Labortechnik Ultra-turrax T25 homogenizer at a speed of 24,000 rpm for 5 min. and the pH of the biomass aliquot was also adjusted to 5.0 by 0.1 M of nitric acid and 0.1 M sodium hydroxide. Fixed known volume (20 mL) of the homogenized biomass suspension was then added to the bottles resulting in 45 mL total solution volumes, unless specified otherwise. The final biomass concentration was about 3 g/L and the copper concentration ranged from about 1 ppm to about 40 ppm unless specified. The mixture was then incubated at 25°C on orbital shaker operated at 200 rpm for a minimum of 24 h. Samples were taken out at different time intervals, transferred to micro-centrifuge tubes and centrifuged to remove the suspended fungal biomass. The metal concentration of the supernatant was then determined by the atomic absorption spectrophotometer at wavelength 324.7 nm. The biosorption experiments were also duplicated.

3.6. Effects of pH on lead and copper biosorption

The pH effects on the Pb and Cu biosorption capacities of selected fungal strains were studied. The batch biosorption experiments were carried out using constant biomass at same initial concentrations with the initial pH ranged from 1 to 8. A series of 500 mL Nalgene polypropylene bottles were prepared with a fixed known volume (25 mL) of same initial concentrations (over 2 mM) of standardized metal (II) nitrate solution and pH of the solution was adjusted to different pH (pH 1 - 8) by 0.1 M of nitric acid and 0.1 M sodium hydroxide. The freeze-dried biomass in dd water was homogenized by Janke-kunkel IKA-Labortechnik Ultra-turrax T25 homogenizer at a speed of 24,000 rpm for 5 min. and the pH of the biomass aliquot was also adjusted to the corresponding pH (pH 1 - 8) by 0.1 M of nitric acid and 0.1 M sodium hydroxide before mixing with the metal solution of the same initial pH. Fixed known volume of the homogenized biomass suspension was added to the bottles and the final biomass concentration was about 3 g/L. The mixture was then incubated at 25°C on orbital shaker operated at 200 rpm for a 24 h. Samples were then taken, transferred to micro-centrifuge tubes and centrifuged to remove the suspended fungal biomass. The metal concentration of the supernatant was then determined by atomic absorption spectrophotometer.

3.7. Effects of treatments on copper biosorption

The effects of different treatments on copper biosorption capacity of *Mucor rouxii* were studied. The four methods studied are: (i) heat treatment, (ii) acid treatment, (iii) alkaline treatment and (iv) formaldehyde treatment. These treatments are described in the following sections. After these treatments, the treated cell was then resuspended in a given amount of dd water and homogenized for 5 min. and pH of the biomass aliquot was then adjusted to 5.0. Twenty mL homogenized biomass suspension was added to the bottles with 25 mL copper (II) nitrate solution, originally at different initial copper concentration, were then added resulting in 45 mL total solution volumes. The

final biomass concentration was about 2 g/L and the copper concentration ranged from about 3 ppm to about 80 ppm unless specified. The mixture was then incubated at 25°C on orbital shaker operated at 200 rpm for a minimum of 24 h. Samples were taken out at different time intervals, transferred to micro-centrifuge tubes and centrifuged to remove the suspended fungal biomass. The copper concentration of the supernatant was then determined by atomic absorption spectrophotometer. The biosorption experiments were also duplicated.

3.7.1. Heat treatment

Five grams freeze-dried filamentous *Mucor rouxii* was weighed and mixed with 500 mL dd water. The biomass was homogenized by Janke-kunkel IKA-Labortechnik Ultra-turrax T25 homogenizer at a speed of 24,000 rpm for 5 min. The biomass suspension aliquot was then autoclaved at 121°C for 15 min. After this step, the biomass was then filtered and washed completely with a large amount of dd water for about 5 times.

3.7.2. Acid treatment

Five grams freeze-dried filamentous *Mucor rouxii* was weighed and mixed with 250 mL 0.1 M nitric acid. The biomass suspension was homogenized for 5 min. The biomass suspension aliquot was then stirred at 25°C continuously for 1 day. The biomass was then filtered and washed completely with a large amount of dd water for about 10 times. The biomass was then resuspensed in a given amount of dd water and then neutralized to pH 5.0 with 1 M diluted sodium hydroxide before the biosorption experiment with copper.

3.7.3. Alkaline treatment

Ten grams freeze-dried filamentous *Mucor rouxii* was weighed and mixed with 100 mL 1.0 M sodium hydroxide and 300 mL dd water. Then the cell suspension was

homogenized in the sodium hydroxide solution for 5 minutes followed by autoclaving at 121°C and 1 kgf/cm^2 for 5 minutes. The resulting gelatinous cell was then filtered and washing completely with a large amount of dd water for about 10 times. The gelatinous cell was then resuspensed in a given amount of dd water and then the pH was adjusted to 5.0 before the copper biosorption experiment.

3.7.4. Formaldehyde treatment

Five grams freeze-dried filamentous *Mucor rouxii* was weighed and mixed with 200 mL dd water. Then the cell suspension was homogenized for 5 min. and 25 mL 37 % formaldehyde and 0.25 g sodium hydroxide pellet were added. The mixture was then vortex-mixed and autoclaved at 121°C at 1 kgf/cm^2 for 10 min. The formaldehyde fixed biomass was then filtered and washed with dd water for about 10 times.

3.8. Effect of medium composition

The new PYG medium contained 0.4% D-glucose, 0.3% Difco bacto peptone and 1% yeast extract and the pH of the medium was adjusted to 4.5 before autoclaved. The composition of the PYG medium was the same as previously used except that the Difco bacto peptone was used instead of the Oxoid mycological peptone. The cell was cultivated at temperature 25°C on an orbital shaker at 200 rpm.

3.9. Comparison of biosorption capacities for different metals

3.9.1. Biosorption of nickel and zinc

The batch biosorption experiments were carried out using constant biomass at different initial metal concentrations. The kinetic and equilbirium studies for nickel and zinc were similar to that for copper biosorption (see Section 3.5.2.) except the final biomass concentration was about 2 g/L and the metal (II) nitrate solution ranged from about 1 mg/L to about 80 mg/L.

3.9.2. Biosorption of other metal cations

The batch biosorption experiments were performed with constant biomass. A series of 500 mL Nalgene polypropylene bottles were prepared with a fixed known volume (25 mL) of approximate concentrations (about 500 ppm) of standardized metal nitrate solution with pH adjusted to 5.0 by 0.1 M of nitric acid and 0.1 M sodium hydroxide. The freeze-dried biomass in dd water was homogenized by Janke-kunkel IKA-Labortechnik Ultra-turrax T25 homogenizer at a speed of 24,000 rpm for 5 min. and the pH of the biomass aliquot was also adjusted to 5.0 by 0.1 M of nitric acid and 0.1 M sodium hydroxide and fixed known volume was added to the bottles, resulting in 45 mL total solution volume, unless specified otherwise. The final biomass concentration was about 4 g/L. The mixture was then incubated at 25°C on orbital shaker operated at 200 rpm for a minimum of 72 h. Samples were taken out at different time intervals, transferred to micro-centrifuge tubes and centrifuged to remove the suspended fungal biomass. The metal concentration of the supernatant was then determined by atomic absorption spectrophotometer at the selected wavelength shown in Table 4. The biosorption experiments were also duplicated.

3.10. Mixed metal (binary system, Pb+Cu) biosorption by *Mucor rouxii*

The batch biosorption experiments were performed with constant biomass at different initial lead and copper concentrations. The maximum concentraion of lead or copper in the mixture was about 3 mM. The mixture solutions of lead and copper were mixed with the initial molar ratio as follows : 10:1, 7:1, 5:1, 3:1, 2:1, 1:1, 0.8:1, 0.6:1 and 0.3:1.

A series of 500 mL Nalgene polypropylene bottles were prepared with a fixed known volume of different concentrations of standardized metal nitrate solutions with pH adjusted to 5.0 by 0.1 M of nitric acid and 0.1 M sodium hydroxide. The freeze-dried biomass in dd water was homogenized by Janke-kunkel IKA-Labortechnik Ultra-turrax T25 homogenizer at a speed of 24,000 rpm for 5 min. and the pH of the biomass

aliquot was also adjusted to 5.0 by 0.1 M of nitric acid and 0.1 M sodium hydroxide. Fixed known volume (20 mL) of the biomass aliquot was added to the bottles, with 25 mL mixed metal solution at different concentration, resulting in 45 mL total solution volume unless specified otherwise. The final biomass concentration was about 3 g/L. The mixture was then incubated at 25°C on orbital shaker operated at 200 rpm for 24 h. The mixture was then centrifuged and the lead and copper concentration in the supernatant were then analysed by atomic absorption spectrophotometer at the selected wavelength 283.3 nm and 324.7 nm respectively.

Chapter 4. Results and Discussion

4.1. Lead and copper biosorption kinetics studies

To study the kinetics of lead and copper biosorption, the lead and copper concentrations after contact with varied amount of biomass in polypropylene bottles were followed as a function of time. The lead biosorption kinetic data for all selected species of fungi are graphically depicted in Figures 5 and 6. A dimensionless concentration term, $[metal]_t/[metal]_0$, the instantaneous metal concentration over initial metal concentration, was plotted against time. The figures show that lead biosorption may be divided into two phases: (i) a fast biosorption first phase with most of the metal ions taken up from solution bound within the first 20 min., and followed by; (ii) a much slower second phase which continued even after 24 h. The copper biosorption data for all selected species of fungi are graphically depicted in Figures 7 and 8. The copper biosorption kinetic behaviour was very similar to that of lead biosorption. These observations suggest that biosorption involves inherently very fast sorption reaction mechanisms based predominantly on chemisorption to the surfaces of the fungal biomass. Further lead or copper uptake by the fungal biomass may be controlled by the diffusion process through the cell or regulated by the intracellular metabolic processes.

Similar biosorption kinetics was observed in other studies. Volesky and Holan (1995) reported that the biosorption processes involved a fast sorption process predominantly on chemisorption last for about 5-15 min. (Kuyucak and Volesky, 1989a and 1989b) and a much slower step of additional metal deposition (Tsezos and Volesky, 1981), perhaps indicating a different secondary metal-binding mechanisms (Holan and Volesky, 1995). Tsezos and Volesky (1982a) proposed that uranium biosorption by *Rhizopus arrhizus* involved 3 steps. The fast process is the uranium coordination to the cell wall chitin amine N and adsorbed to the chitin network structure. Then a slower rate of precipitation reaction of $UO_2(OH)_2$ within the chitin microcrystalline cell wall structure occurred. Similar observations are reported by Gadd *et al.* (1988). They

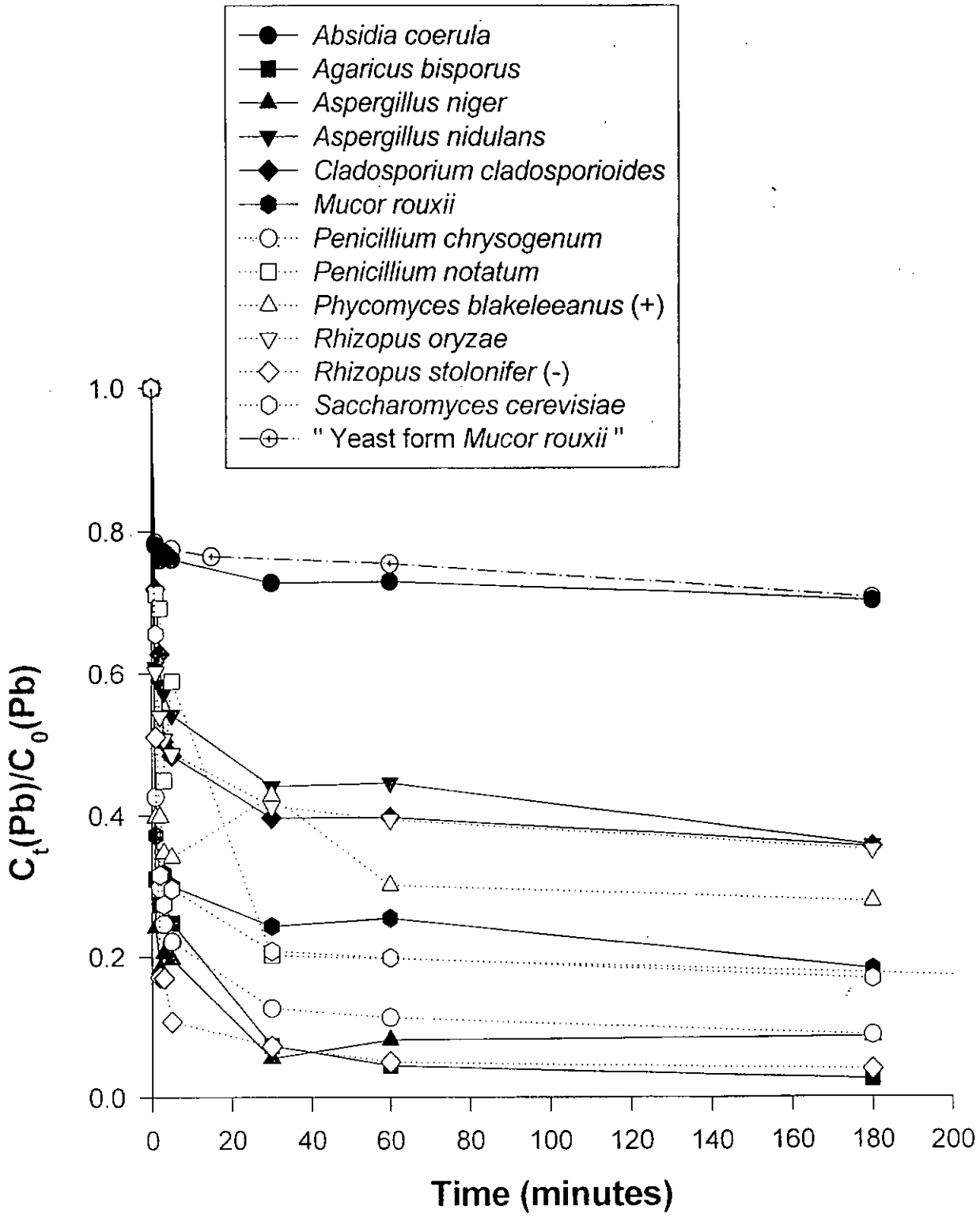

Figure 5. Kinetics of lead biosorption by selected fungal biomass (data set a)

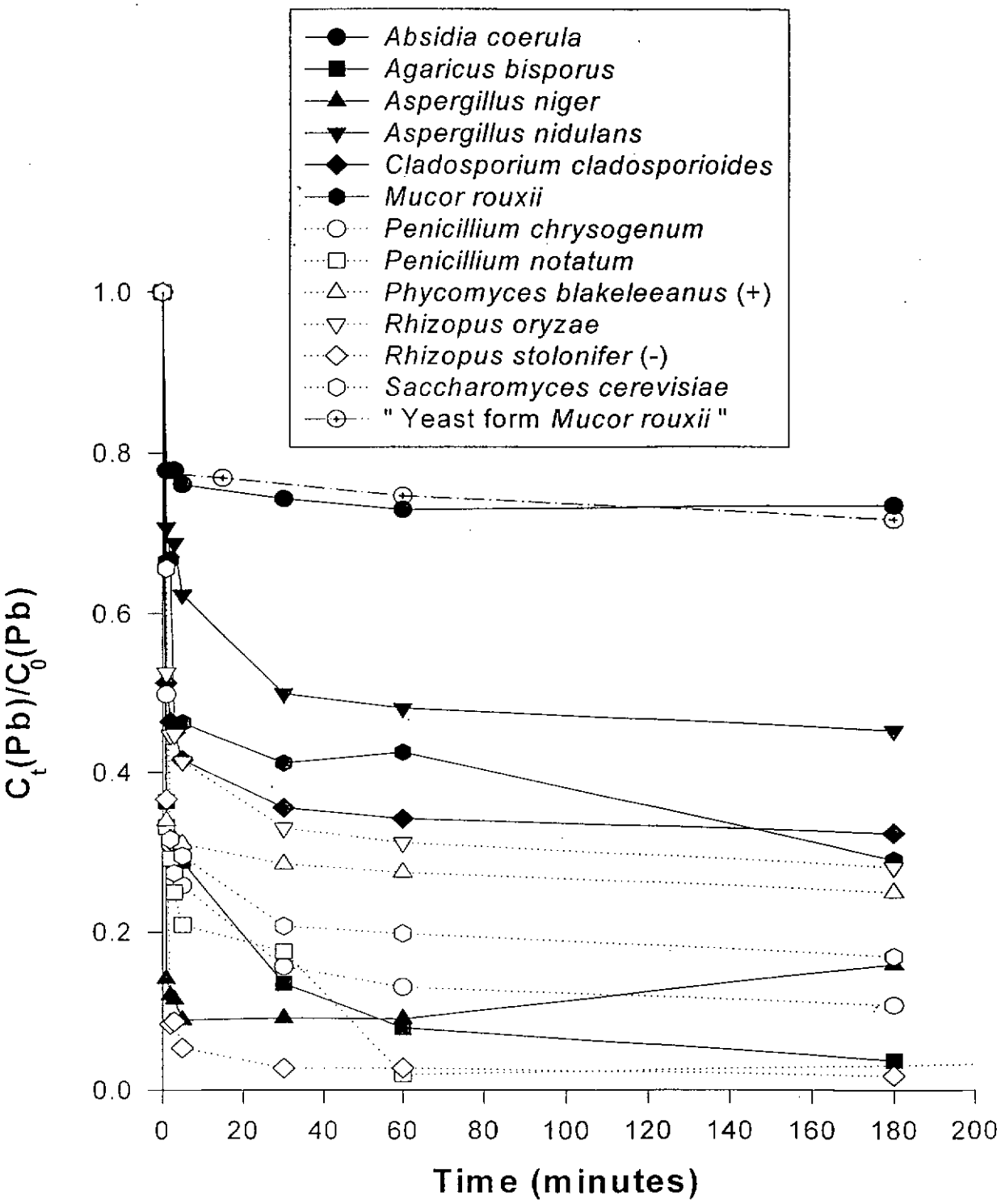

Figure 6. Kinetics of lead biosorption by selected fungal biomass (data set b)

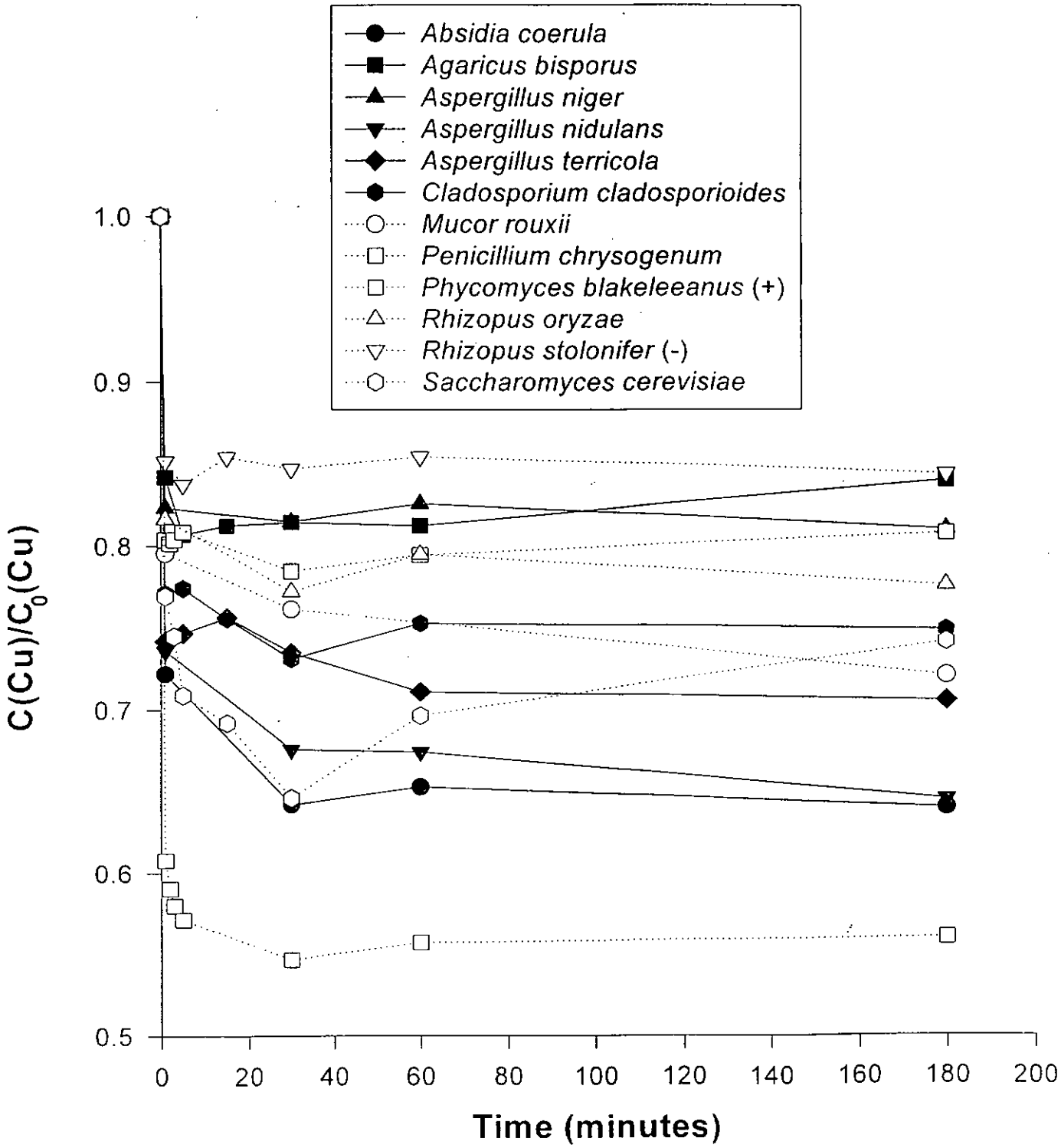

Figure 7. Kinetics of copper biosorption by selected fungal biomass (data set a)

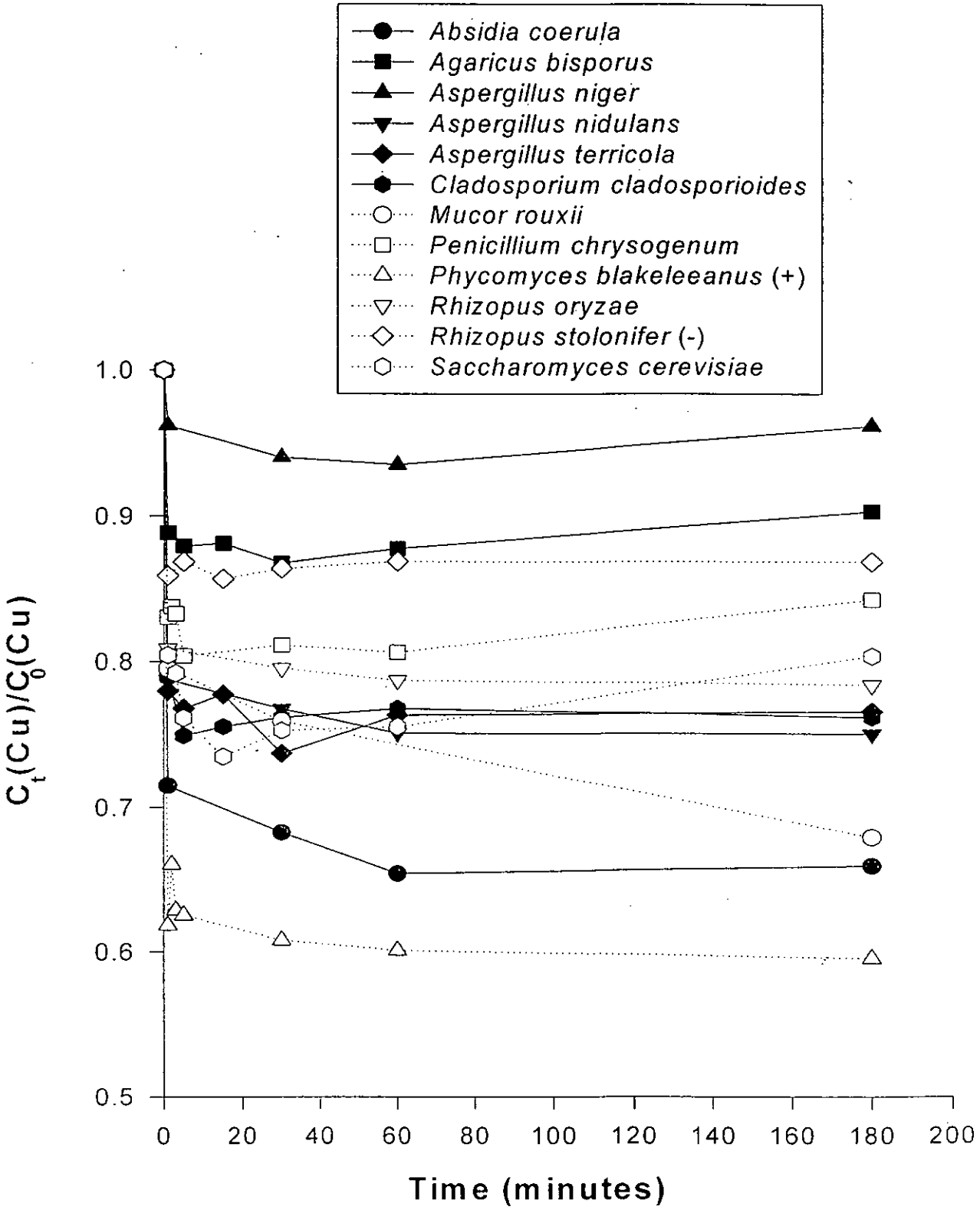

Figure 8. Kinetics of copper biosorption by selected fungal biomass (data set b)

observed that U and Sr uptake by *R. arrhizus* and *S. cerevisiae*, even in the absence of metabolism and intracellular bioaccumulation process, the complete equilibrium were not reached even after 3 hours of reaction time. Gadd (1990) suggested that the crystallization within the cell wall structure may account for the slow process.

4.2. Lead and Copper Equilibrium Studies

The biosorption capacities of different fungal species were compared and evaluated quantitatively using the biosorption isotherms derived from the equilibrium data. Figures 9 and 10 are plots of the lead biosorption capacities q (in mg lead/g dried weight biomass) against residual lead equilibrium concentration remaining in the solution, C_e (in ppm). A linear relationship was not observed for any of the species. The examined biomass types may be separated into two groups. The first group is composed of the types that the biosorption capacities q became saturated at C_e as low as 20 ppm. The species, *Absidia coerula*, *Agaricus bisporus*, *Aspergillus nidulans*, *Cladosporium cladosporioides*, *Penicillium chrysogenum*, *Penicillium notatum*, *Phycomyces blakeleeanus* (+), *Rhizopus oryzae*, *Saccharomyces cerevisiae* and 'yeast form' *Mucor rouxii* form this group. The second group exhibited much higher biosorption capacities that did not become saturated at C_e as high as 100 ppm. The species, *Aspergillus niger*, *Mucor rouxii*, and *Rhizopus stolonifer* (-) belong to this group. Among these species, *A. niger* and *M. rouxii* showed the highest biosorption capacities in excess of 500 mg/g.

Figures 11 and 12 are plots of the copper biosorption capacities q (in mg copper/g dried weight biomass) against residual copper equilibrium concentration remaining in the solution, C_e (in ppm). Among the species, *Aspergillus nidulans*, *Cladosporium cladosporioides*, *Mucor rouxii and Phycomyces blakeleeanus* (+) showed the highest biosorption capacities in excess of 10 mg/g over the concentration range studied. The copper biosorption capacities of fungal species, *Penicillium chrysogenum*, *Phycomyces blakeleeanus* (+) *and Rhizopus oryzae*, did not reached saturation over the

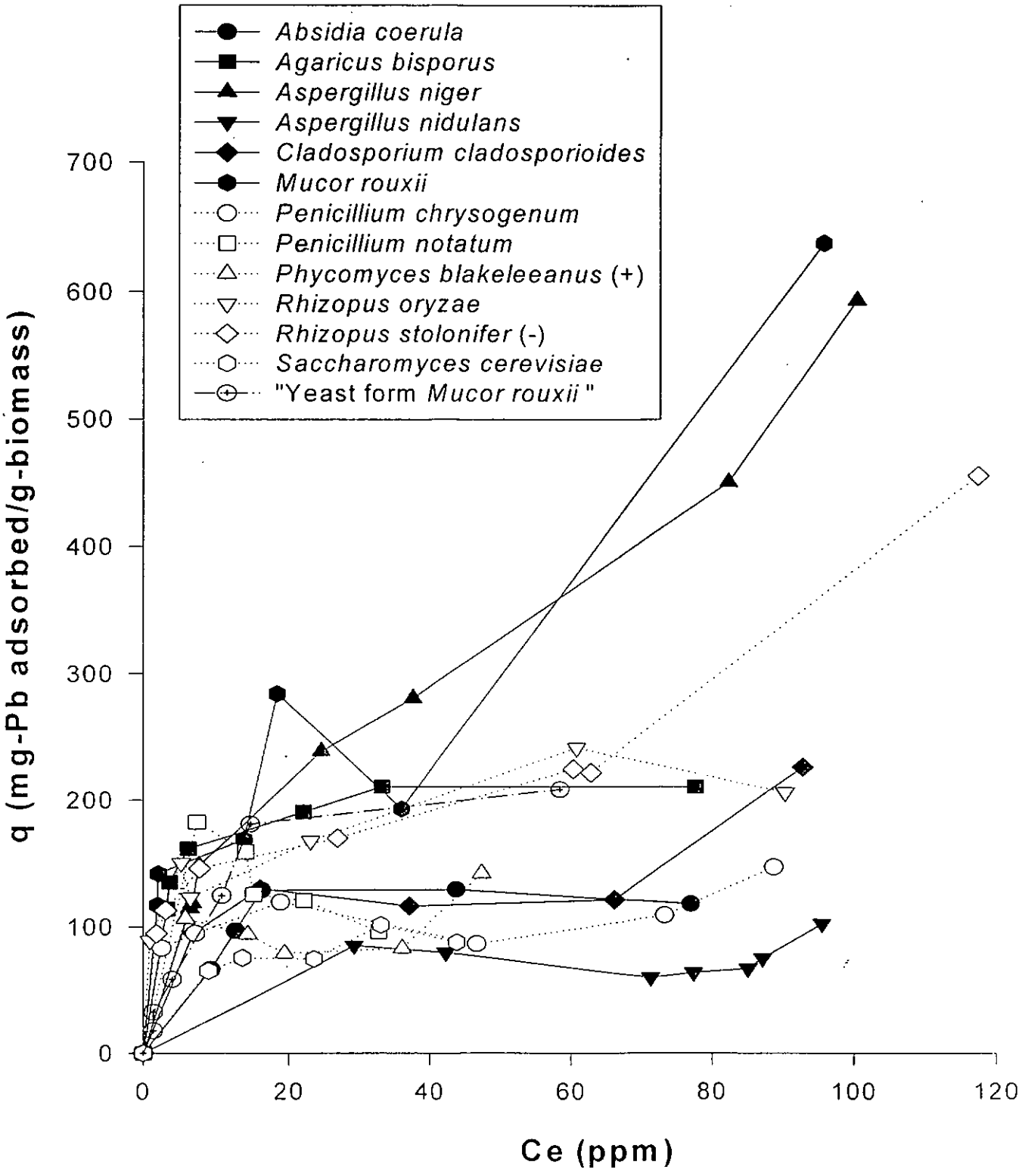

Figure 9. Equilibrium isotherms of lead biosorption for selected fungal biomass (data set a)

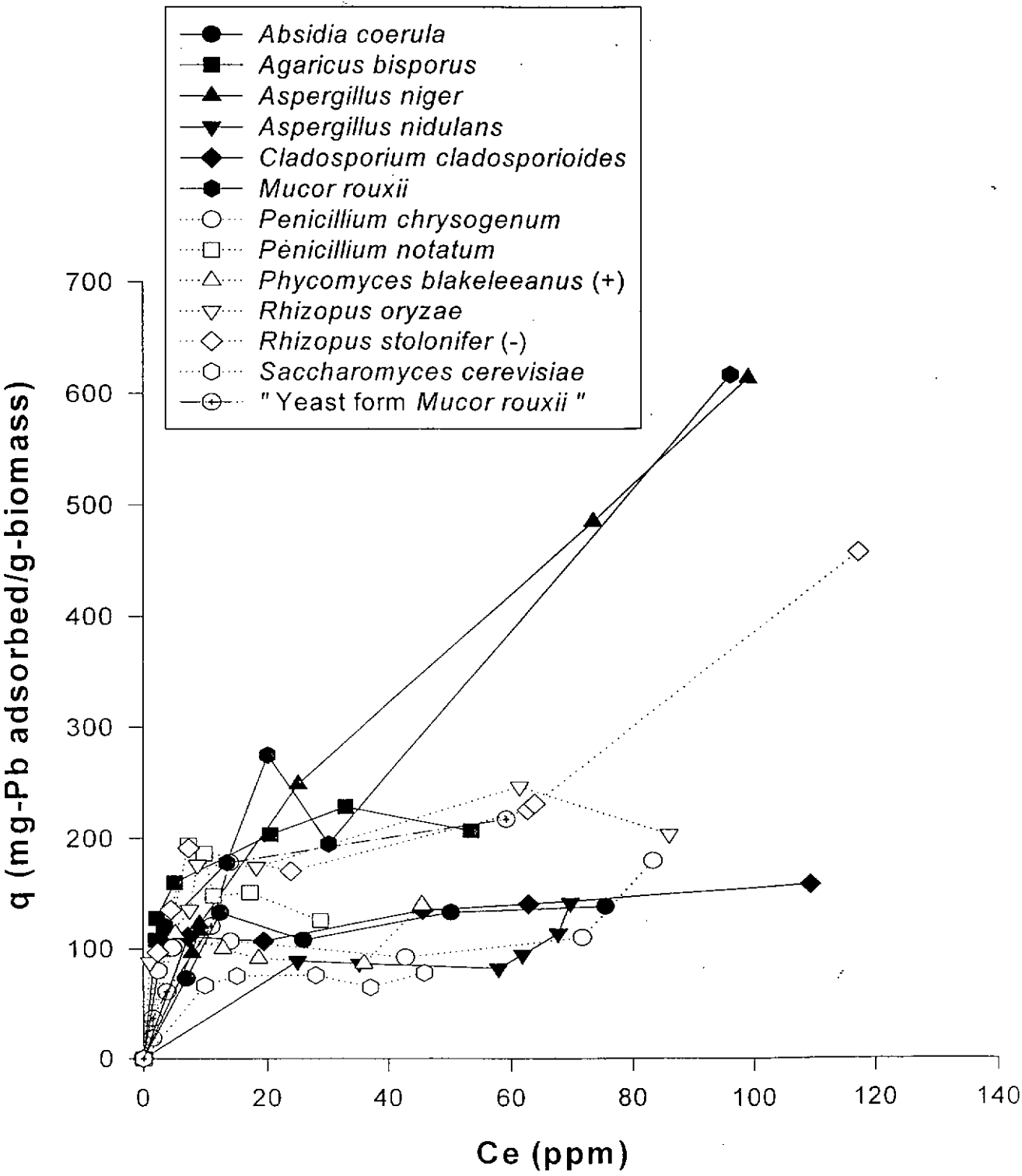

Figure 10. Equilibrium isotherms of lead biosorption for selected fungal biomass (data set b)

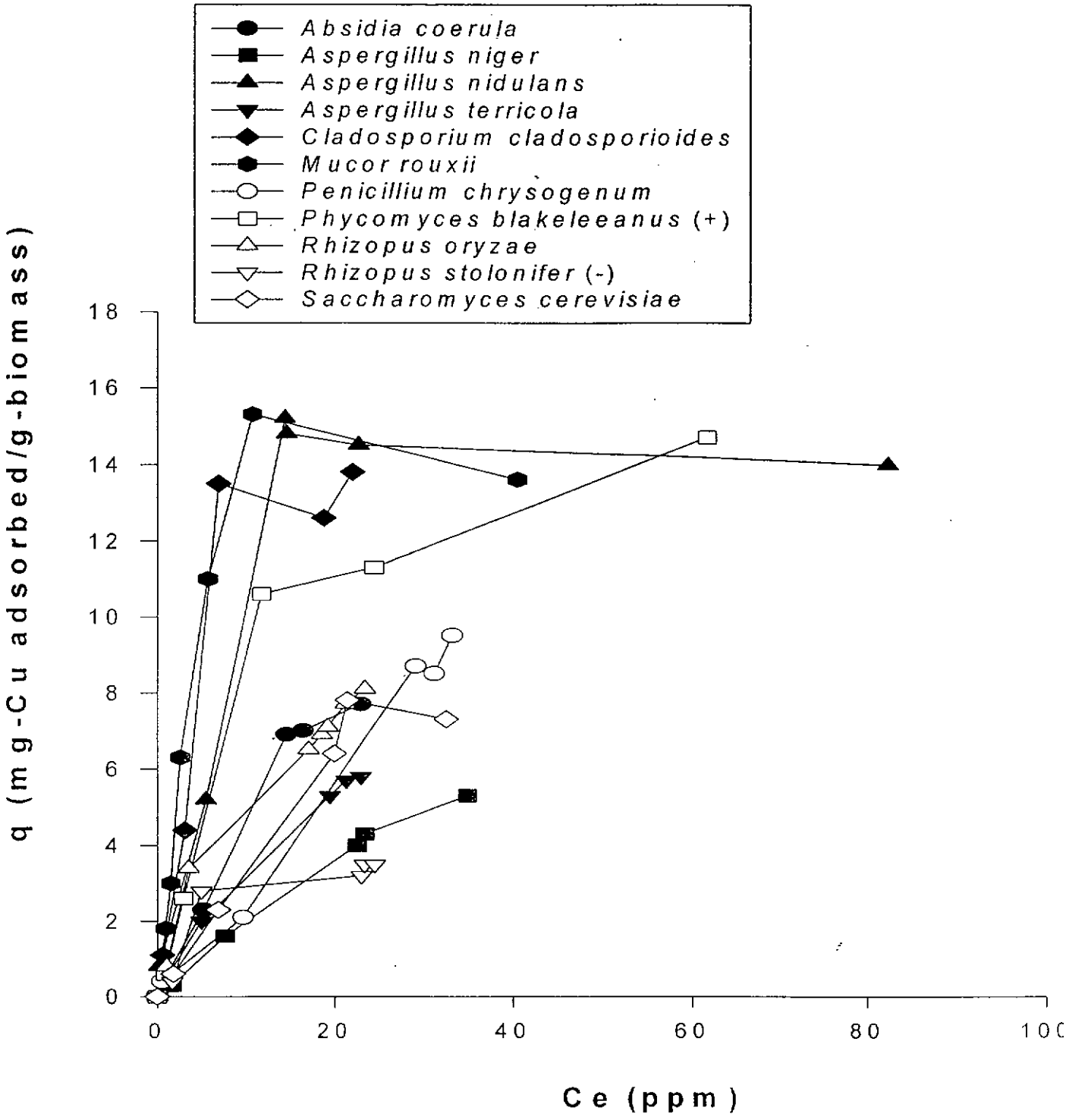

Figre 11.Equilibrium isotherms of copper biosorption for selected fungal biomass (data set a)

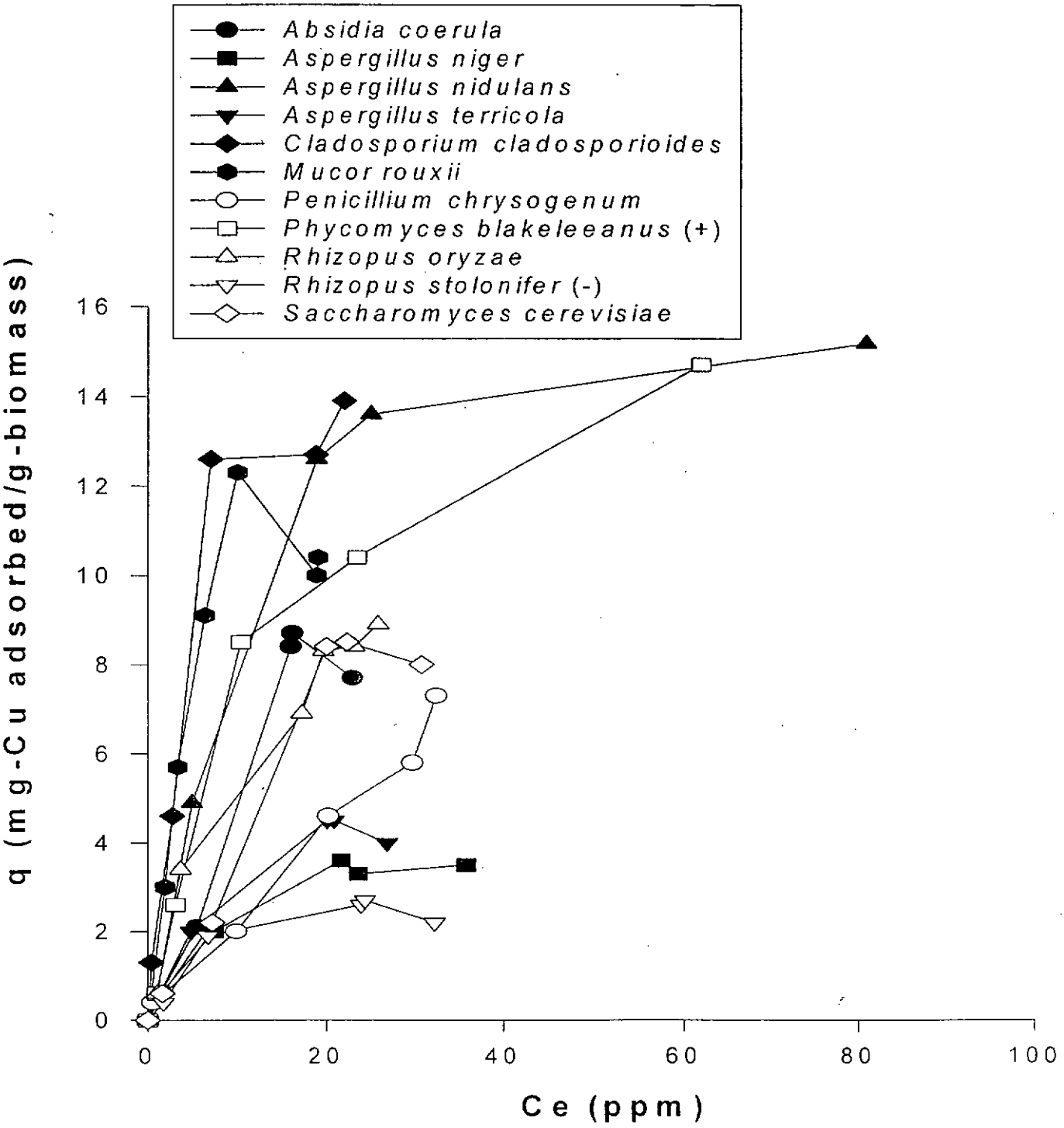

Figure 12. Equilibrium isotherms of copper biosorption for selected fungal biomass (data set b)

limited concentration range studied. Since most determined biosorption isotherms present a shape similar to that of common activated carbon adsorption isotherms, the biosorption data were fitted with most widely used adsorption isotherm models, *Langmuir* and *Freundlich* isotherms.

4.2.1. *Langmuir* isotherm model

The linearlized *Langmuir* isotherm plots for lead biosorption are shown in Figures 13-16 for all the selected fungi. The *Langmuir* parameters determined (q_{max} and K) from the linearlized plot and the regression coefficient for all the fungal species examined are shown in Table 5. These figures and table clearly show that the lead biosorption of most species conforms to the *Langmuir* model over the range of lead concentrations examined. Among all the examined species, *A. niger* showed the highest theoretical maximum biosorption capacity (q_{max}) 857.1±202.0 mg Pb/g biomass with biosorption affinity, K 0.0196±0.0077 ppm^{-1}. The species *M. rouxii* exhibited the next best theoretical maximum biosorption capacity (741.8±38.9 mg Pb/g biomass) but with higher biosorption affinity (0.0285±0.0036 ppm^{-1}) compared with *A. niger*.

The linearlized *Langmuir* isotherm plots for copper biosorption are shown in Figures 17-20 for all the selected fungi. The *Langmuir* parameters determined (q_{max} and K) from the linearlized plot and the regression coefficient for all the fungal species examined are shown in Table 6. These figures and tables clearly show that the copper biosorption of most species except *Absidia coerula*, *Penicillium chrysogenum* and *Saccharomyces cerevisiae* conforms to the *Langmuir* model over the range of concentrations examined. Among all the examined species which fit the *Langmuir* model, *Phycomyces blakeleeanus* (+) showed the highest average theoretical maximum biosorption capacity (q_{max}) 20.3±0.15 mg Cu/g biomass with biosorption affinity k, 0.0462 ± 0.0013 ppm^{-1}. The species *Cladosporium cladosporioides* exhibited the next best theoretical maximum biosorption capacity (18.05±1.36 mg Cu/g biomass)

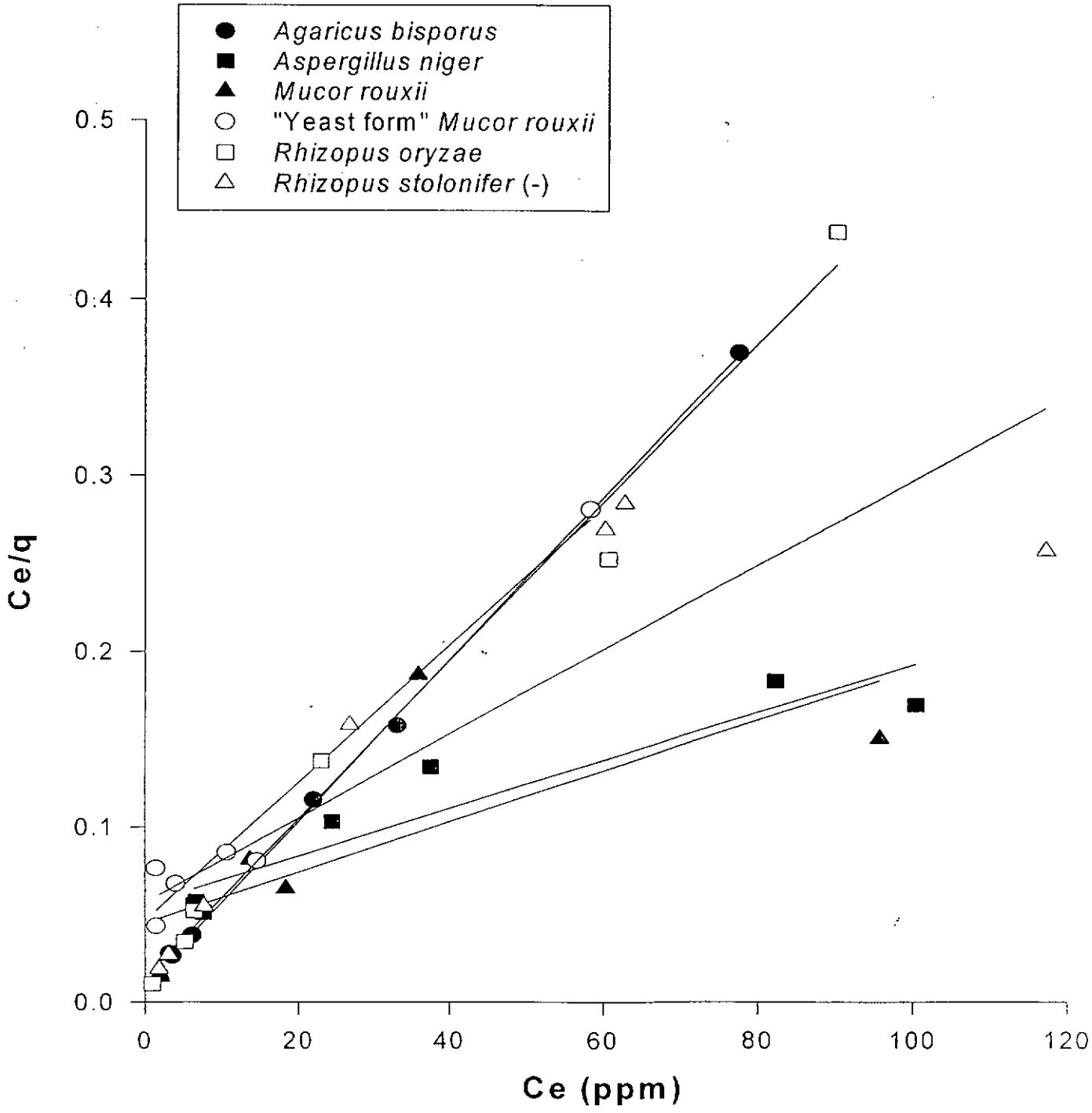

Figure 13. Linearized *Langmuir* isotherms of lead biosorption (data set a)

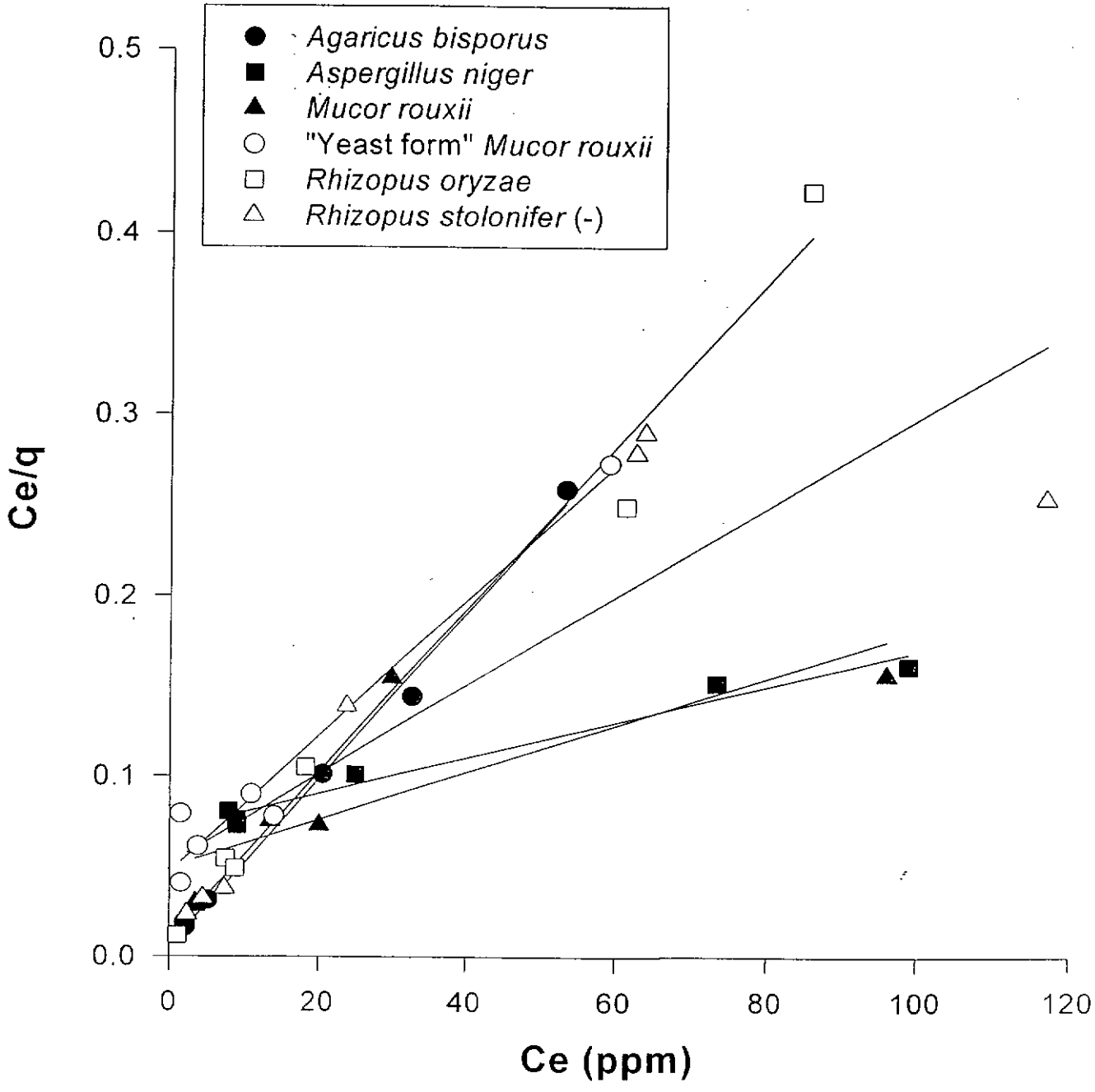

Figure 14. Linearized *Langmuir* isotherms of lead biosorption (data set b)

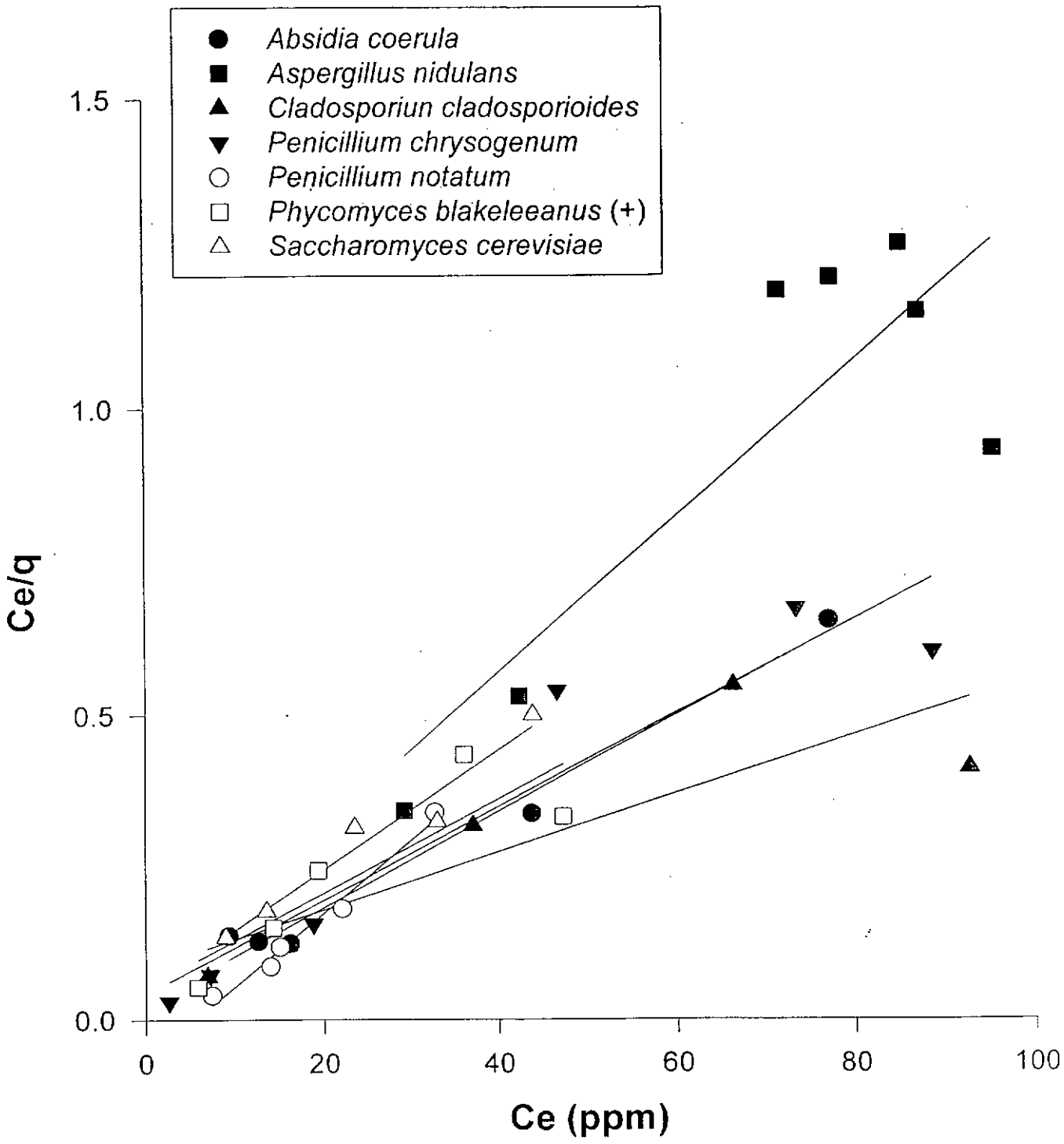

Figure 15. Linearized Langmuir isotherms of lead biosorption (data set a)

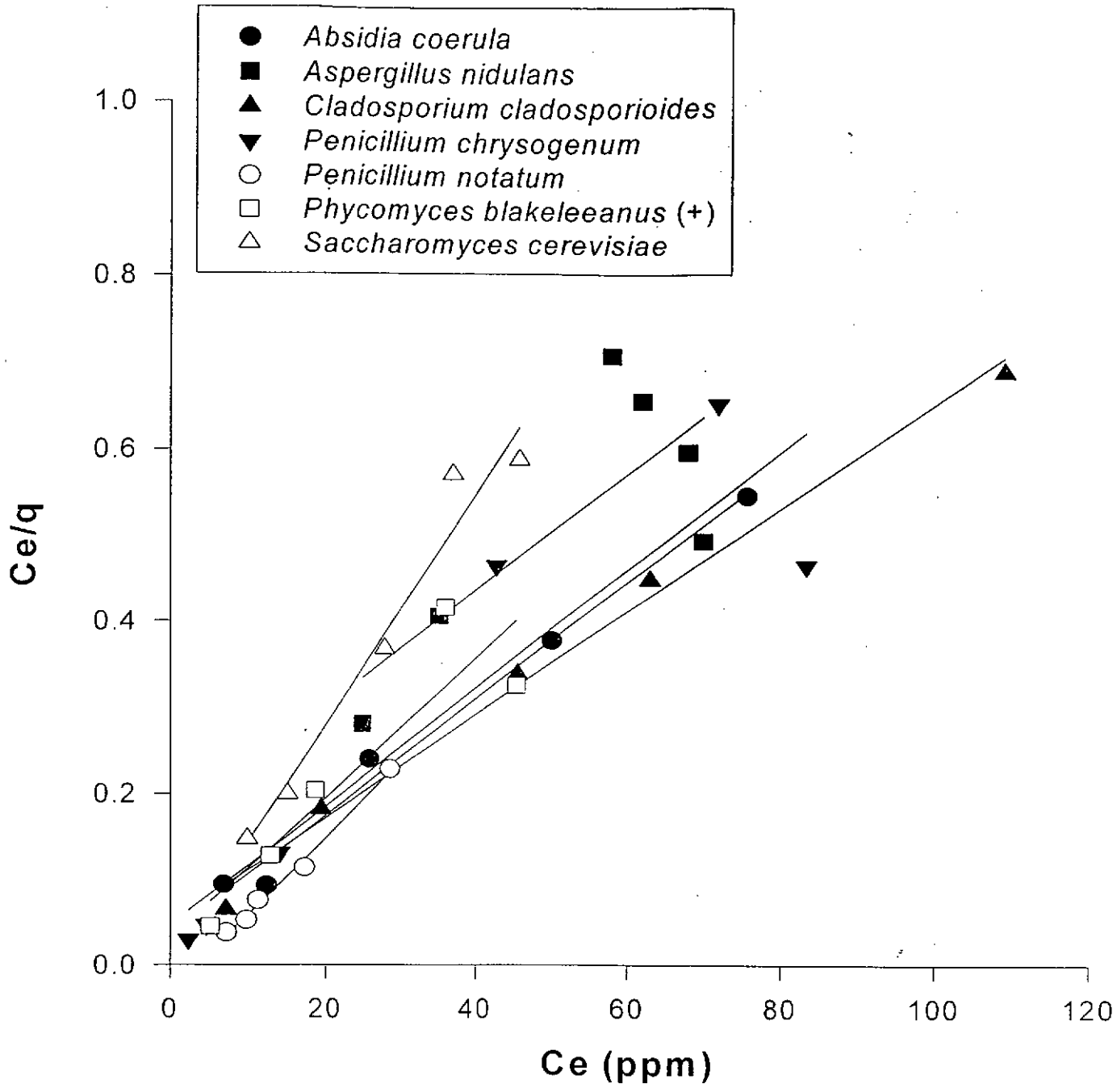

Figure 16. Linearized *Langmuir* isotherms of lead biosorption (data set b)

Table 5. *Langmuir* parameters obtained from linearized *Langmuir* isotherm plots

Experiment	Set 1			Set 2			Average value	
Fungal strains	**q_{max}(1st)**	**b(1st)**	**r^2**	**q_{max}(2nd)**	**b(2nd)**	**r^2**	**Average q_{max}**	**Average b**
Absidia coerula	126.5823	0.2904	0.9815	147.0588	0.1753	0.9891	136.8206 ± 14.4791	0.2329 ± 0.0814
Agaricus bisporus	217.3913	0.4259	0.9994	217.3913	0.6970	0.9947	217.3913 ± 0.0000	0.5615 ± 0.1917
Aspergillus niger	714.2857	0.0250	0.8897	1000.0000	0.0141	0.9738	857.1429 ± 202.0305	0.0196 ± 0.0077
Aspergillus nidulans	78.7402	0.2075	0.7258	147.0588	0.0412	0.6011	112.8995 ± 48.6085	0.1244 ± 0.1176
Cladosporium cladosporioides	208.3333	0.0558	0.7348	166.6667	0.1172	0.9918	187.5000 ± 29.4627	0.0865 ± 0.0434
Mucor rouxii	714.2857	0.0301	0.5310	769.2308	0.0259	0.6325	741.7583 ± 38.8521	0.0285 ± 0.0036
"Yeast form *Mucor rouxii* "	256.4103	0.0832	0.9662	270.2703	0.0781	0.9632	263.3403 ± 9.8005	0.0807 ± 0.0036
Penicillium chrysogenum	129.8701	0.1754	0.9035	144.9275	0.1450	0.8434	137.3988 ± 10.6472	0.1602 ± 0.0215
Penicillium notatum	83.3333	-0.1896	0.9814	112.3596	-0.2967	0.9931	97.8465 ± 20.5247	-0.2432 ± 0.0757
Phycomyces blakeleeanus(+)	129.8701	0.1395	0.7549	123.4568	0.2492	0.825	126.6635 ± 4.5349	0.1944 ± 0.0776
Rhizopus oryzae	222.2222	0.3125	0.9843	222.2222	0.3782	0.9811	222.2222 ± 0.0000	0.3454 ± 0.0465
Rhizopus stolonifer (-)	416.6667	0.0423	0.7425	400.0000	0.0479	0.7448	408.3334 ± 11.7851	0.0451 ± 0.0040
Saccharomyces cerevisiae	102.0408	0.1918	0.9521	74.6269	1.1356	0.9637	88.3339 ± 19.3846	0.6637 ± 0.6674

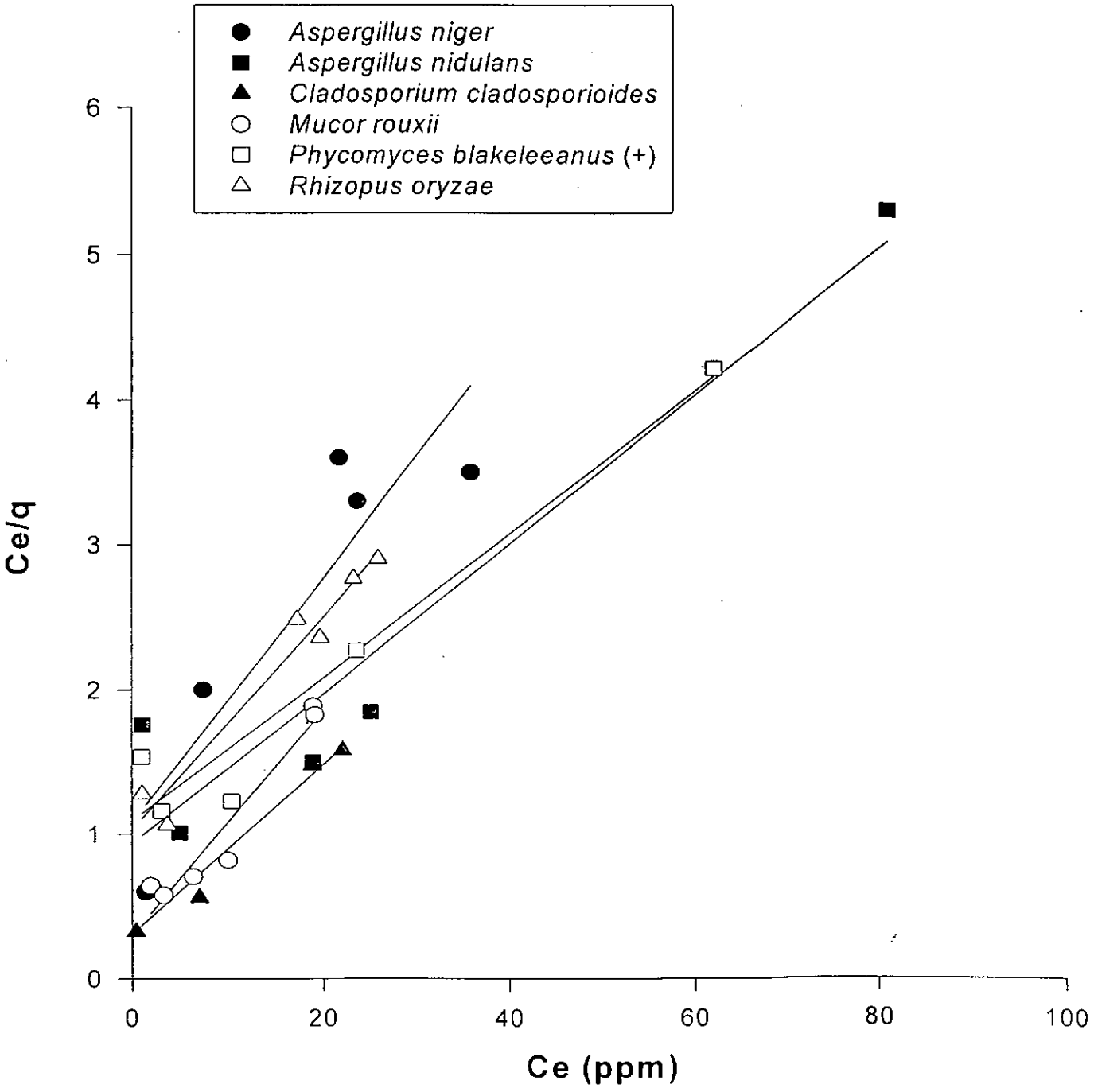

Figure 17. Linearized *Langmuir* isotherms of copper biosorption (data set a)

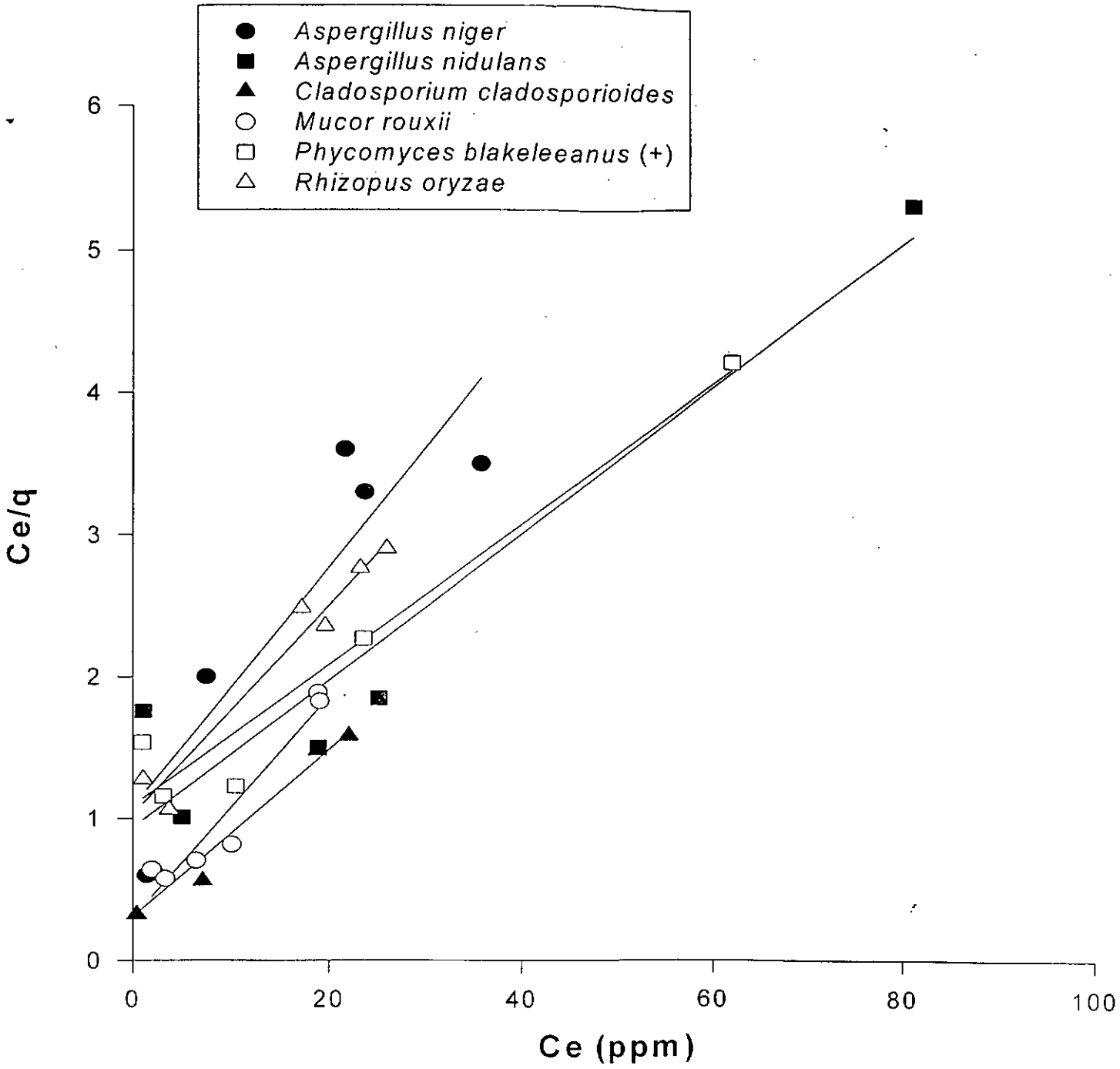

Figure 18. Linearized *Langmuir* isotherms of copper biosorption (data set b)

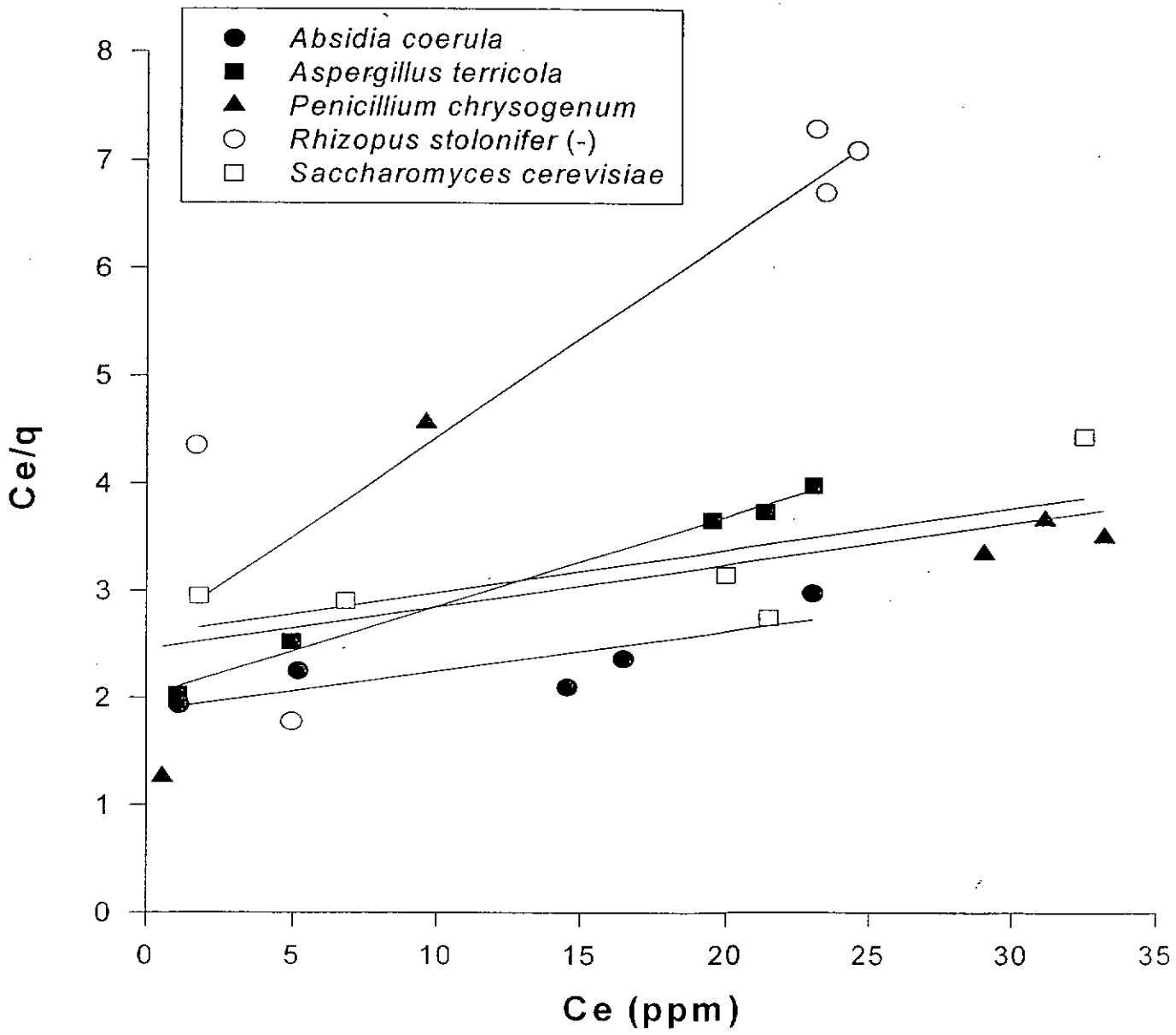

Figure 19. Linearized *Langmuir* isotherms of copper biosorption (data set a)

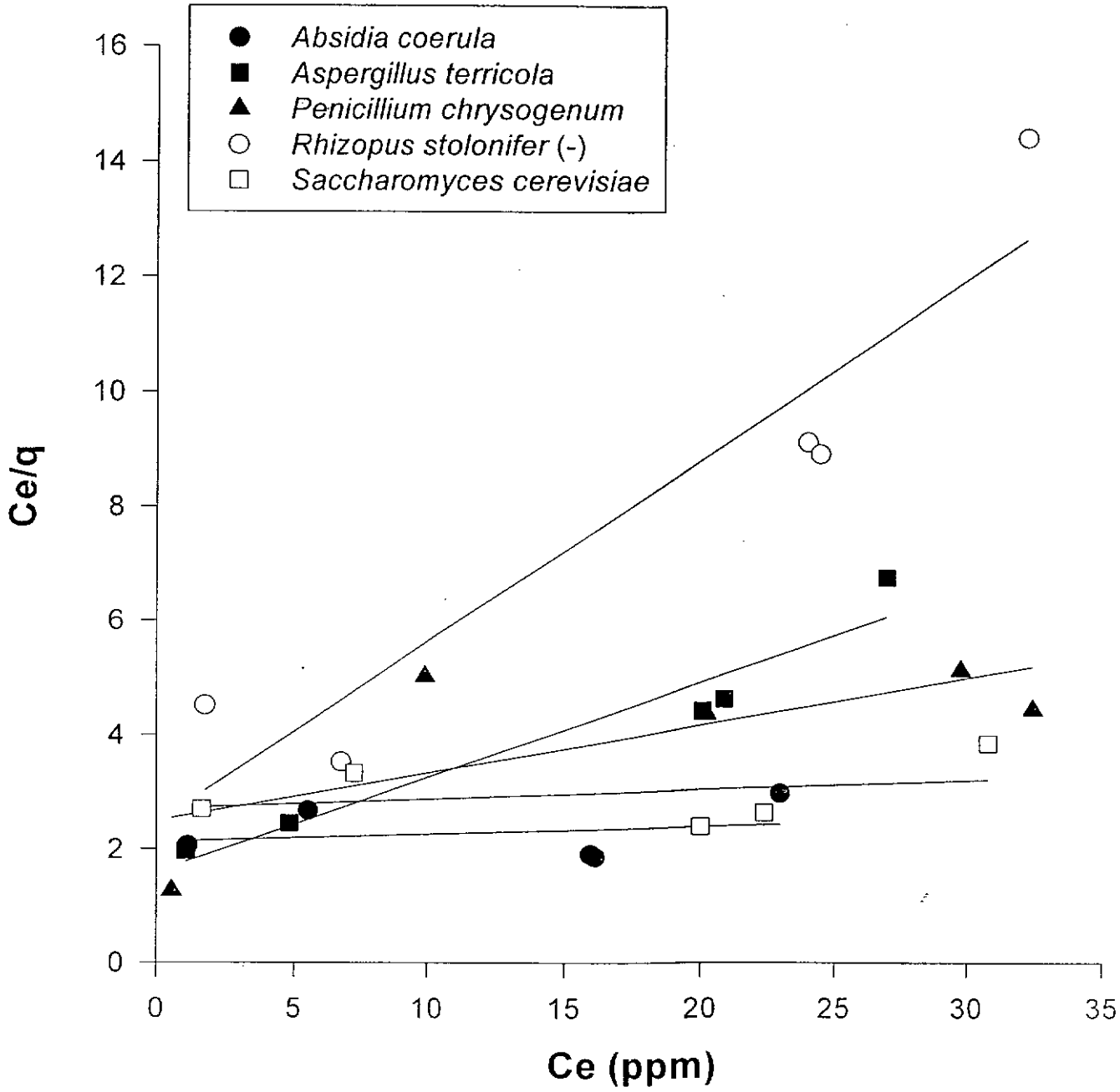

Figure 20. Linearized *Langmuir* isotherms of copper biosorption (data set b)

Table 6. *Langmuir* parameters obtained from linearized *Langmuir* isotherm plots

Experiment	Set 1			Set 2			Average value	
Fungal strains	q_{max}(1st)	b(1st)	r^2	q_{max}(2nd)	b(2nd)	r^2	Average q_{max}	Average b
Absidia coerula	27.0270	0.0197	0.6702	74.6268	0.0063	0.0561	50.8269 ± 33.6581	0.0130 ± 0.0095
Aspergillus niger	13.4590	0.0190	0.9519	4.5475	0.1128	0.9750	9.0033 ± 6.3014	0.0659 ± 0.0663
Aspergillus nidulans	14.7275	0.3409	0.9829	19.3424	0.0552	0.9175	17.0350 ± 3.2632	0.1981 ± 0.2020
Aspergillus terricola	11.9474	0.0416	0.9927	6.0423	0.1035	0.9345	8.9949 ± 4.1755	0.0726 ± 0.0438
Cladosporium cladosporioides	19.0114	0.1223	0.9048	17.0940	0.1882	0.9645	18.0527 ± 1.3558	0.1553 ± 0.0466
Mucor rouxii	15.3610	0.2426	0.9701	12.8205	0.2593	0.9303	14.0908 ± 1.7964	0.2510 ± 0.0118
Penicillium chrysogenum	25.2525	0.0162	0.2277	12.0192	0.0333	0.4931	18.6359 ± 9.3574	0.0248 ± 0.0121
Phycomyces blakeleeanus(+)	20.4082	0.0471	0.9112	20.2020	0.0453	0.9515	20.3051 ± 0.1458	0.0462 ± 0.0013
Rhizopus oryzae	11.3636	0.0869	0.9516	13.5870	0.0715	0.9553	12.4753 ± 1.5722	0.0792 ± 0.0109
Rhizopus stolonifer (-)	5.4259	0.0713	0.762	3.1686	0.1273	0.8805	4.2973 ± 1.5962	0.0993 ± 0.0396
Saccharomyces cerevisiae	25.1256	0.0154	0.5019	59.5238	0.0062	0.1101	42.3247 ± 24.3232	0.0108 ± 0.0065

but with higher biosorption affinity (0.1553 ± 0.0466 ppm $^{-1}$) compared with *Phycomyces blakeleeanus* (+). Comparison of the regression coefficients calculated for lead and copper biosorption show that the *Langmuir* isotherm model fits the lead biosorption data better than the copper biosorption data for most fungi studied.

4.2.2. *Freundlich* isotherm model

The linearlized *Freundlich* isotherm plots for lead are shown in Figures 21 and 22 for the five selected fungi which conformed to the *Freundlich* model reasonably well. The constants, k and n, for the *Freundlich* isotherms for each are given in Table 7. These five are *Agaricus.bisporus*, *Agaricus niger*, *Mucor rouxii* (both filamentous and yeast form), *Rhizopus oryzae* and *Rhizopus stolonifer* (-). The biosorption data of the other species, those with lower biosorption capacities, do not fit the isotherm (Figure 23 and 24). The *Freundlich* isotherm cannot be applied to all values of C_e since at saturation, q_{max} is a constant, independent of further increases in C_e. The five fungal species with low biosorption capacities became saturated with metal ions at C_e as low as 15 ppm, as a result, the *Freundlich* isotherm no longer applied at C_e higher than 20 ppm.

The linearlized *Freundlich* isotherm plots for copper are shown in Figures 25-28 for the all the fungi studied. The constants, k and n, for the *Freundlich* isotherms for each are given in Table 8. These figures and table clearly show that the copper biosorption of most species conforms reasonably well to the *Freundlich* model over the range of concentrations examined. Comparison of the regression coefficients calculated for lead and copper biosorption show that *Freundlich* isotherm model fits the copper biosorption data much better than lead biosorption data over the range of concentration examinated. The lowest regression coefficient obtained was 0.766 for *Rhizopus stolonifer* (-).

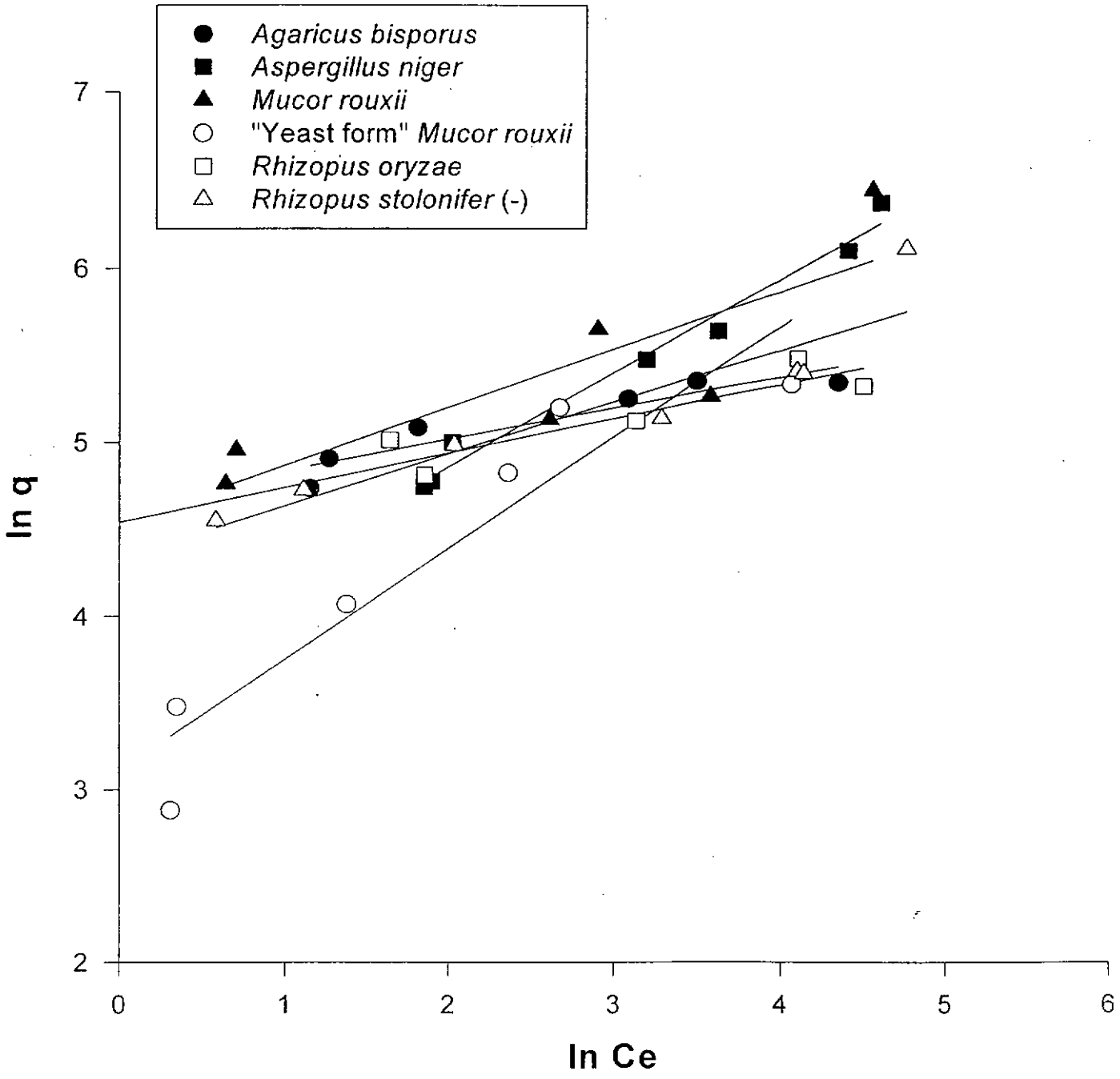

Figure 21. Linearized *Freundlich* isotherms of lead biosorption (data set a)

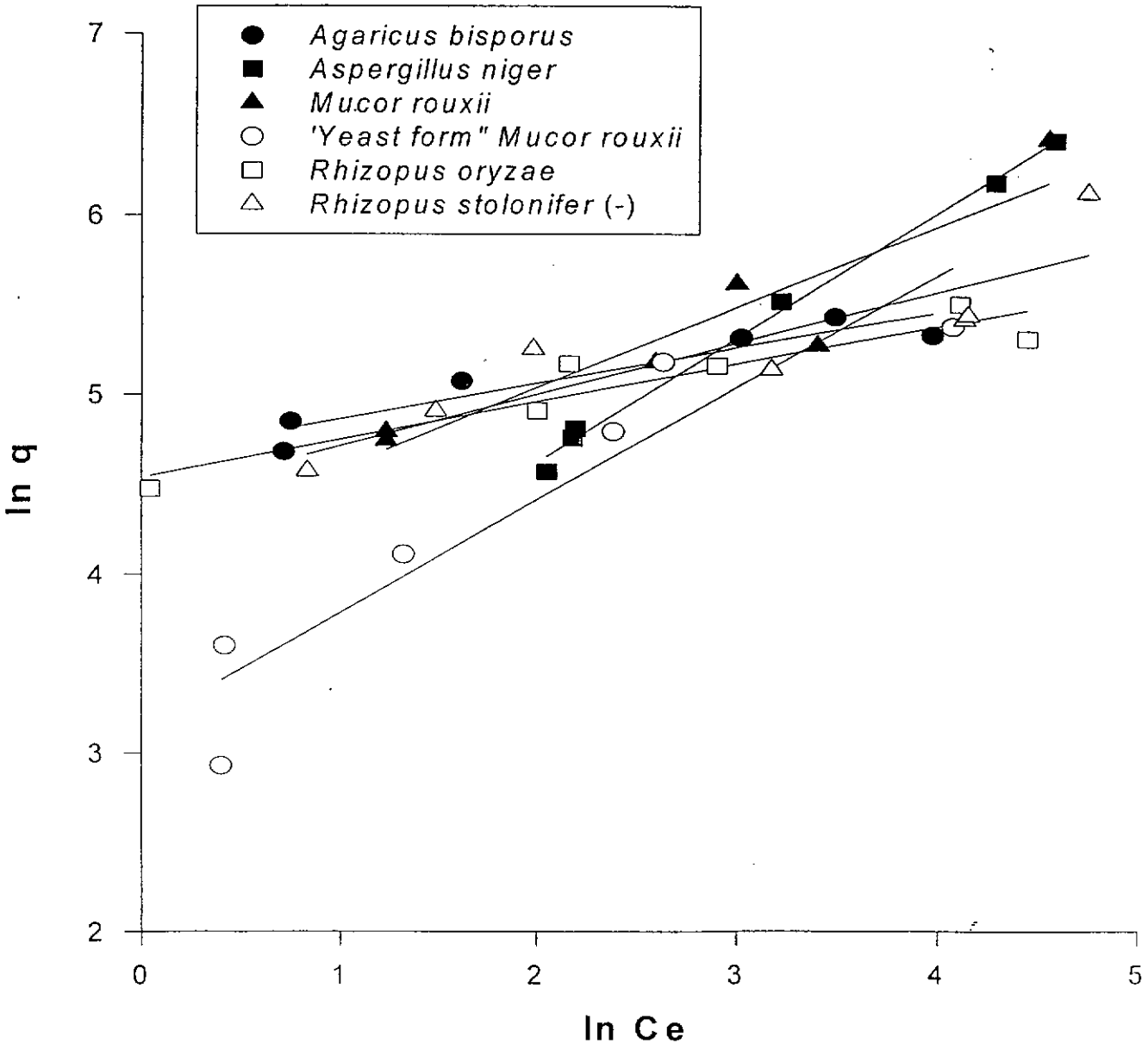

Figure 22. Linearized *Freundlich* isotherms of lead biosorption (data set b)

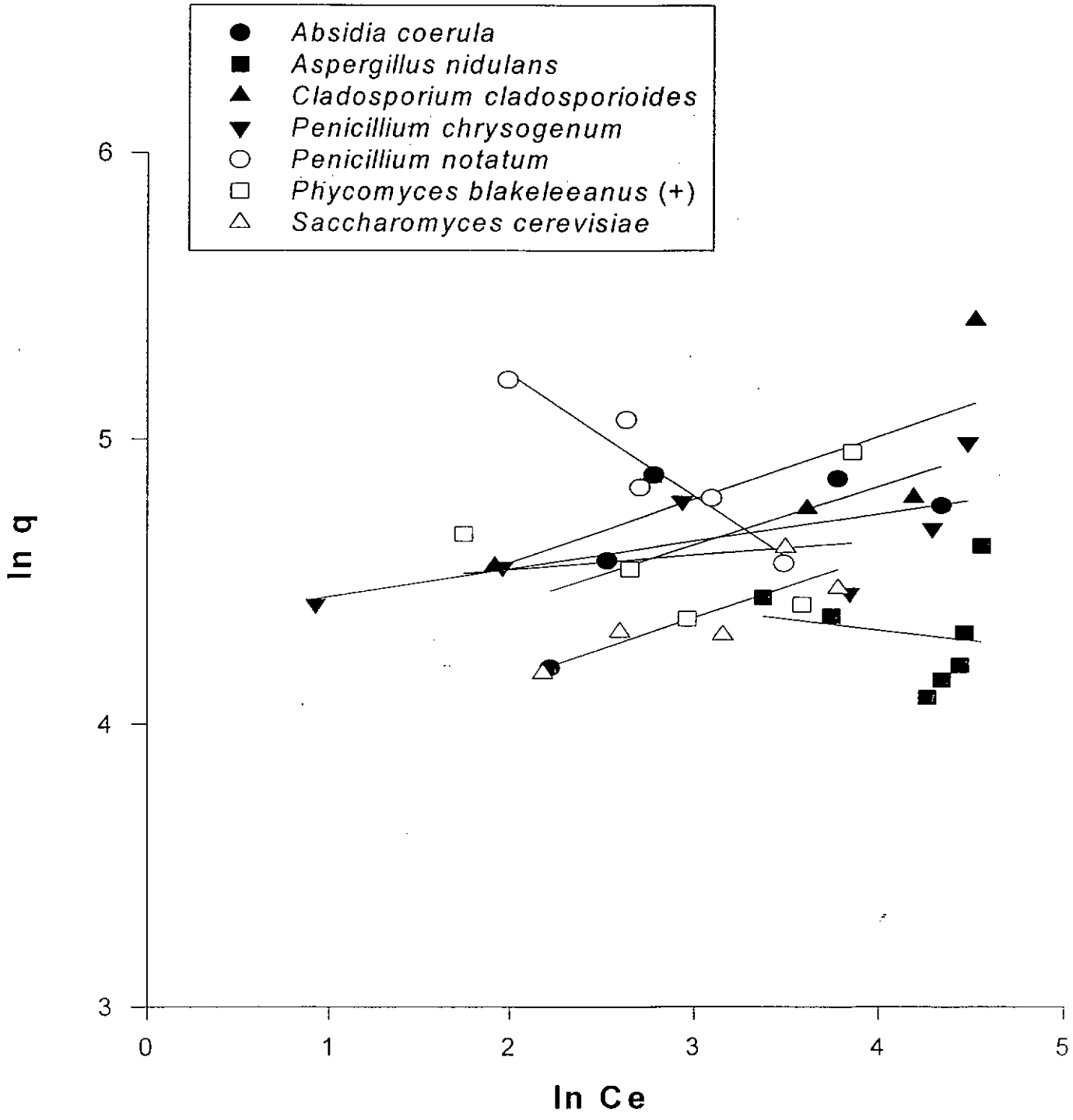

Figure 23. Linearized *Freundlich* isotherms of lead biosorption (data set a)

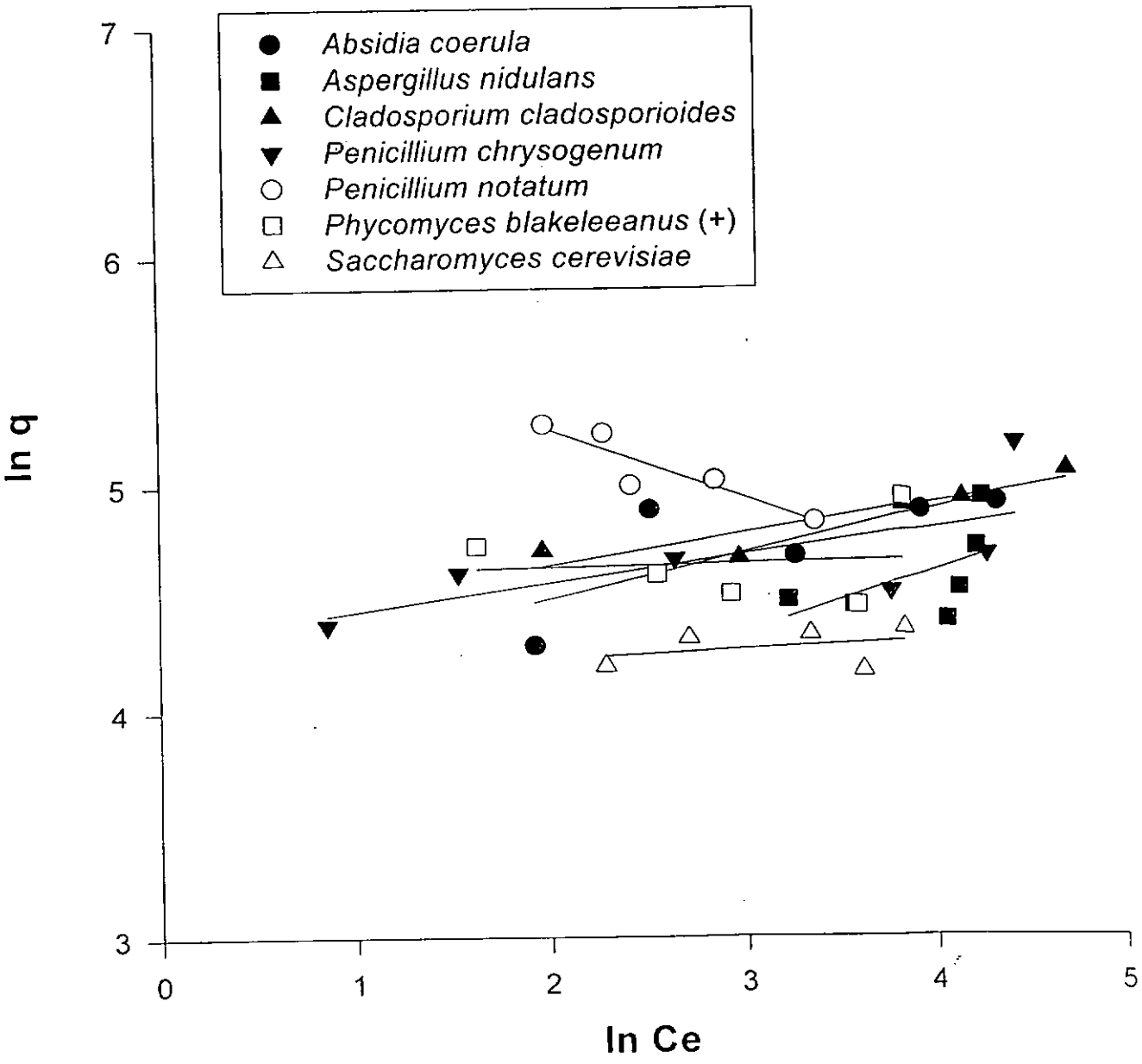

Figure 24. Linearized *Freundlich* isotherms of lead biosorption (data set b)

Table 7. *Freundlich* parameters obtained from linearized *Freundlich* isotherm plots

Experiment	Set 1			Set 2			Average value	
Fungal strains	**n(1st)**	**k(1st)**	**r^2**	**n(2nd)**	**k(2nd)**	**r^2**	**Average n**	**Average k**
Absidia coerula	4.7755	54.3748	0.4460	4.9237	59.6802	0.5593	4.8496 ± 0.1048	57.0275 ± 3.7515
Agaricus bisporus	5.5648	105.3196	0.8708	5.0454	106.1337	0.8927	5.3051 ± 0.3673	105.7267 ± 0.5757
Aspergillus niger	1.8484	43.5757	0.9817	1.4400	25.2468	0.9956	1.644 ± 0.2888	34.4113 ± 12.9605
Aspergillus nidulans	-13.6240	101.9518	0.0306	3.5778	33.3514	0.3211	-5.0231 ± 12.1635	67.6516 ± 48.5078
Cladosporium cladosporioides	4.4944	61.6332	0.5350	7.0671	78.3198	0.8310	5.7808 ± 1.8192	69.9765 ± 11.7992
Mucor rouxii	2.9967	93.0539	0.7266	2.2336	62.8845	0.8676	2.6152 ± 0.5396	77.9702 ± 21.3344
" Yeast form *Mucor rouxii* "	1.5667	22.4794	0.8918	1.6008	23.6343	0.8802	1.5838 ± 0.0241	23.0569 ± 0.8166
Penicillium chrysogenum	10.2354	77.3933	0.4067	8.0645	75.0834	0.4525	9.1500 ± 1.5351	76.2384 ± 1.6333
Penicillium notatum	-2.3419	437.4227	0.9060	-3.2744	348.6261	0.8430	-2.8082 ± 0.6594	393.0244 ± 62.7887
Phycomyces blakeleeanus(+)	19.4553	84.6394	0.0329	64.5161	99.9730	0.0049	41.9857 ± 31.8628	92.3062 ± 10.8425
Rhizopus oryzae	5.0531	93.7845	0.9040	4.7642	93.6814	0.8819	4.9087 ± 0.2043	93.7330 ± 0.0729
Rhizopus stolonifer (-)	3.3535	76.4319	0.8634	3.5002	83.7051	0.7884	3.4269 ± 0.1037	80.0685 ± 5.1429
Saccharomyces cerevisiae	4.5662	41.0381	0.7029	26.0417	63.7520	0.0851	15.3040 ± 15.1855	52.3951 ± 16.0612

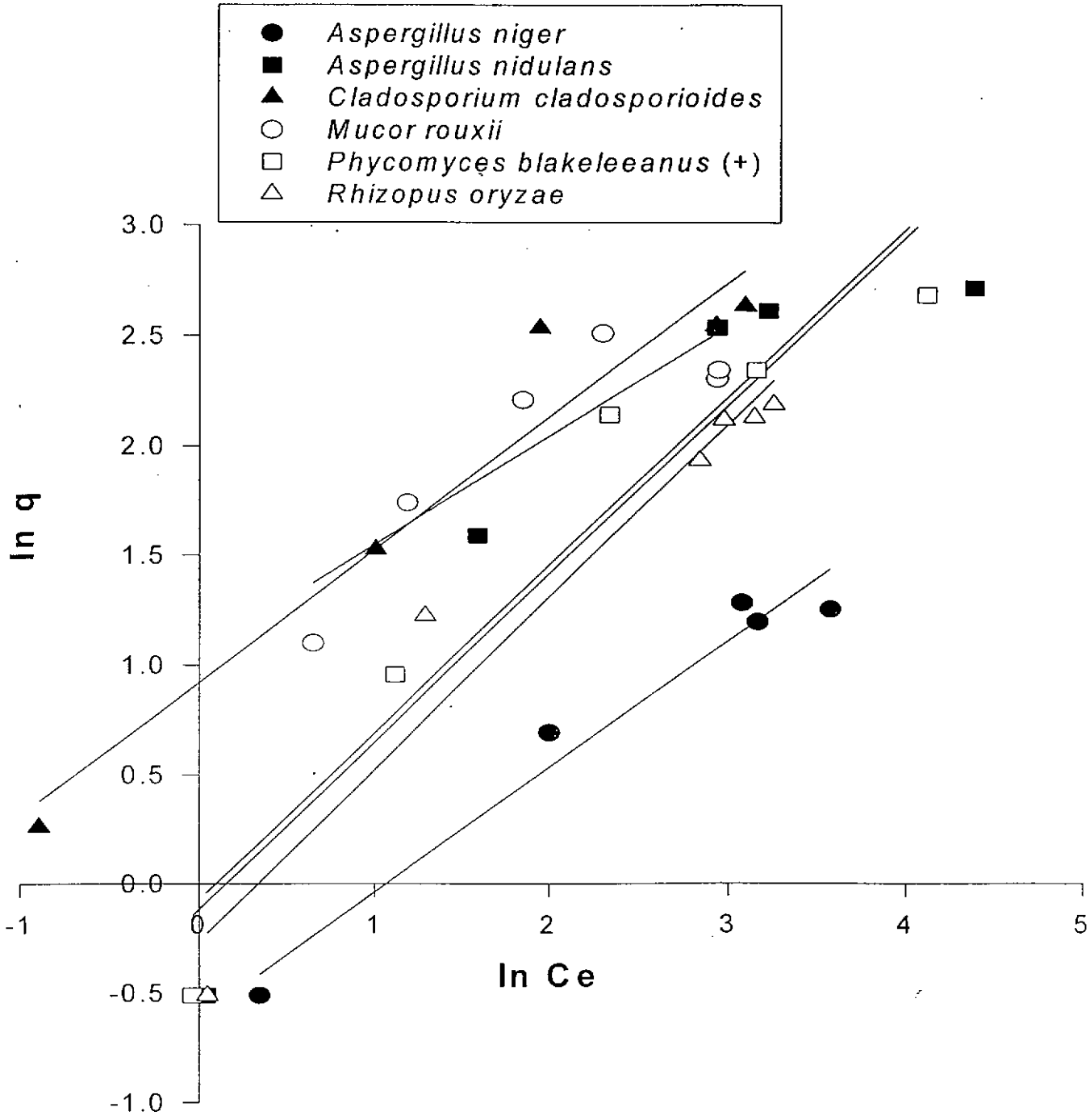

Figure 25. Linearized *Freundlich* isotherms of copper biosorption (data set a)

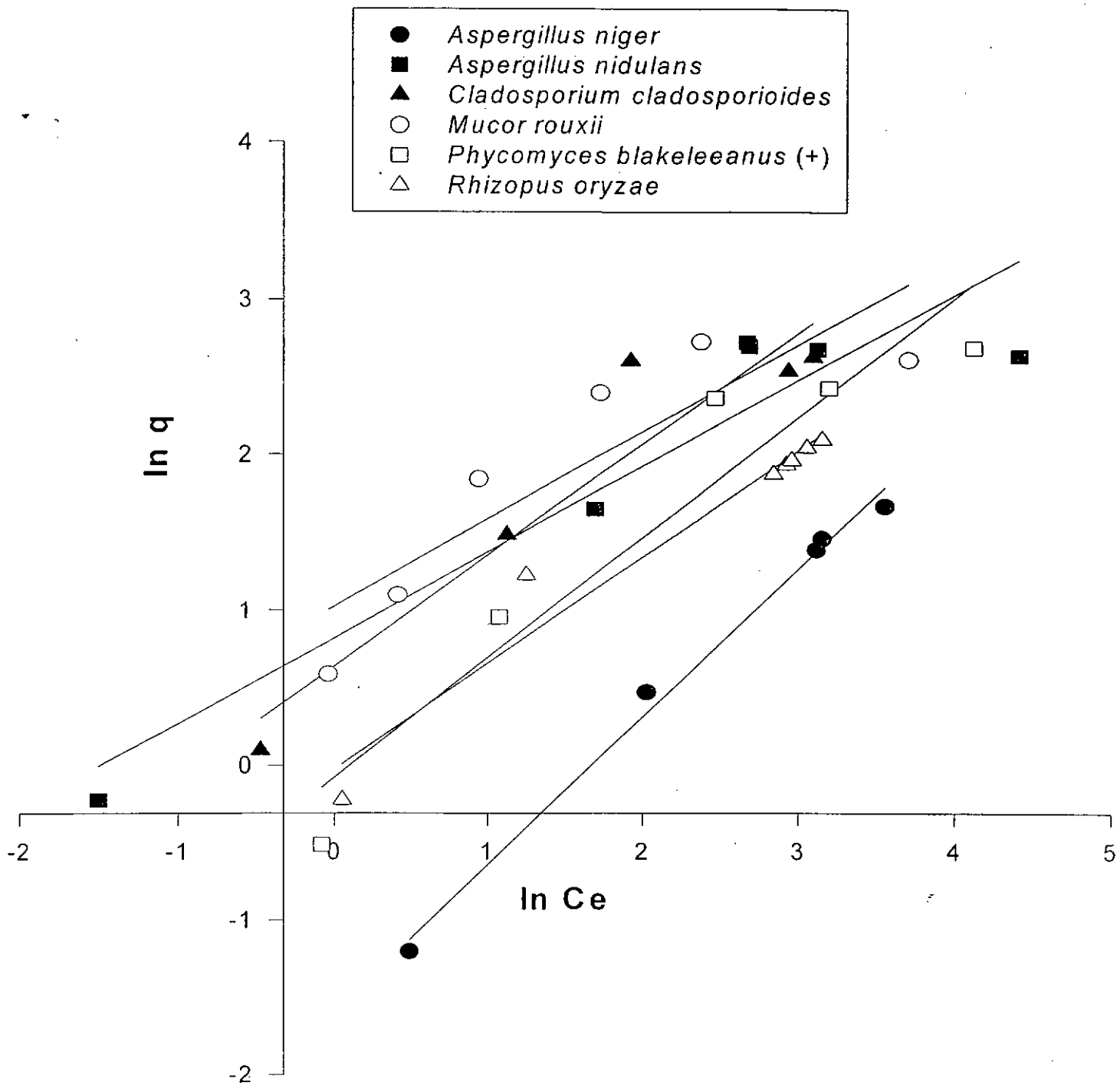

Figure 26. Linearized *Freundlich* isotherms of copper biosorption (data set b)

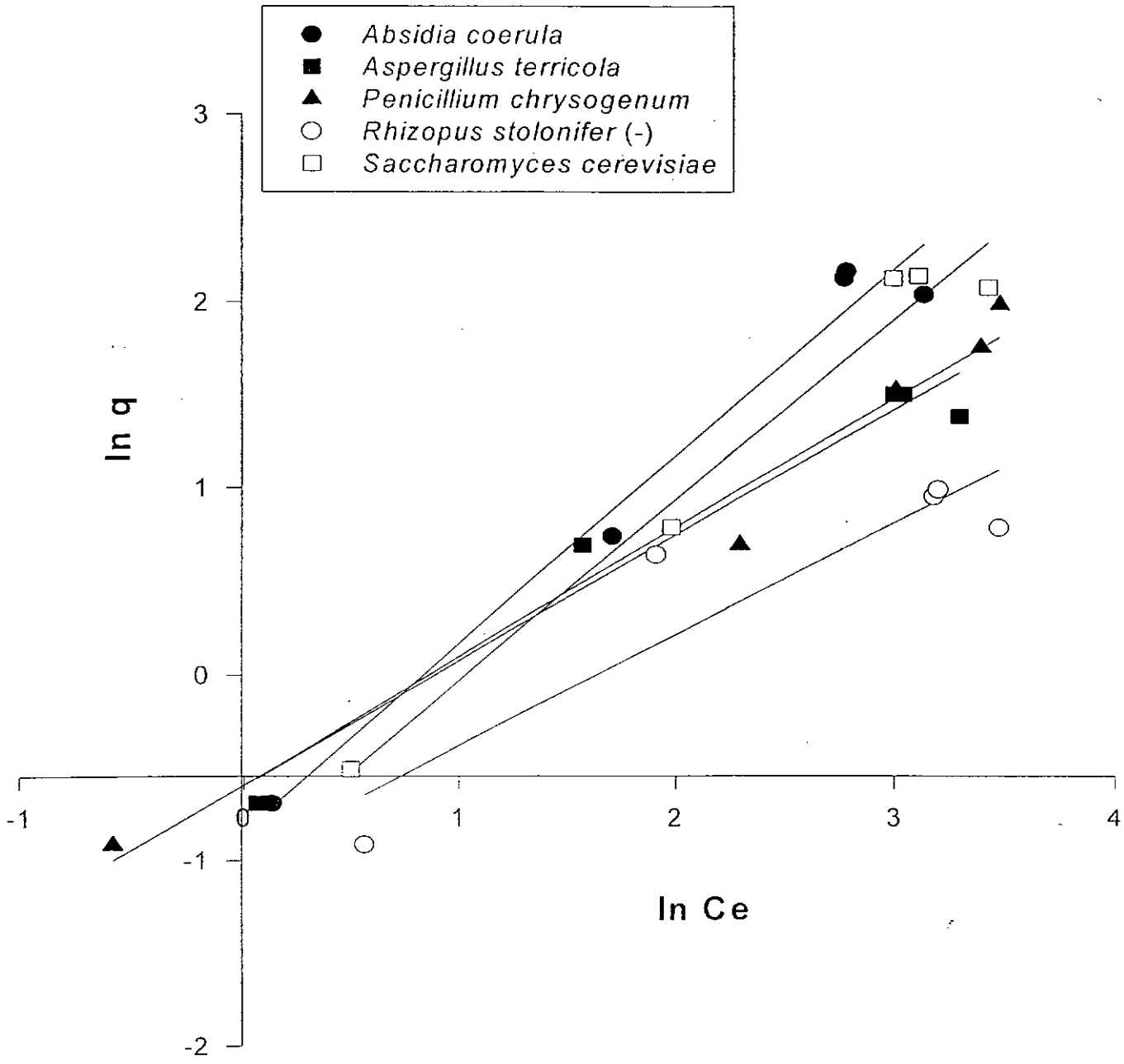

Figure 27. Linearized *Freundlich* isotherms of copper biosorption (data set a)

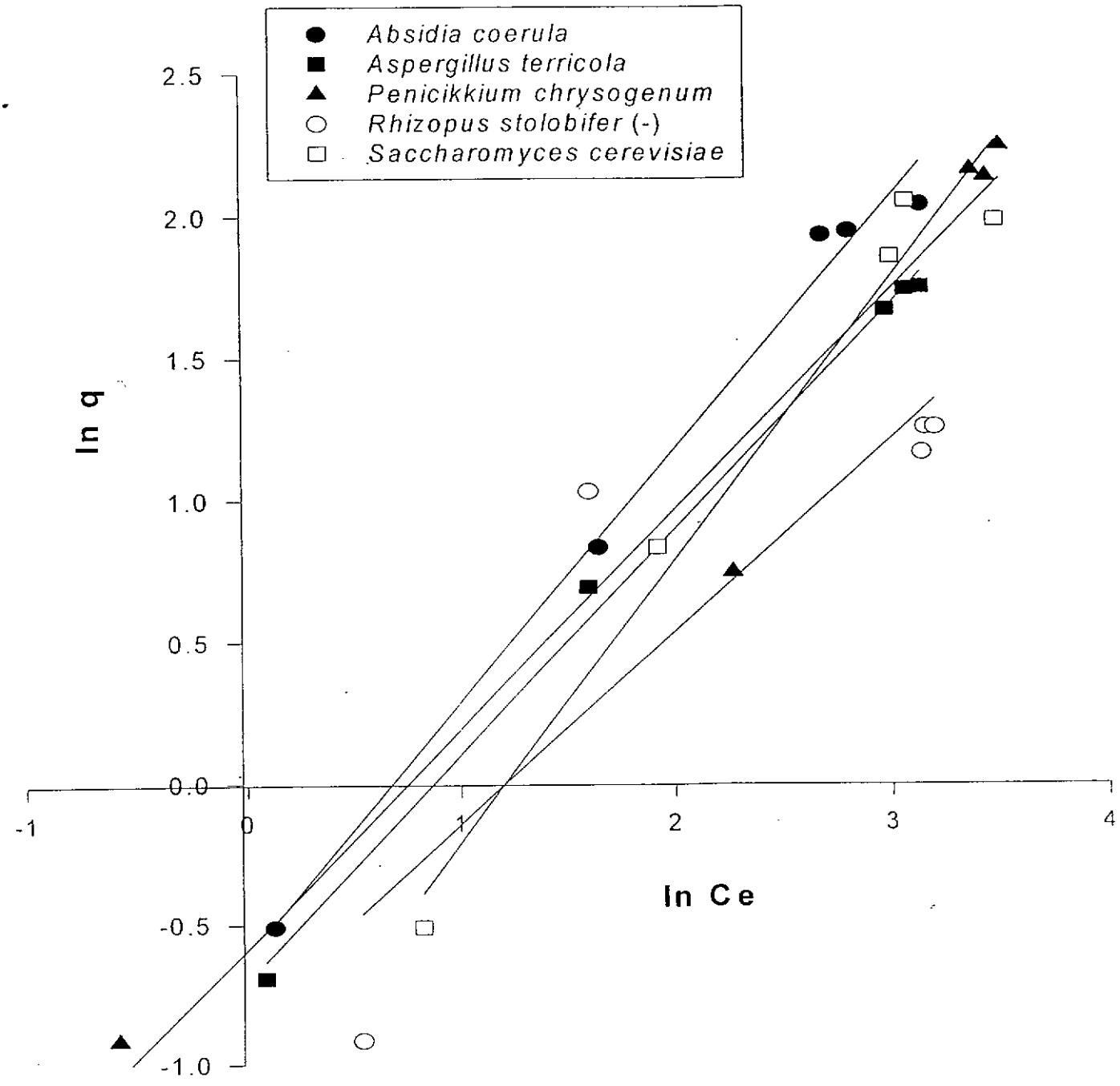

Figure 28. Linearized Freundlich isotherms of copper biosorption (data set b)

Table 8. *Freundlich* parameters obtained from linearized *Freundlich* isotherm plots

Experiment	Set 1			Set 2			Average value	
Fungal strains	n(1st)	k(1st)	r^2	n(2nd)	k(2nd)	r^2	Average n	Average k
Absidia coerula	1.1207	0.5468	0.9901	0.9952	0.4328	0.9731	1.0580 ± 0.0887	0.4898 ± 0.0806
Aspergillus niger	1.0499	0.2030	0.9927	1.7464	0.5427	0.9633	1.3982 ± 0.4925	0.3729 ± 0.2402
Aspergillus nidulans	1.8106	2.2735	0.8852	1.3084	0.9279	0.8771	1.5595 ± 0.3551	1.6007 ± 0.9515
Aspergillus terricola	1.2538	0.4988	0.9958	1.4848	0.5498	0.9616	1.3693 ± 0.1633	0.5243 ± 0.0361
Cladosporium cladosporioides	1.4008	1.8944	0.9009	1.6521	2.5080	0.9398	1.5265 ± 0.1777	2.2012 ± 0.4339
Mucor rouxii	1.7870	2.7902	0.7845	2.0206	2.8680	0.7739	1.9965 ± 0.2963	2.8291 ± 0.0550
Penicillium chrysogenum	1.2885	0.5576	0.9689	1.4449	0.5519	0.9770	1.3667 ± 0.1106	0.5548 ± 0.0040
Phycomyces blakeleeanus(+)	1.2972	0.9262	0.9123	1.3051	0.8889	0.9240	1.3012 ± 0.0056	0.9076 ± 0.0264
Rhizopus oryzae	1.4646	0.9740	0.9489	1.2719	0.7673	0.9416	1.3683 ± 0.1363	0.8707 ± 0.1462
Rhizopus stolonifer (-)	1.4717	0.4391	0.7661	1.6708	0.3748	0.8426	1.5713 ± 0.1408	0.4070 ± 0.0455
Saccharomyces cerevisiae	1.0803	0.3734	0.9764	1.0312	0.3670	0.9742	1.0558 ± 0.0347	0.3702 ± 0.0045

4.2.3. Comparison of *Langmuir* and *Freundlich* isotherm models

For lead biosorption, the comparison of the regression coefficients determined for the two biosorption models (Tables 5 and 7) show that both fit reasonably well the biosorption for the five fungal species with higher biosorption capacities; the fit of *Langmuir* isotherm usually results in higher regression coefficients, hence indicating slightly better suitability of this model. Moreover, The *Langmuir* model can be applied over a wider range of metal equilibrium concentration compared with *Freundlich* model. For the concentration range examined, from 0 to 100 ppm, *Langmuir* model fits reasonably well the biosorption data of all the fungal strains while the *Freundlich* model can only fit five only.

For copper biosorption, the comparison of the regression coefficients calculated for the two biosorption models (Tables 6 and 8) show that *Freundlich* model generally fit reasonably well the biosorption data for all the fungal species and *Langmuir* model can fit all but three species over the concentration range studied.

4.3. Effects of pH on lead and copper biosorption

Among all the species selected for lead and copper biosorption experiments, *Mucor rouxii* exhibited a very high lead biosorption capacity for lead and moderate copper biosorption capacity. Since the strain can be applied to develop potentially cost-effective biosorbent for removing and recovering lead and copper from effluents, it is selected for further studies. As reported by many researchers, pH is an important factor affecting biosorption. Experiments, therefore, were carried out in duplicate (set a and set b) for investigating the effect of pH.

Figures 29 and 30 are plots of mean percentage of metal removal against initial pH of the metal nitrate solutions. In Figure 29, the lead biosorption capacity shows a general increaing trends with increasing pH. The maximum lead biosorption occurred at pH 6.0 with about 74 % lead removed. However, the control experimental data demonstrated that lead started to precipitate at pH higher than 6.0.

Figure 30 shows that the copper biosorption capacity increased with pH increase until 5.0 (before occurrence of precipitation) and the maximum percentage of copper removed was about 54 %. The control experimental data demonstrated that copper started to precipitate at pH 7.0.

The biosorption capacity increased with the solution pH until an optimum pH was reached. Sag and Kutsal (1995) proposed that the nature of chemical interactions between metals and microbial cells and the isoelectric point of particular cell types may explain the effect of pH on metal biosorption. At pH values above the isoelectric point of the cell, the overall surface charge is negative. The ionic state of cell wall ligands such as carboxyl, phosphate and amino groups would enhance the uptake of heavy metal cations. On the other hand, as the pH is lowered, the overall surface charge will become positive and limited the approach of the positively charged metal cations. Besides, protons may compete with metal ions for the ligands. Therefore, the interactions between the metal ions and microbial cells decreased.

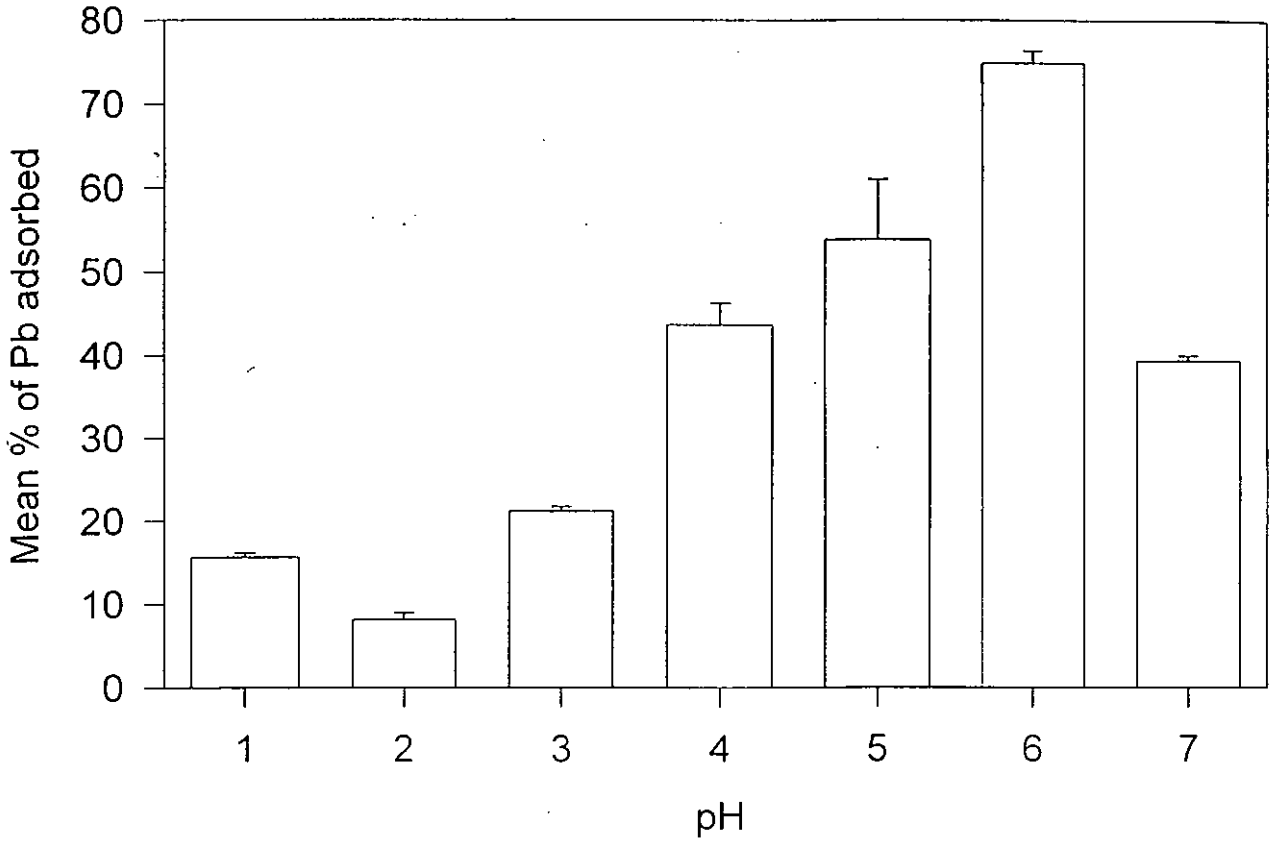

Figure 29. Effect of initial pH on lead biosorption by filamentous *Mucor rouxii*

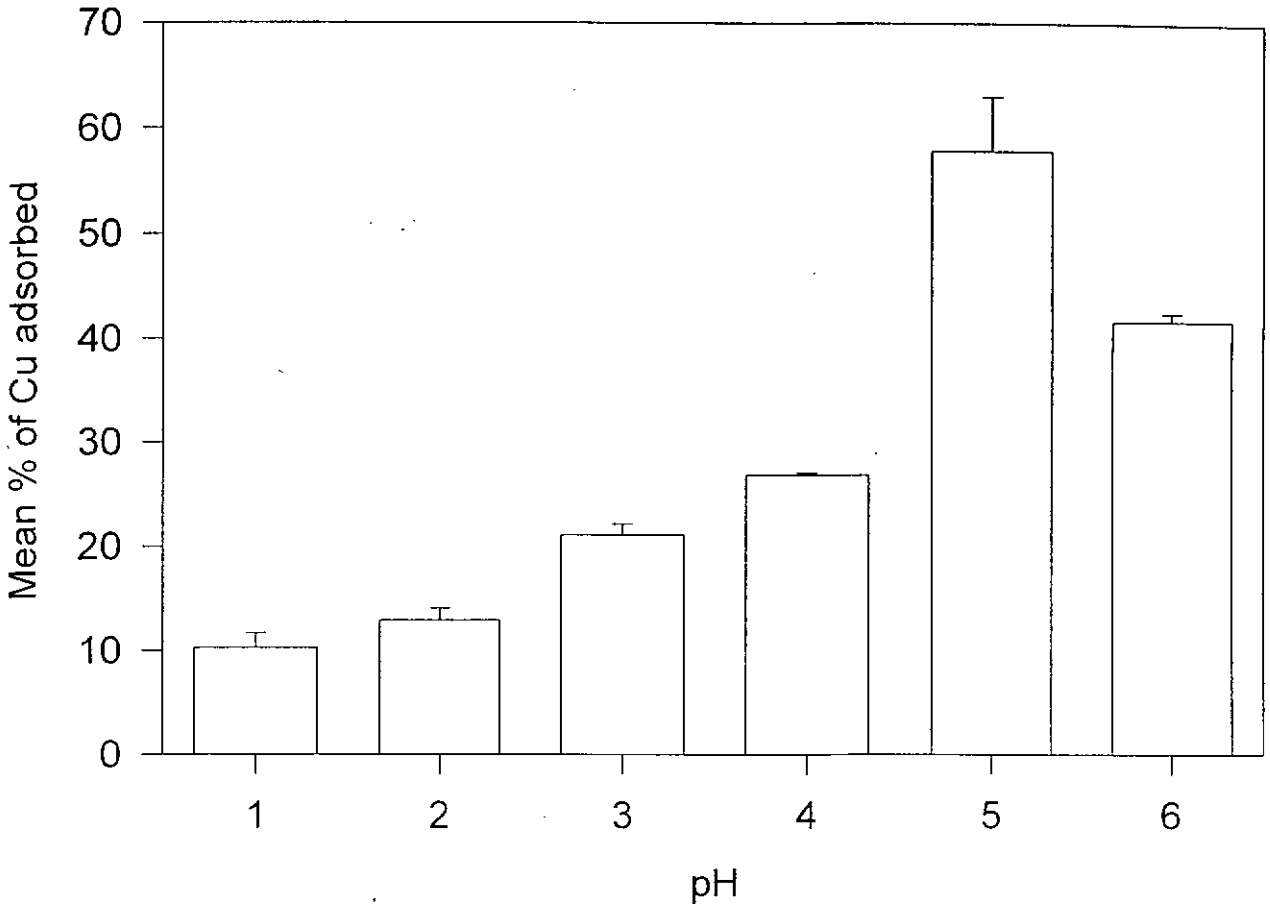

Figure 30. Effect of initial pH on copper biosorption by filamentous *Mucor rouxii*

Zhou and Kiff (1991) suggested that the nature of the cell surface metal binding sites and solution chemistry of metals in water under different pH values might explain the effect of pH on metal biosorption. At low pH values, the cell wall ligands would be closely associated with the hydronium ions (H_3O^+) and restrict the approach of the metal cations as a result of the repulsive force created. At high pH values, however, more cell wall ligands would be exposed and carried negative charges with the consequence of increasing metal cations attraction. The uptake decreased at a much higher pH due to the occurrence of metal precipitation (Brady and Duncan, 1994). Niu *et al.* (1993) suggested that the decrease in metal ions uptake at higher pH might due to the biomass deterioration.

4.4. Effects of treatments on copper biosorption

Several studies have shown that chemical modification of the microbial biomass such as *Saccharomyces cerevisiae* (Huang *et al.*, 1988) and *Penicillium* (Galun *et al.*, 1987) affected metal biosorption. The effects of different treatment methods on kinetics and equilibrium of copper biosorption by *Mucor rouxii* are reported in this section.

The methods examined include heat treatment, acid treatment, alkaline treatment and formaldehyde treatment. Figures 31.a and 31.b plot the effect of treatment on copper biosorption kinetics and Figures 32 and 33 the effect on copper equilibrium isotherms. While Figures 34 and 35 depict *Langmuir* isotherms, Figures 36 and 37 the *Freundlich* isotherms.

4.4.1. Kinetic studies

To study the effect of different treatment methods on kinetics of copper biosorption by *M. rouxii*, the copper concentrations of a series of copper nitrate solution after contact with same amount of biomass in polypropylene bottles were followed as a function of time. The copper biosorption kinetic data for *Mucor rouxii* are plotted

graphically in Figures 31.a and 31.b. The dimensionless metal concentration, $[Cu]_t/[Cu]_0$, the instantaneous metal concentration over initial metal concentration is plotted against time. The biosorption kinetics of both autoclaved and formaldehyde cross-linked biomass is similar to that of untreated mycelial biomass (Figures 31.a and 31.b). The process may be divided into two phases: (i) a fast first phase with most of the metal ions taken up from solution bound within the first 20 min., and followed by; (ii) a much slower second phase which continued even after 24 h. However, after 30 hours, the bulk residual copper concentration decreased suddenly but gradually and significantly for the next 80 h. for both native mycelial and autoclaved *Mucor rouxii* (Figure 31.b). But the bulk copper concentration changed very little after 30 h. for the formaldehyde cross-linked biomass.

There may be several possible explanations for the sudden increase of copper uptake. But active uptake was certainly not responsible since the kinetic pattern of autoclaved cells is very similar to that of native cells (Figures 31.a and 31.b). This piece of observation also confirms that metal uptake by fungal biomass is primarily a metabolic-independent or passive process. Gadd (1990) reported that active intracellular uptake of metals by biomass was unlikely a significant mechanism of metal uptake at relatively high metal concentrations. The sudden increase of copper uptake after 30 hours may be caused by the influx of copper ions into the cell compartment through the cell wall and cell membrane. The long exposure period to high copper concentration solution may rupture the cell wall membrane structure, which in turn allow the copper cations to penetrate into the cell compartment. The cell wall rupture may also expose potential binding sites for more copper uptake.

The cross-linking pretreatment with formaldehyde would strength the cell wall and prevent cell rupture which in turn block the diffusion of copper ions into the cell compartments. Consequently, the bulk copper concentrations remained unchanged after 30 hours.

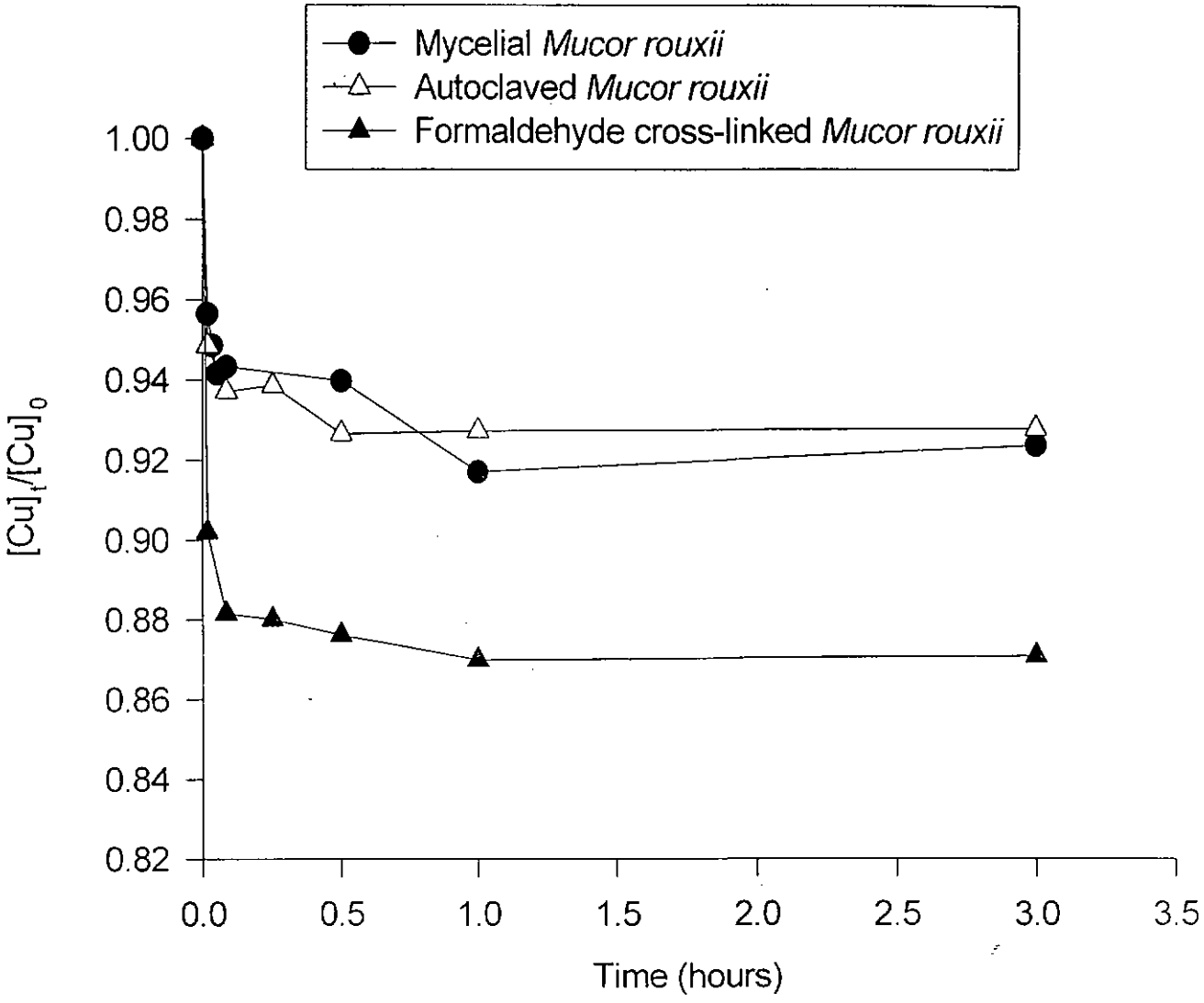

Figure 31.a. Effect of treatments on copper biosorption kinetics after short period of exposure

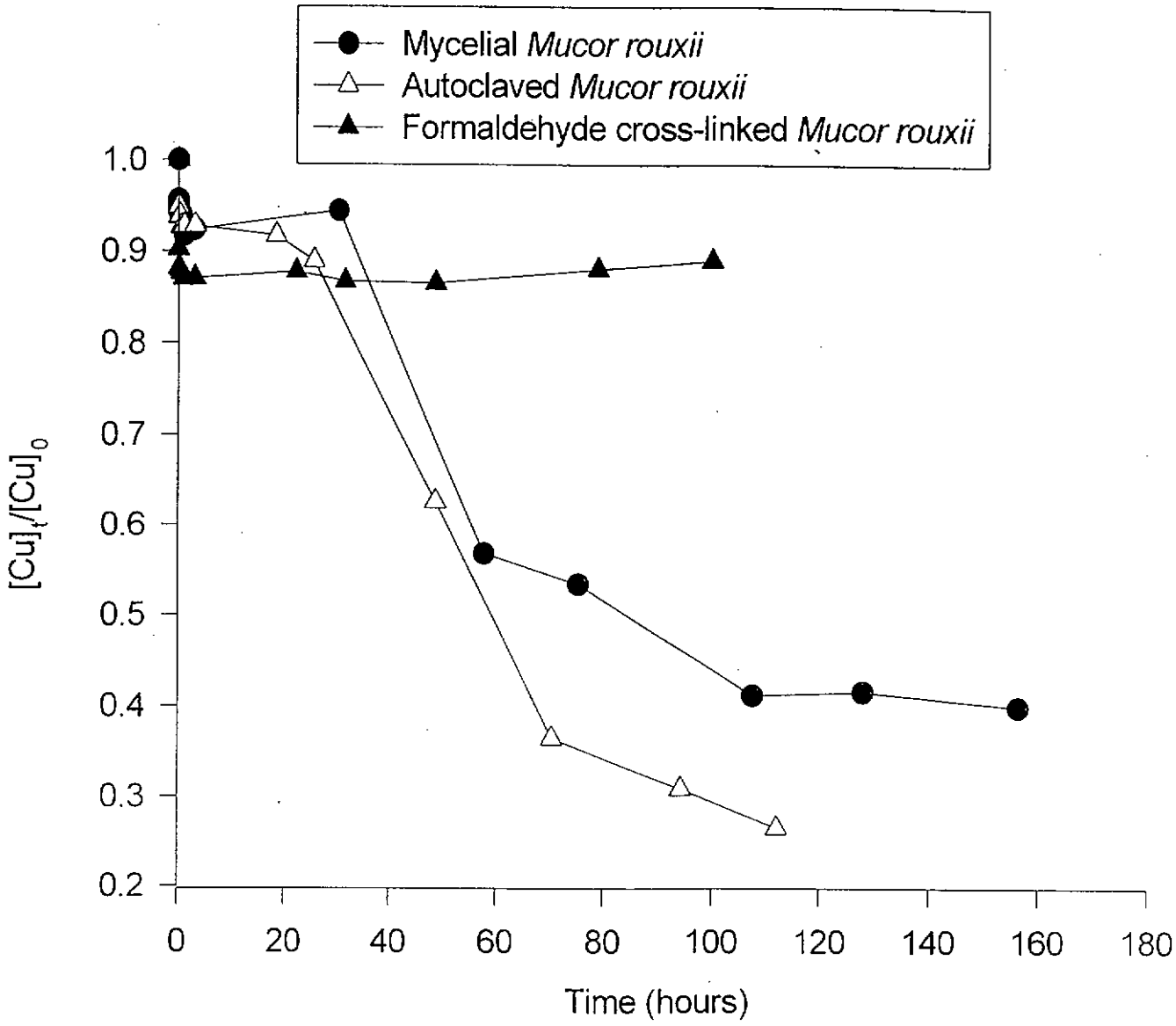

Figure 31.b. Effect of treatments on copper biosorption kinetics after long period of exposure

4.4.2. Effect of heat treatment on equilibrium isotherm

A number of researchers suggested that heat treatment would improve biosorption capacity while others claimed that heat treatment would have no effect. Siegel (1986b) reported that the heat treatment on mycelium of *Penicillium* species would decrease the percentage of lead uptake at equilibrium. Pons and Fuste (1993) reported that uranium uptake by immobilized *Pseudomonas* strain EPS 5028 cells was 47% higher after heat treatment.

In this study, *Mucor rouxii* was autoclaved for 15 min. at 121^{0}C before the biomass was employed for copper biosorption studies. The equilibrium biosorption isotherms are plotted in Figures 32 and 33, which show that the biosorption capacity (q) of the autoclaved biomass decreased significantly especially at lower copper equilibrium concentrations. Only at high copper equilibrium concentration did the autoclaved biomass achieve metal uptake comparable to the untreated biomass. The steeper biosorption isotherm in Figure 32 indicates that the untreated biomass bound copper more strongly than the autoclaved biomass. From Table 9, the predicted *Langmuir* parameter, q_{max} for autoclaved biomass is equal to 18.19±0.23 mg Cu/g biomass which was slightly higher than the mean value for untreated biomass (q_{max} = 14.09±1.80 mg Cu/g biomass). However, the biosorption affinity, K for autoclaved biomass (0.0328±0.0060 ppm^{-1}) is much lower than the value for the untreated biomass (0.2510±0.0118 ppm^{-1}). Autoclaving biomass at high temperature may cause the damage of some functional groups on the fungal cell wall and hence decrease the biosorption ability of the materials.

If a comparison is made between the *Langmuir* (Figures 34 and 35) and *Freundlich* isotherm plot (Figures 36 and 37), the latter one shows a better fit for the equilibrium data with a larger correlation coefficient (Table 10).

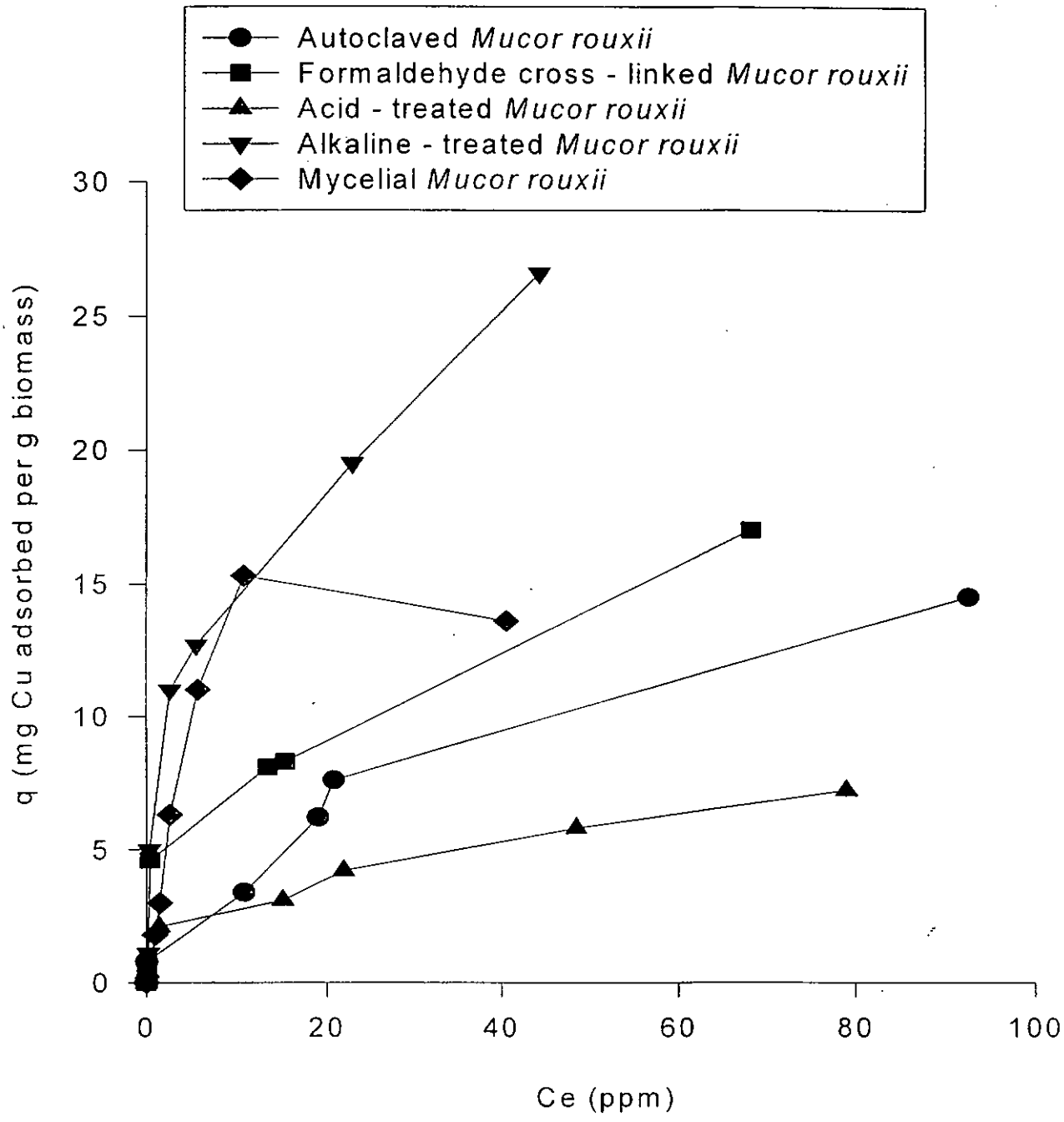

Figure 32. Copper equilibrium isotherms for different types of treated *Mucor rouxii* (data set a)

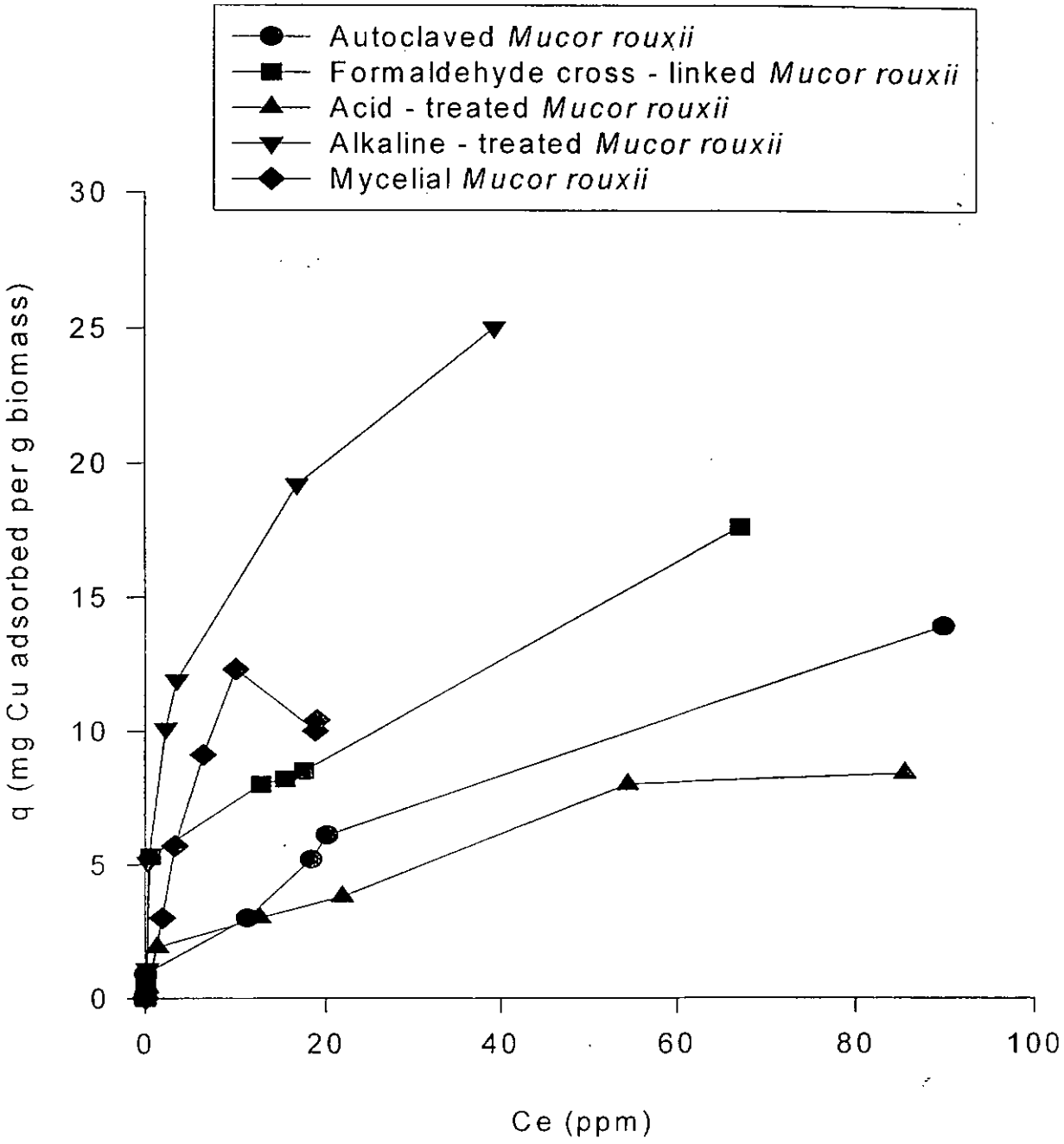

Figure 33. Copper equilibrium isotherms for different types of treated *Mucor rouxii* (data set b)

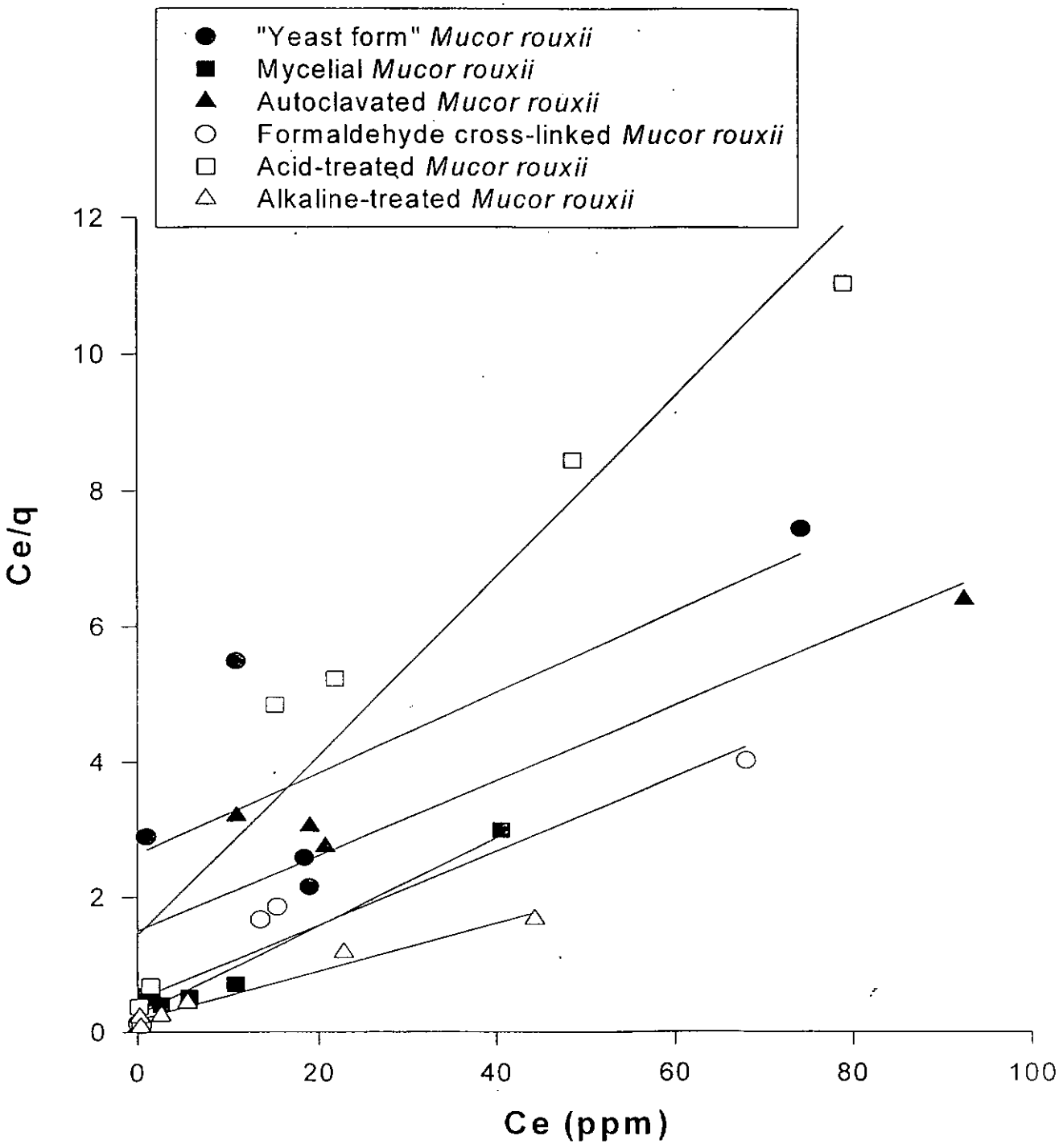

Figure 34. Linearized Langmuir isotherms for copper biosorption by different types of treated *Mucor rouxii* (data set a)

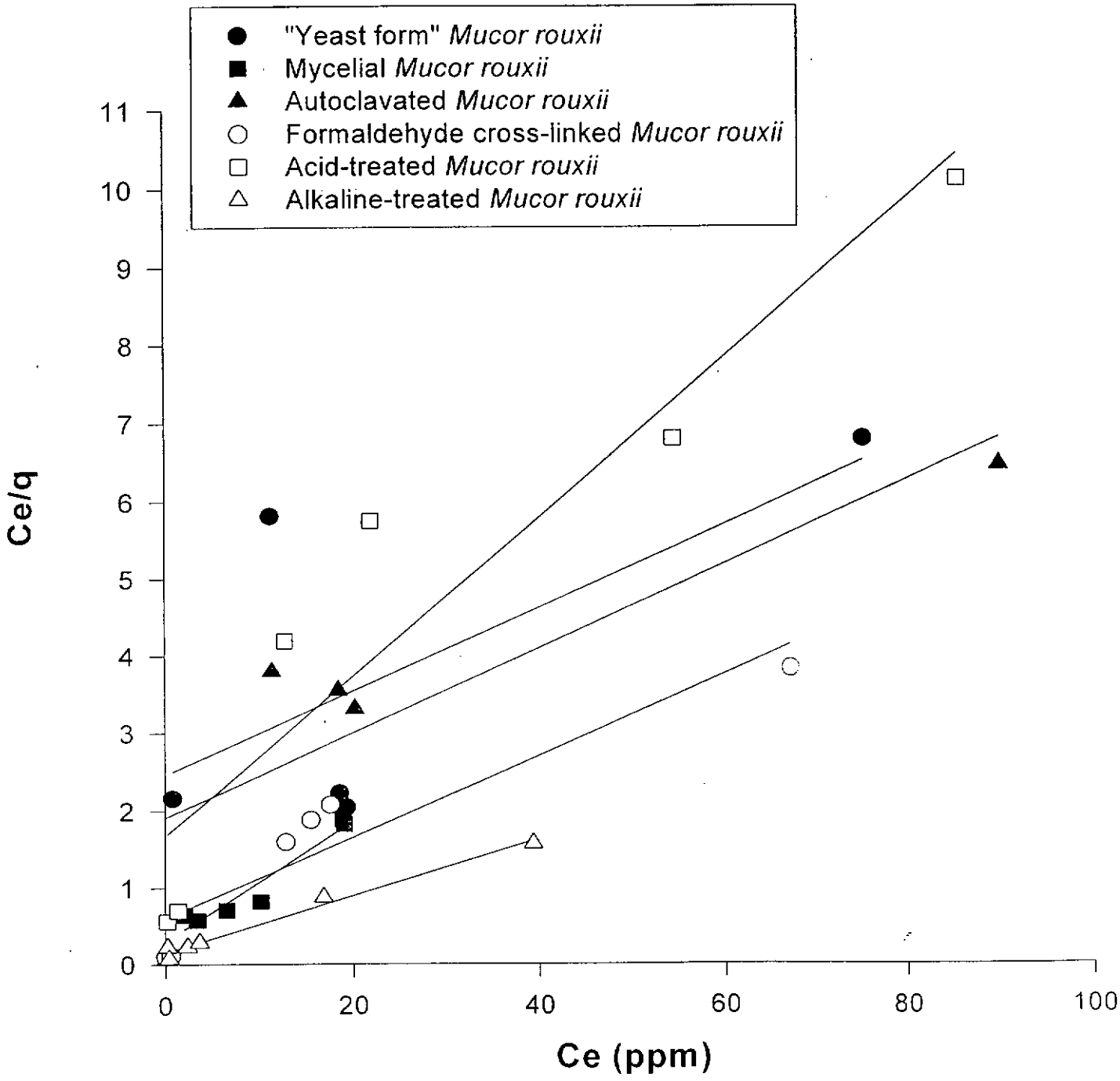

Figure 35. Linearized Langmuir isotherms for copper biosorption by different types of treated *Mucor rouxii* (data set b)

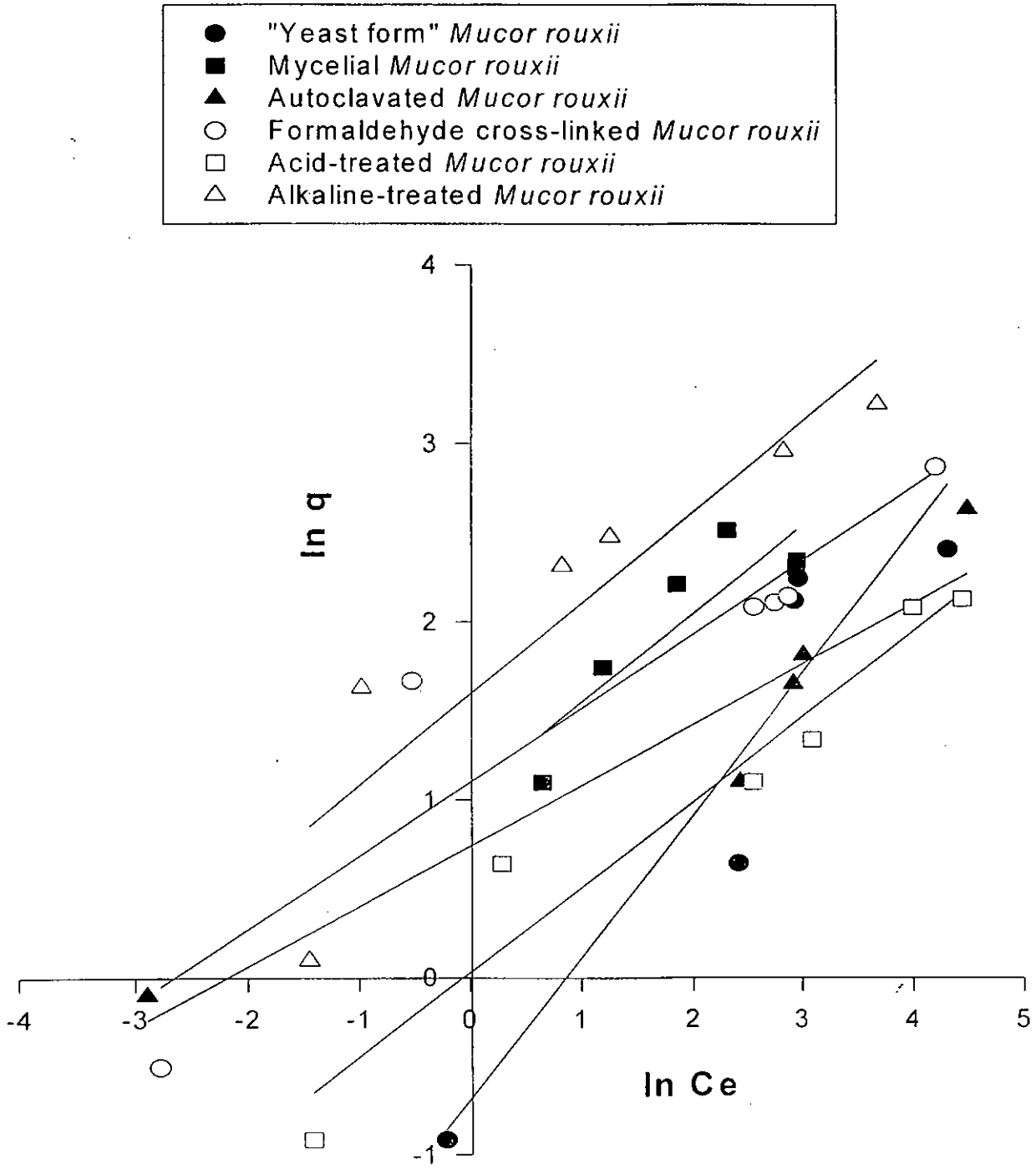

Figure 36. Linearized *Freundlich* isotherms for copper biosorption by different types of treated *Mucor rouxii* (data set a)

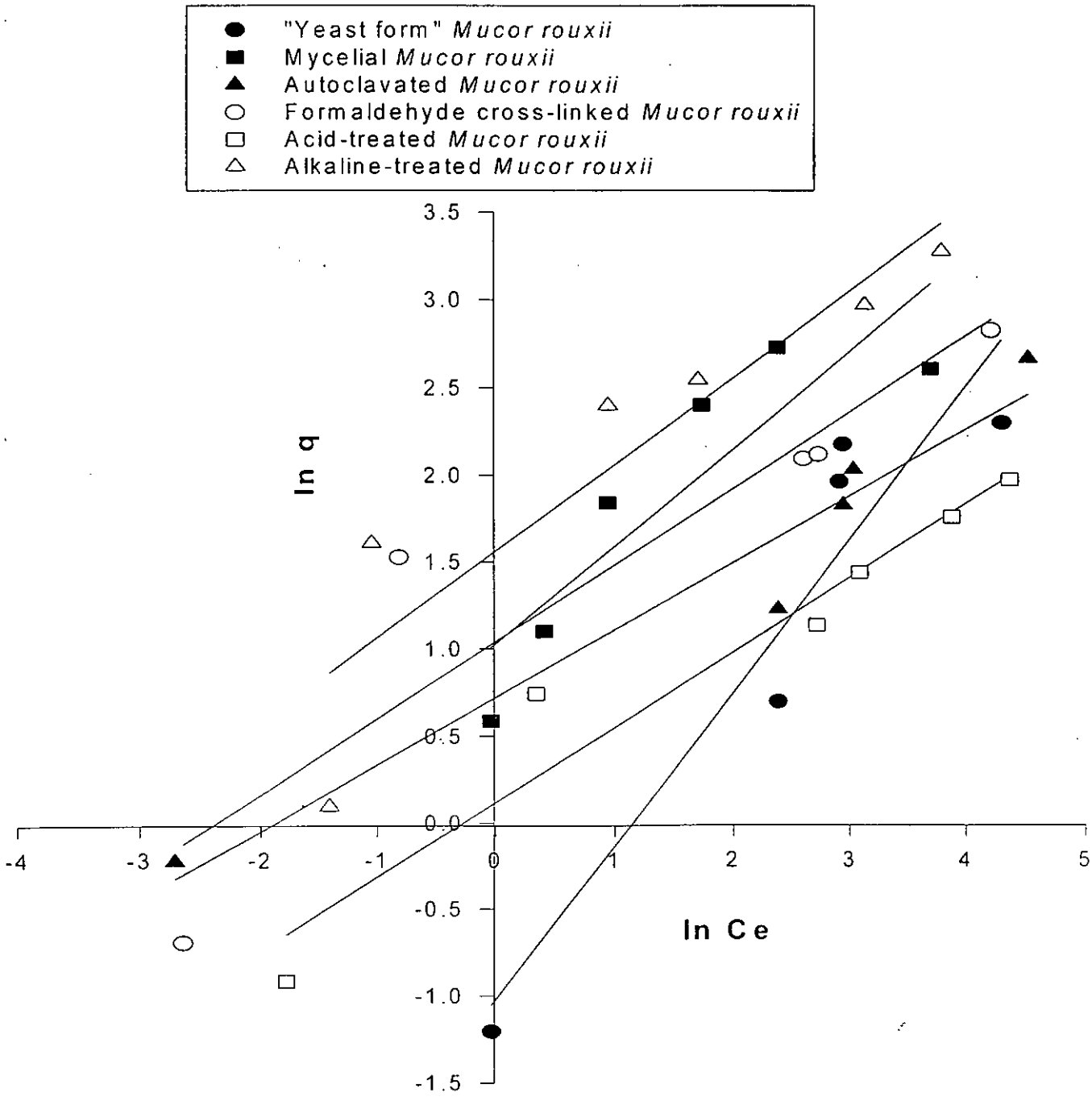

Figure 37. Linearized *Freundlich* isotherms for copper biosorption by different types of *Mucor rouxii* (data set b)

Table 9. *Langmuir* parameters for copper biosorption of different types of treated *Mucor rouxii*

Experiment	Set 1			Set 2			Average value	
Fungal materials	**q_{max}(1st)**	**K(1st)**	**r^2**	**q_{max}(2nd)**	**K(2nd)**	**r^2**	**Average q_{max}**	**Average b**
Mycelia Mucor rouxii	15.36	0.2426	0.970	12.82	0.2593	0.930	14.09 ± 1.80	0.2510 ± 0.0118
Autoclavated Mucor rouxii	18.02	0.0370	0.824	18.35	0.0285	0.726	18.18 ± 0.23	0.0328 ± 0.0060
Formaldehyde cross-linked Mucor rouxii	18.25	0.1134	0.921	19.08	0.0867	0.871	18.67 ± 0.59	0.1001 ± 0.0189
Acid-treated Mucor rouxii	7.56	0.0921	0.933	9.73	0.0615	0.888	8.64 ± 1.53	0.0768 ± 0.0216
Alkaline-treated Mucor rouxii	28.01	0.1967	0.971	27.10	0.2349	0.986	27.55 ± 0.64	0.2158 ± 0.0270

Table 10. *Freundlich* parameters for copper biosorption of different types of treated *Mucor rouxii*

Experiment	Set 1			Set 2			Average Value	
Fungal materials	**n(1st)**	**k(1st)**	**r^2**	**n(2nd)**	**k(2nd)**	**r^2**	**Average n**	**Average k**
Mycelial Mucor rouxii	1.787	2.7902	0.785	2.021	2.8680	0.774	1.904 ± 0.165	2.8291 ± 0.0550
Autoclaved Mucor rouxii	2.593	0.4863	0.949	2.942	2.0978	0.909	2.768 ± 0.247	1.2921 ± 1.1395
Formaldehyde cross-linked Mucor rouxii	2.275	2.8292	0.854	2.413	3.0021	0.871	2.344 ± 0.097	2.9157 ± 0.1223
Acid-treated Mucor rouxii	2.327	1.1251	0.941	2.085	1.0278	0.942	2.206 ± 0.172	1.0765 ± 0.0688
Alkaline-treated Mucor rouxii	2.014	4.7636	0.834	1.960	4.9150	0.832	1.987 ± 0.038	4.8393 ± 0.1071

4.4.3. Effect of acid treatment on equilibrium isotherm

Few investigators have considered the effect of acid treatment on biosorption. Galun *et al.* (1987) reported that acid treatment with diluted HCl had no effect on sebsequent uptake of nickel at pH 5.5 but had significantly improved the cadmium uptake and may have slightly improved copper and zinc uptake. Acid treatment may be able to remove metal ions such as potassium, a component present in the growth medium, which may be immobilized on the surfaces of the biomass; hence free metal binding sites for uptake of more metal ions.

Figures 32 and 33 show that the acid-treated *Mucor rouxii* exhibited a decrease in copper biosorption capacity as compared to the filamentous intact cells over the concentration range studied. The linearized *Langmuir* isotherm plots are shown in Figures 34 and 35. The predicted *Langmuir* isotherm parameters, maximum biosorption capacity (q_{max}) of copper was 8.64±1.54 mg Cu/g biomass (Table 9) which is about half the biosorption capacity of the intact filamentous cell. The *Freundlich* model (Figures 36 and 37) fit the equilibrium data of acid-treated cell better with a larger correlation coefficient than the *Langmuir* model.

The fungal biomass was immersed in HNO_3 for one day. The long acid exposure time may denature the fungal cell surface and decreased the metal uptake capacity.

4.4.4. Effect of alkaline treatment on equilibrium isotherm

The effect of NaOH treatment on copper biosorption was studied. *Mucor rouxii* treated with NaOH doubled the amount of copper biosorption compared to biosorption by the native cells (Figures 32 and 33). The *Langmuir* parameter calculated, q_{max} was 27.56±0.64 mg Cu/g biomass, much higher than that of native cells (Table 9). The *Langmuir* biosorption affinity, K (Table 9), determined was 0.2158±0.0270 ppm^{-1} which was close to the untreated cells in magnitude.

Other researchers have also observed that alkaline treatment of biomass enhanced its metal biosorption capacity. Galun *et al.* (1987) reported that NaOH pre-treated *Penicillium* biomass would improve the uptake of cadmium, copper, nickel and zinc. Luef *et al.* (1991) suggested that the removal of amorphous polysaccharides from the fungal cell wall by alkali treatment generated more accessible space in the glucan-chitin skeleton, hence allowing more zinc ions to precipitate at the cell wall. *M. rouxii* belongs to the chitosan-chitin group. Alkaline treatment may remove the amorphous polysaccharides on the fungal cell wall and thus expose copper-binding chitosan present in the chitosan-chitin skeleton allowing biosorption of more copper ions. Alkaline treatment can also destroy autolytic enzymes that cause putrification of fungal cells.

The *Freundlich* isotherm plot (Figures 36 and 37) gave a lower correlation coefficient than the *Lanmguir* model (see Tables 9 and 10). The *Langmuir* model shows a better fit of the equilibrium data than the *Freundlich* one. The results suggest that the adsorption process may be homogeneous rather than heterogeneous in nature.

4.4.5. Effect of formaldehyde treatment on equilibrium isotherm

For industrial operation, it is desirable to employ packed bed reactor for metal removal. However, the low mechanical rigidity of fungal material would cause difficulties in preparing such reactor. The release of cell component materials and their precipitation in metal containing solutions have to be considered too for the scale-up of the biosorption process (de Carvalho, 1994). Pretreating the biomass with formaldehyde may solve some of these problems. The cross-linking treatment with formaldehyde would confer mechanical strength and prevent leaching of cell materials. The biosorption capacity of the materials in such a cross-linking reaction depends on the extent of cross - linking (de Carvalho, 1994) and the cross-linking reagent (Holan and Volesky, 1993). The effect of formaldehyde treatment on copper biosorption was studied.

Figures 32 and 33 shows that the formaldehyde cross-linked biomass exhibited a lower capacity for copper compared with the native filamentous biomass until at very high residual equilibrium copper concentration. The calculated *Langmuir* isotherm parameters for copper uptake by native biomass and formaldehyde treated biomass were compared (Table 9). The calculated q_{max} of formaldehyde treated biomass was 18.67±0.59 mg Cu/g biomass which was slightly higher than that obtained for native filamentous cell. However, the *Langmuir* biosorption affinity predicted, K was 0.1001±0.0189 ppm^{-1} which was lower than the value calculated for the native cells. The formaldehyde treatment alters the biosorption behaviour of the fungal biomass towards copper. The lower biosorption affinity indicates that the formaldehyde treated biomass bound copper more strongly than the native biomass. Comparison of the regression coefficients calculated for the *Langmuir* and *Freundlich* models (Tables 9 and 10) shows that both fit reasonably well the biosorption data of formaldehyde-treated biomass.

4.5. Effect of medium composition

The effects of medium composition on lead and copper biosorption of *Mucor rouxii* was investigated. The morphology of *Mucor rouxii* was found to change from the filamentous form to yeast form when mycological peptone (Oxoid) was replaced with bacto peptone (Difco) in the growth medium. Bartnicki-Garcia and Nickerson (1962a and 1962b) also reported that the morphology of *Mucor rouxii* changed from the filamentous form to yeast form when incubated in CO_2 atmosphere at the same medium composition.

The equilibrium uptake of lead and copper by the filamentous and yeast forms of *Mucor rouxii* was compared (Figures 38 and 39). The filamentous biomass of the culture grown on medium containing mycological peptone showed the higher maximum lead uptake of 600 mg Pb/g biomass which is about 200 % higher than that obtained

with yeast typed biomass grown on bacto peptone. The *Langmuir* and *Freundlich* isotherm parameters determined and the regression coefficients were summarized in Tables 11 and 12. While the copper biosorption equilibrium isotherm was L-type for filamentous form of biomass, the isotherm was S-type for yeast form of biomass (Figure 39). The maximum copper uptake obtained with filamentous form was slightly lowered than that obtained with yeast form. However the steeper biosorption isotherm (Figure 39) indicates that the filamentous typed biomass bound copper more strongly than the yeast typed biomass. The *Langmuir* and *Freundlich* isotherm parameters calculated and the equilibrium coefficients were summarized in Tables 11 and 12.

The difference observed in the metal biosorption behaviour between filamentous and yeast types of biomass may be accounted by the difference in cell wall compositions and the morphologies between the two types of biomass. Mannose has been reported to be present in most species of yeasts whereas it is not found in the species of filamentous fungi (Bartnicki-Garcia and Nickerson, 1962a and 1962b).

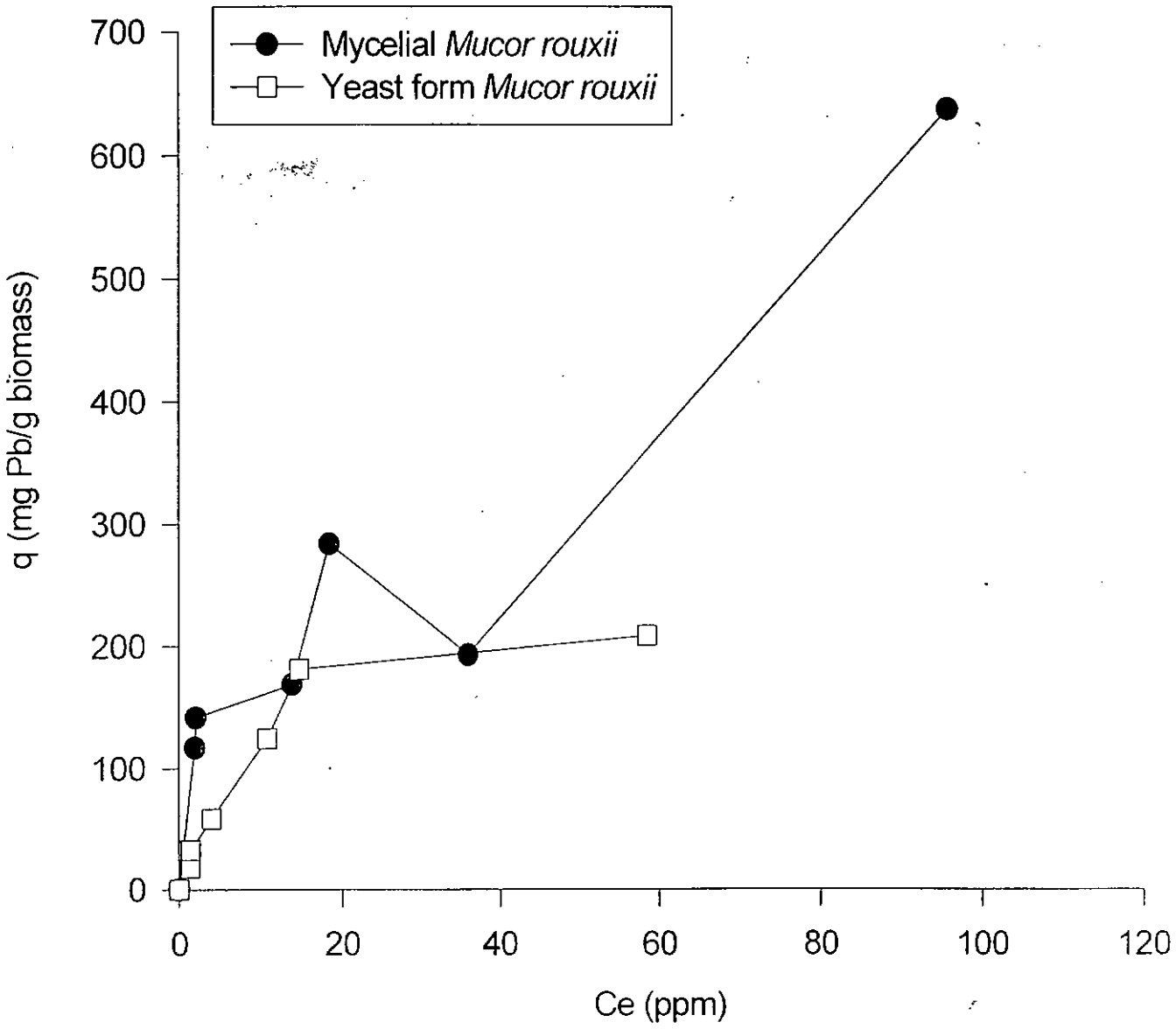

Figure 38. Effect of culture medium composition on lead biosorption by *Mucor rouxii*

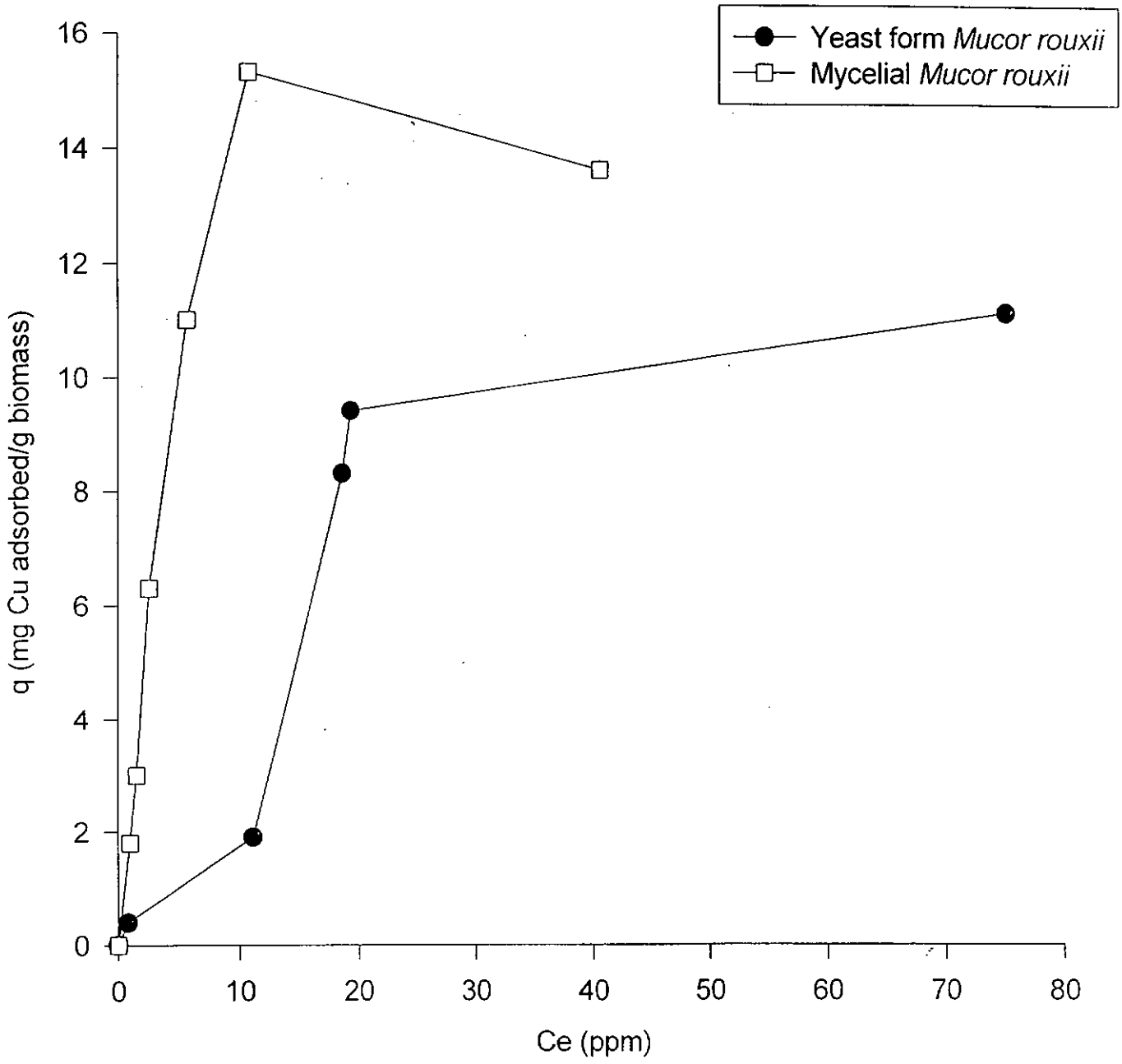

Figure 39. Effect of culture medium composition on copper biosorption by *Mucor rouxii*

Table 11. *Langmuir* parameters for lead and copper biosorption by yeast form and filamentous *Mucor rouxii*

Metals	Fungal materials	Average q_{max} (mg metal/g biomass)	Average K	Average r^2
Lead	Yeast form *Mucor rouxii*	741.76 ± 38.82	0.0285 ± 0.0036	0.582
	Filamentous form *Mucor rouxii*	263.35 ± 9.80	0.0807 ± 0.0036	0.965
Copper	Yeast form *Mucor rouxii*	17.68 ± 1.23	0.0222 ± 0.0004	0.512
	Filamentous form *Mucor rouxii*	14.09 ± 1.80	0.2510 ± 0.0118	0.950

Table 12. *Freundlich* parameters for lead and copper biosorption by yeast form and filamentous *Mucor rouxii*

Metals	Fungal materials	Average n	Average k	Average r^2
Lead	Yeast form *Mucor rouxii*	2.616 ± 0.540	77.97 ± 21.33	0.797
	Filamentous form *Mucor rouxii*	1.584 ± 0.024	23.06 ± 0.81	0.886
Copper	Yeast form *Mucor rouxii*	1.190 ± 0.080	0.4309 ± 0.0991	0.884
	Filamentous form *Mucor rouxii*	1.904 ± 0.165	2.829 ± 0.055	0.779

4.6. Comparison of biosorption capacities for different metals

4.6.1. Kinetic studies of nickel and zinc biosorption

To study the kinetics of nickel and zinc biosorption, the concentrations after contact with a given amount of biomass in polypropylene bottles were followed as a function of time. The kinetic data are graphically depicted in Figure 40 for nickel and Figure 41 for zinc. The metal concentration is plotted against time. Figures 40 and 41 show that the kinetic pattern for nickel and zinc biosorption was similar to that for lead and copper biosorption. The process may be divided into two phases: (i) a fast biosorption first phase with most of the metal ions taken up from solution bound within the first 10 min. and followed by; (ii) a much slower second phase which continued even after 24 h. These observations suggest that the first phase in biosorption involves inherently a very fast chemisorption adsorption process. Further metal uptake by the fungal biomass may be controlled by the diffusion process through the cell or regulated by the intracellular metabolic processes.

4.6.2. Equilibrium isotherm for nickel and zinc

The biosorption capacities of species *Mucor rouxii* for nickel and zinc were compared and evaluated quantitatively using the biosorption isotherms derived from the equilibrium data. Figure 42 is plots of the metal biosorption capacities, q (in mg metal adsorbed/g dried weight biomass), against residual metal equilibrium concentration remaining in the solution, C_e (in mg/L). A linear relationship was not observed too for this species. For nickel biosorption, the biosorption capacity q became saturated at C_e as low as 10 ppm. The maximum biosorption capacity q_{max} for nickel was about 15 mg Ni adsorbed per g biomass. For zinc biosorption, the biosorption capacity did not become saturated at C_e even over 35 ppm. The maximum biosorption capacity (mg/g) for zinc was higher than that obtained for nickel (Figure 42).

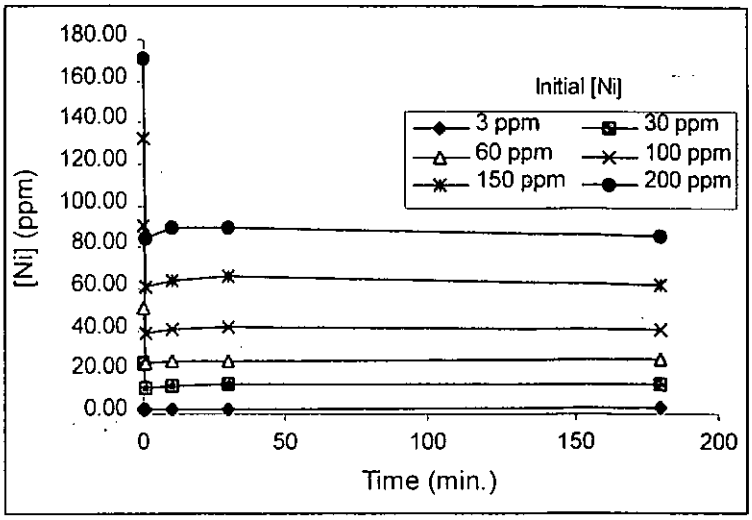

Figure 40. Nickel biosorption of kinetics of filamentous *Mucor rouxii*

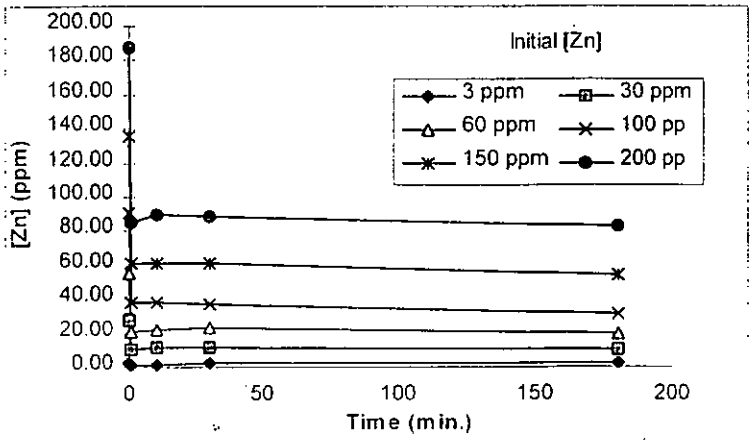

Figure 41. Zinc biosorption kinetics of filamentous *Mucor rouxii*

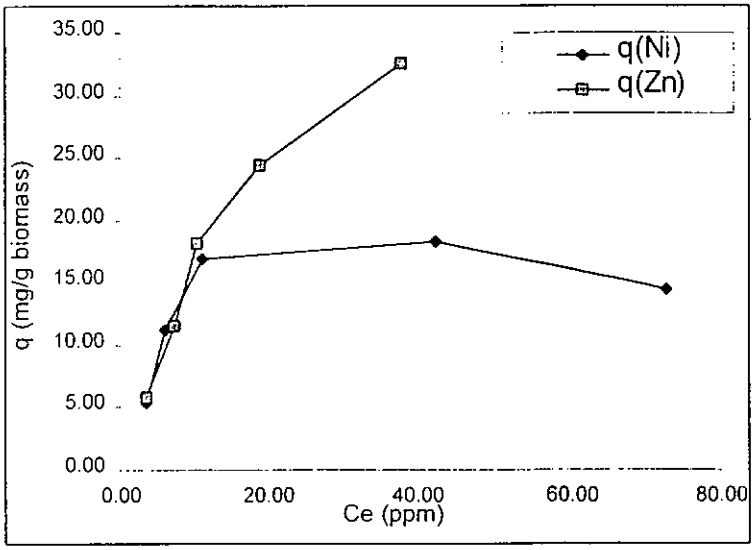

Figure 42. Equilibrium isotherm of nickel and zinc biosorption by filamentous *Mucor rouxii*

4.6.3. *Langmuir* biosorption isotherm for nickel and zinc

The linearlized *Langmuir* isotherm plots for nickel and zinc are shown in Figures 43 and 45. The *Langmuir* parameters determined (q_{max} and K) from the linearlized plots and the regression coefficients for *Mucor rouxii* species are summarized in Table 13. Figures 43 and 45 clearly show that the nickel and zinc biosorption of *Mucor rouxii* conforms to the *Langmuir* model over the range of metal concentrations examined. For zinc biosorption, *Mucor rouxii* showed a higher theoretical maximum biosorption capacity (q_{max}) 65.74±10.26 mg Zn/g biomass with biosorption affinity (K) 0.0319±0.0049 ppm^{-1}. For nickel biosorption, the theoretical maximum biosorption capacity was determined to be 16.3989±0.7782 mg Ni/g biomass but with higher biosorption affinity K (0.3642±0.1534 ppm^{-1}) compared with Zn biosorption.

4.6.4. *Freundlich* biosorption isotherm for nickel and zinc

The linearlized *Freundlich* isotherm plots are shown in Figures 44 and 46 for nickel and zinc biosorption of *Mucor rouxii*. The constants, k and n, for the *Freundlich* isotherms are given in Table 14. The zinc biosorption equilibrium data conformed to the *Freundlich* model reasonably well. However, the nickel biosorption data did not fit the isotherm. The *Freundlich* isotherm cannot be applied to all values of C_e since at saturation, q_{max} is a constant, independent of further increases in C_e. *Mucor rouxii* with low nickel biosorption capacity became saturated at C_e as low as 10 mg/L, consequently, the *Freundlich* isotherm no longer applied at C_e higher than 10 mg/L.

Comparison of the regression coefficients calculated for the two biosorption models (Tables 13 and 14) shows that both fit very well for zinc biosorption, but only *Langmuir* model can fit nickel biosorption. The *Langmuir* model can be applied over a wider range of nickel equilibrium concentration compared with *Freundlich* model.

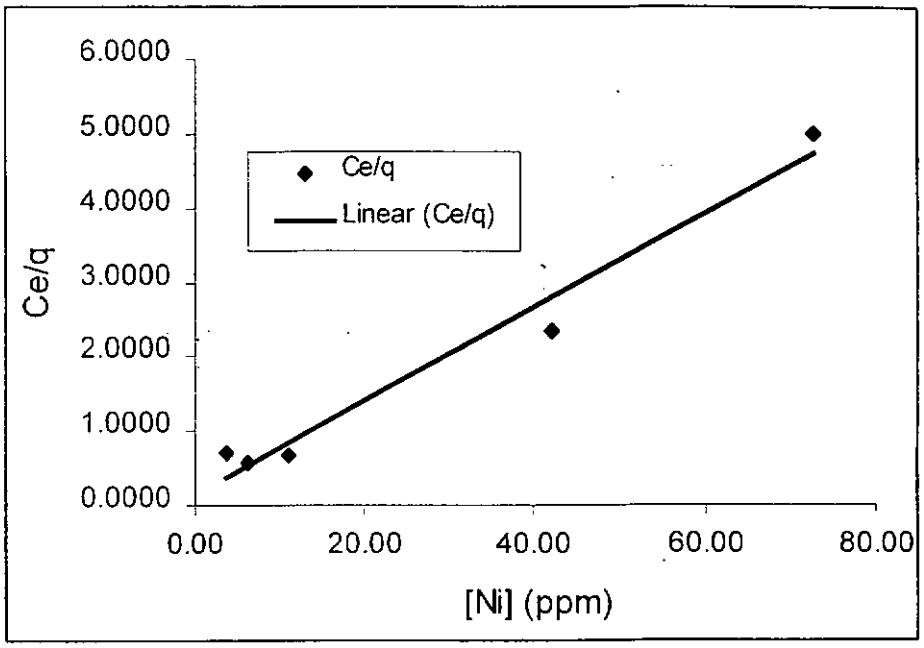

Figure 43. Linearized *Langmuir* isotherms of nickel biosorption by filamentous *Mucor rouxii*

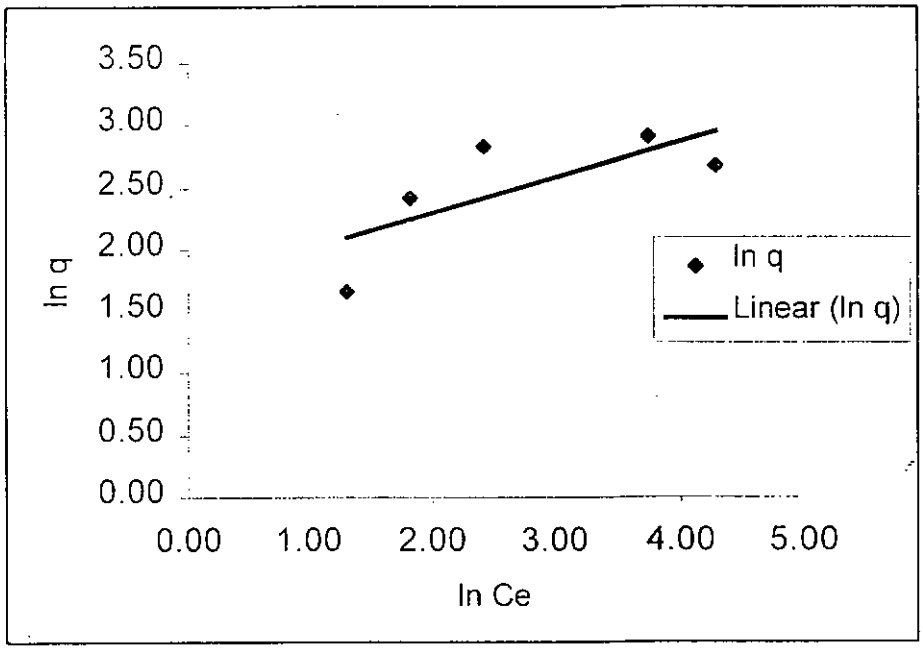

Figure 44. Linearized *Freundlich* isotherm of nickel biosorption by filamentous *Mucor rouxii*

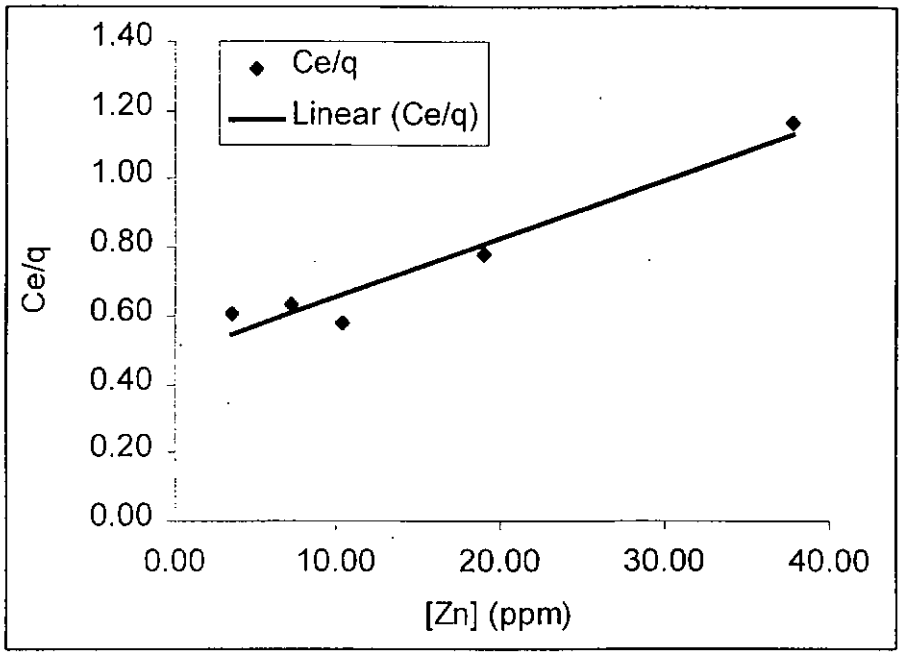

Figure 45. Linearized *Langmuir* isotherm of zinc biosorption by filamentous *Mucor rouxii*

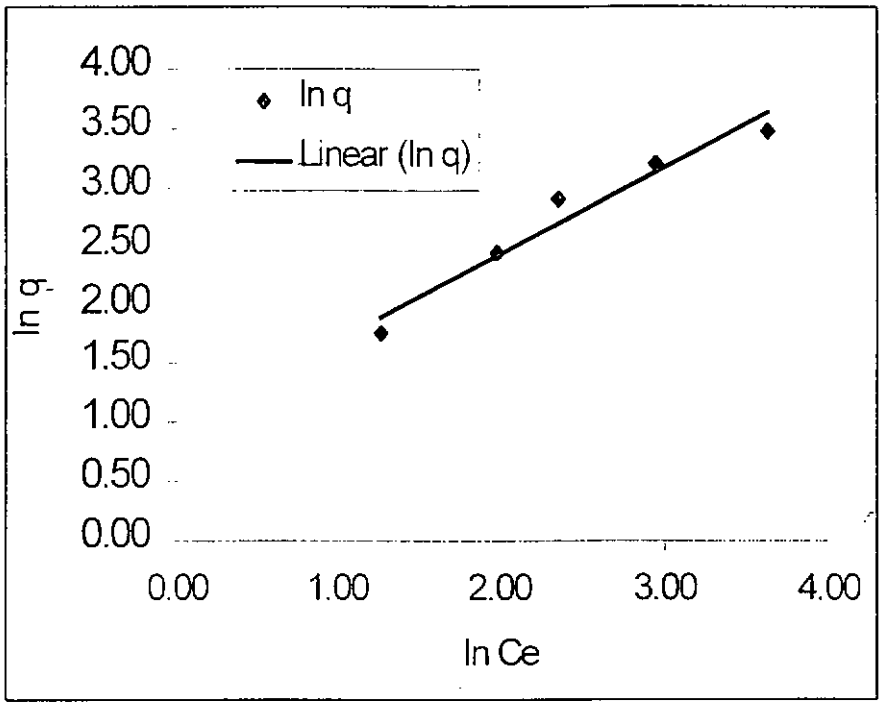

Figure 46. Linearized *Freundlich* isotherm of zinc biosorption by filamentous *Mucor rouxii*

Table 13. *Langmuir* parameters for Ni^{2+} and Zn^{2+} biosorption by *Mucor rouxii*

Experiment	Set 1			Set 2			Average value	
Metals	q_{max}(1st)	b(1st)	r^2	q_{max}(2nd)	b(2nd)	r^2	Average q_{max}	Average b
Nickel	15.8479	0.4727	0.9692	16.9492	0.2557	0.9793	16.3989 ± 0.7782	0.3642 ± 0.1534
Zinc	58.4795	0.0353	0.9417	72.9927	0.0284	0.9823	65.7361 ± 10.2624	0.0319 ± 0.0049

Table 14. *Freundlich* parameters Ni^{2+} and Zn^{2+} biosorption by *Mucor rouxii*

Experiment	Set 1			Set 2			Average value	
Metals	n(1st)	k(1st)	r^2	n(2nd)	k(2nd)	r^2	Average n	Average k
Nickel	3.4710	5.5511	0.5324	3.0157	4.8496	0.5791	3.2433 ± 0.3220	5.2004 ± 0.4960
Zinc	1.3727	2.6669	0.9526	1.2758	2.5239	0.9977	1.3243 ± 0.0685	2.5954 ± 0.1011

4.6.5. Other cations

The biosorption capacities of species *Mucor rouxii* for lead, copper, zinc, nickel, sodium, silver, magnesium, chromium, cadmium and cobalt were compared and evaluated quantitatively. The biosorption capacity q_e (mmol./g biomass) at C_e over 100 ppm for different cations were arranged in the following descending order: $Pb^{2+} > Zn^{2+} > Mg^{2+} > Cr^{3+} > Cd^{2+} > Ag^{+} > Ni^{2+} > Cu^{2+} > Co^{2+} > Na^{+}$. In order to facilitate a comparison of the results, most of the data in this study were obtained with a single counterion, nitrate, and a pH 5.0. Nitrate salts are usually soluble, and the nitrate ion forms only weak complexes with metals (Cotton and Wilkinson, 1996). Hence nitrate anions would not interfere with metal biosorption. To avoid complexation of the metals with other anions, unbuffered solutions were used in all the biosorption experiments (Tobin *et al.*, 1984).

Figure 47.a shows the plot of the maximum biosorption capacity against the ionic radius. The ionic radii of different metals is obtained from Sargent-Welch Scientific Company. However. there is no correlation between biosorption capacity and ionic radius. The observations are quite a contrast to those reported by Tobin *et al.* (1984) who has found that the amount of metal uptake by *Rhizopus arrhizus* was directly related to ion radii of the metal cations, except for Cr^{3+}, and the alkali metal cations.

Figure 47.b plots the maximum biosorption capacity against a charge/radius term, Z^2/r or charge density factor. Z is the oxidation state or ion charge and r is the ionic radius (Andres *et al.*, 1993; Crist *et al.*, 1994). The figure shows an increasing trend of maximum biosorption capacities with increasing Z^2/r. The maximum biosorption capacities correlate better with Z^2/r than with r.

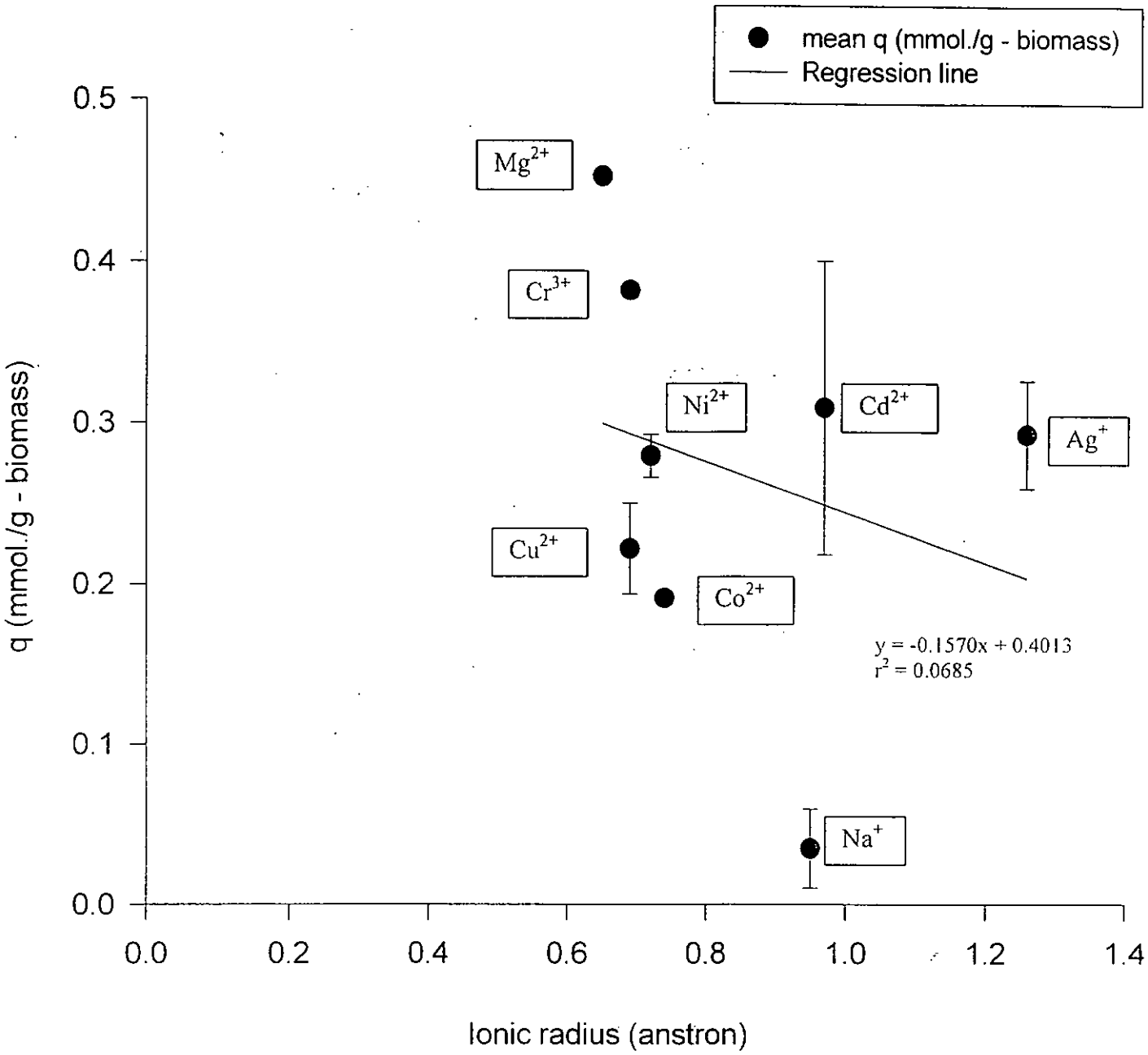

Figure 47.a. Plot of biosorption capacity of metal cations against ionic radius

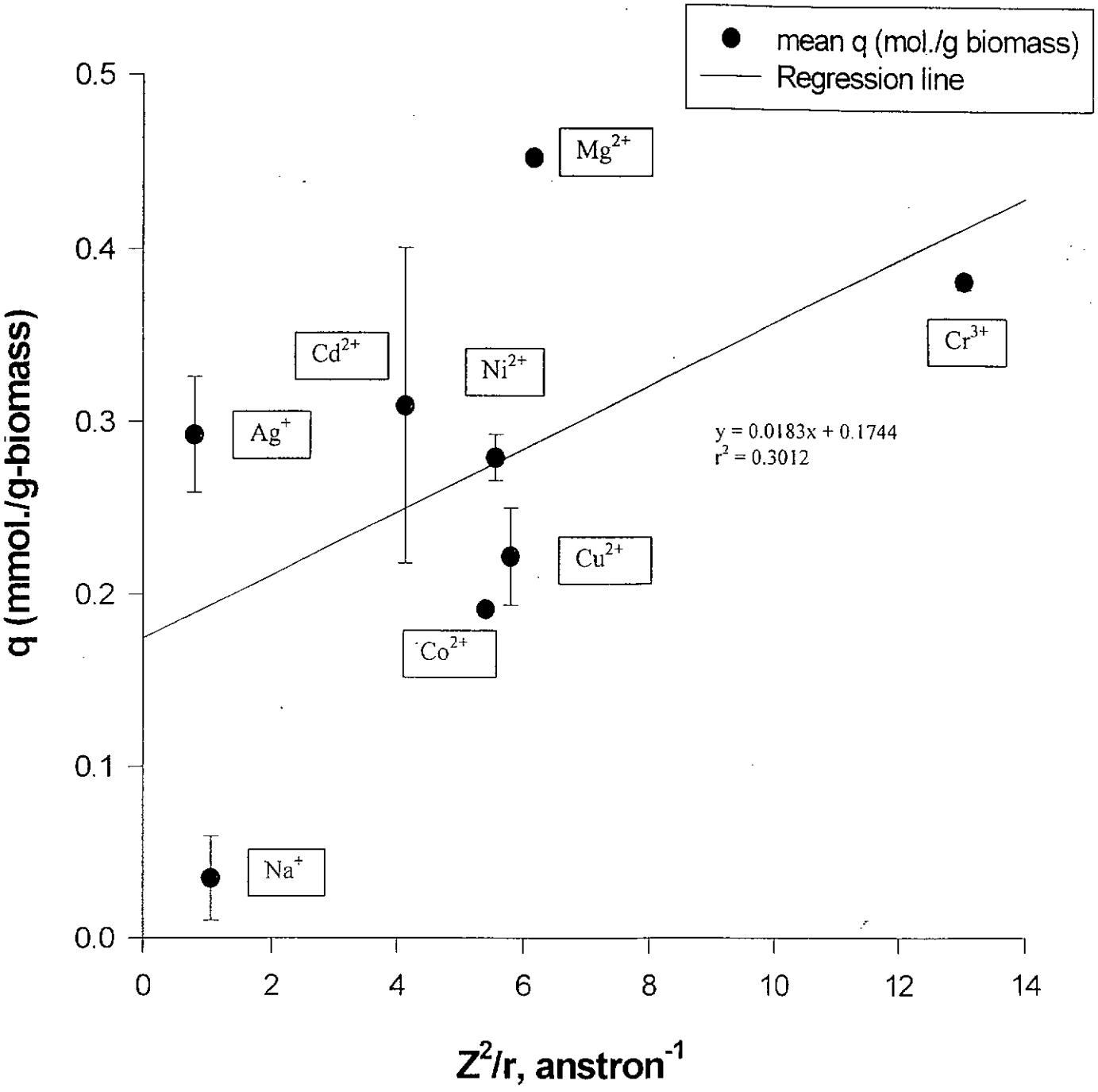

Figure 47.b. Plot of biosorption capacity of metal cations against Z^2/r

It is proposed that a significant portion of the uptake is due to coordination of functional groups on molecules in the biomass to the metal ions. These functional groups may include carboxylate, amine, phosphate, sulfhydryl, hydroxyl, etc. The alkali metal ion, Na^+ (and likely the others, which are not determined in this study) was not significantly adsorbed by the biomass. This group of metals does not form complexes with most ligands (Cotton and Wilkson, 1996). The absence of significant biosorption of this ion is consistent with the proposed biosorption mechanism of the nonalkali ions by the biomass, involving binding by functional groups. Zinc (II) and lead (II) were adsorbed at anormalously high levels. The criteria based on Z and r alone are not satisfactory at the moment. The absence of the additional bonding parameters such as atomic electronegativity, coordination number and ionic radius variations dependent on bond character may explain for the poor linear relationship established. The poor linear relationship established may imply that the material is selective towards lead rather than other metal cations.

4.7. Lead and copper (II) biosorption from binary metal mixtures by *Mucor rouxii*

4.7.1. Two-dimensional analysis (Scatchard plots analysis)

Scatchard plot (Scatchard, 1949) has been commonly used to describe binding of ligands (usually small molecules) to macromolecules. This plot has been adopted to describe binding of metal ions to biomass. For instance, Rose (1996) employed Scatchard plots for data analysis of the competitive binding of calcium in the presence of magnesium or zinc to *Streptococcus sanguis* and Purified *S. sanguis* cell walls. The Figures 48.a - 48.g show the Scatchard plots for lead binding by *Mucor rouxii* biomass in the presence of 0, 0.1, 0.3, 0.55, 1.72, 1.90 and 2.50 mM copper. These Figures were used to derive the capacity (X_0) and the association constant (K) (or binding affinity) of the metal-binding sites. A plot of bound metal concentration divided by free-metal concentration ($q_M/[M]_e$) versus the bound metal concentration (q_M) gives a slope of -K and the abscissa intercept X_0. All the parameters determined are summarized in Table 15. The plots for the Scatchard model (Hirs and Timasheff, 1978; Andres *et al.*, 1993) can qualify the nature of binding sites in their interaction with the ligands. Figures 48.a - 48.g show that as the copper concentration in the binary metal mixtures increased, the Scatchard plots for lead binding changed from 'L-shape' curves (Figures 48.a - 48.c) to straight line (Figures 48.f - 48.g). The biosorption systems (Figures 48.a - 48.e) can be depicted by two interesting curve targents ('L-shape' curve) representing two linear contributions of different slope. This indicates the presence of at least two types of binding sites, corresponding to strong and weak binding affinity. Furthermore, concave curve forms suggest negative cooperation, reflecting binding priority of one type of sites with respect to another. A number of potential metal binding sites including amino, carboxyl, phospate, sulfhydryl or hydroxyl groups, are present on the surfaces of fungal biomass. Each functional group exhibits its specification towards metal ions.

When initial copper concentration increased to about 2 mM, the Scatchard plots changed to straight line. This observation suggests that the binding of lead changed to

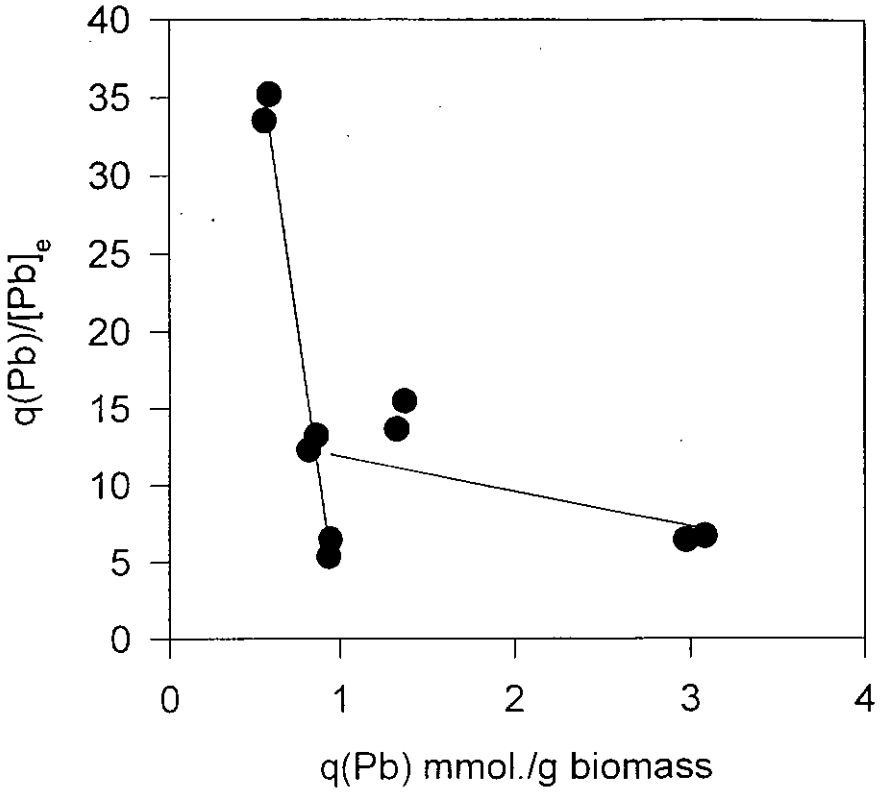

Figure 48.a. Scatchard plot for Pb biosorption at initial [Cu] = 0 mM

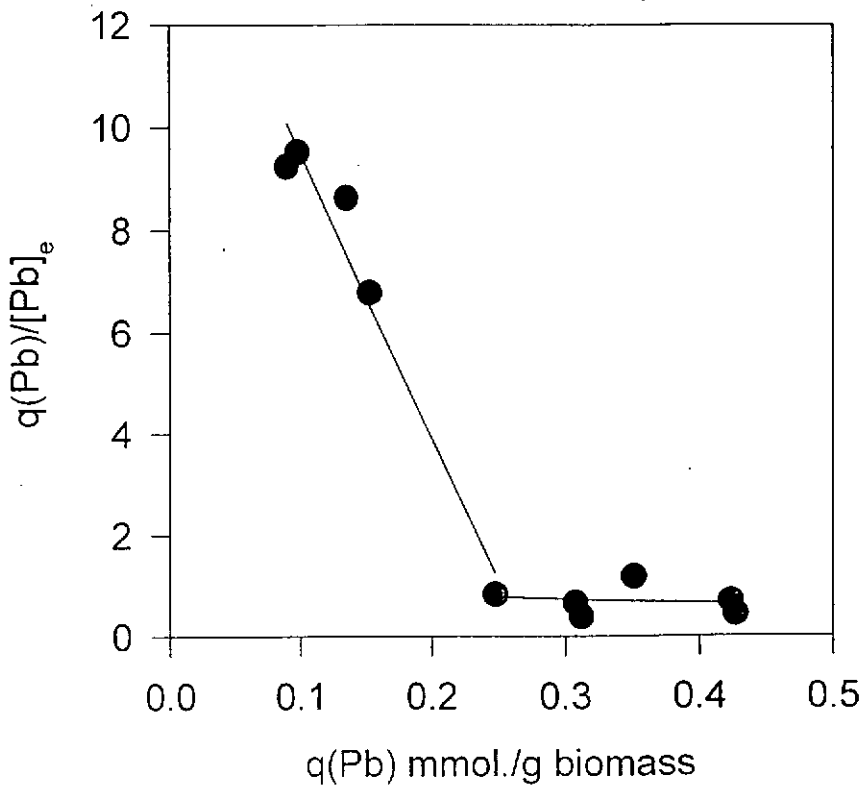

Figure 48.b. Scatchard plot for Pb biosorption at initial [Cu] = 0.1 mM

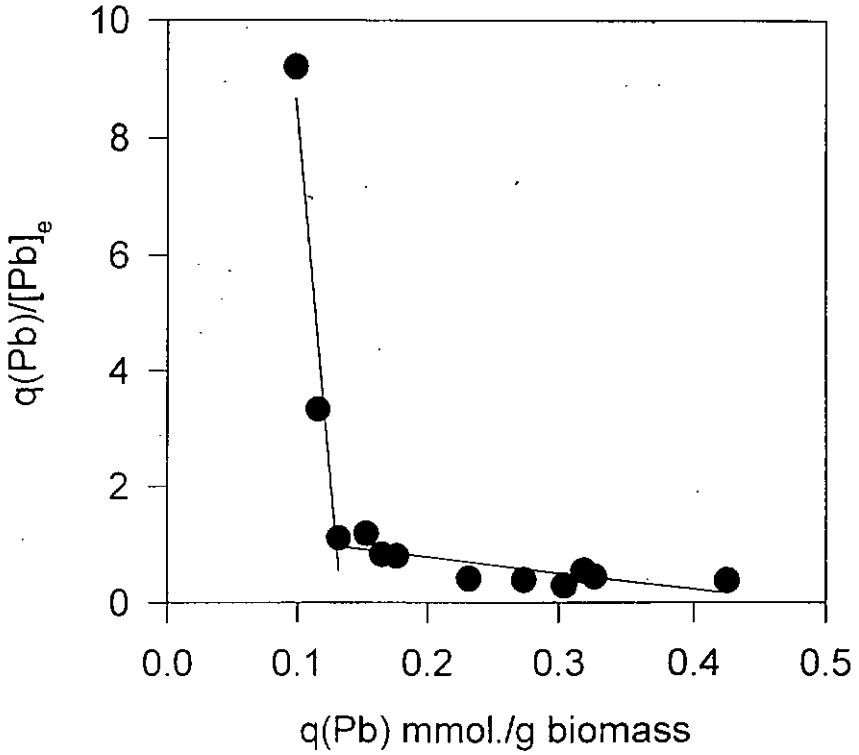

Figure 48.c. Scatchárd plot for Pb biosorption at initial [Cu] = 0.3 mM

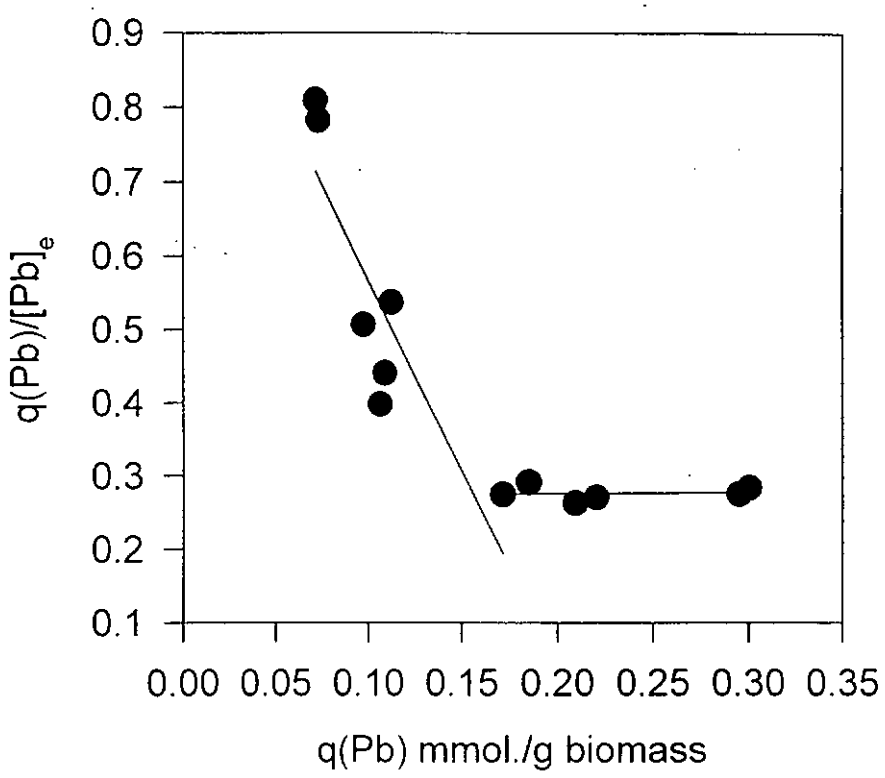

Figure 48.d. Scatchard plot for Pb biosorption at initial [Cu] = 0.55 mM

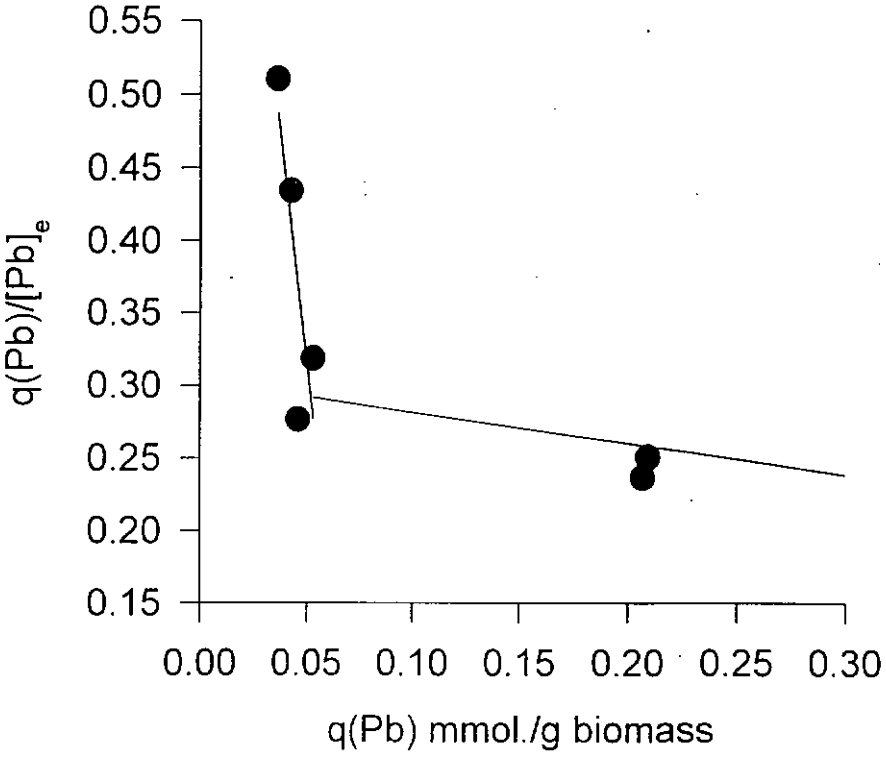

Figure 48.e. Scatchard plot for Pb biosorption at initial [Cu] = 1.72 mM

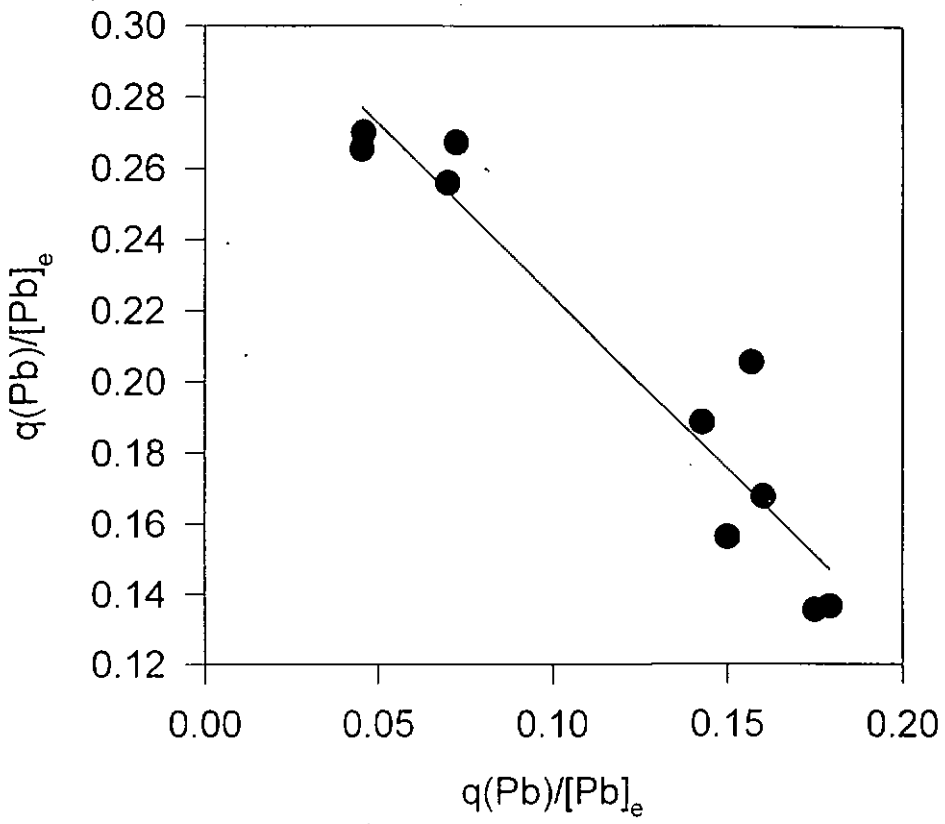

Figure 48.f. Scatchard plot for Pb biosorption at initial [Cu] = 1.9 mM

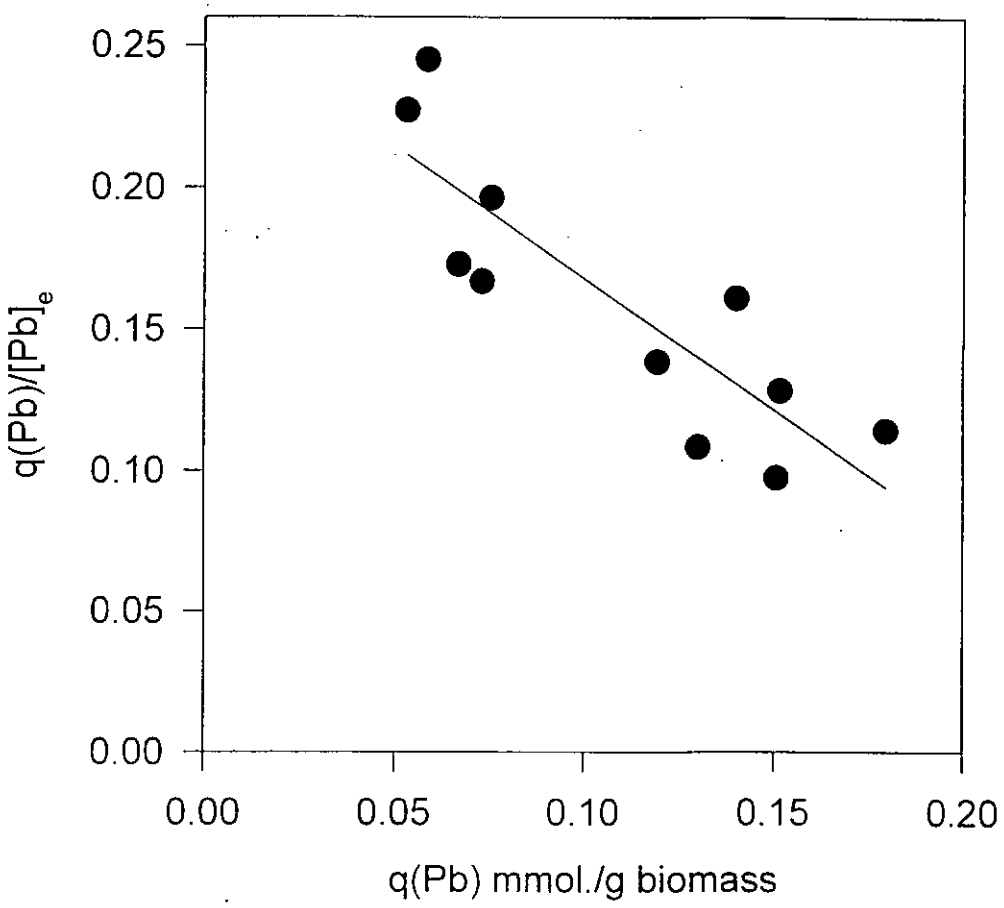

Figure 48.g. Scatchard plot for Pb biosorption at initial [Cu] = 2.5 mM

Table 15. A summary of Scatchard parameters, K and X_0 , for (Pb + Cu) system

Initial [Cu] (mM)	Average **K**	Average $\mathbf{X_0}$	r^2
0.0	76.7989 ± 5.7410	1.0105 ± 0.1041	0.978
	2.2920 ± 2.1755	9.659 ± 1.734	0.270
0.10	55.7557 ± 6.7636	0.2705 ± 0.0482	0.958
	0.8012 ± 2.0221	1.2193 ± 3.4739	0.038
0.30	244.5599 ± 57.3112	0.1344 ± 0.0370	0.948
	2.7722 ± 0.7017	0.4814 ± 0.1937	0.661
0.55	5.1803 ± 1.2417	0.2093 ± 0.0699	0.777
	(-0.0163 ± 0.0897)	(-16.7310 ± 92.7813)	(0.0082)
1.72	12.5072 ± 6.1142	0.0752 ± 0.0427	0.677
	0.2133 ± 0.1260	1.4192 ± 1.0127	0.037
1.90	0.9723 ± 0.1092	0.3305 ± 0.0555	0.908
2.50	0.9290 ± 0.1860	0.2807 ± 0.0845	0.735

single-binding site when copper concentration increased to about 2 mM. When few copper cations were present, there may be two or more binding sites responsible for lead binding. However, at high copper concentrations, copper cations may become a true competitor for one of the lead binding sites.

4.7.2. Three-dimensional biosorption isotherm experimental surfaces

A two-dimensional biosorption isotherm is used to represent the biosorption equilibrium data of a single metal system. The most appropriate way of representing the biosorption equilibrium data of a binary metal system is to construct a three-dimensional (3-D) biosorption isotherm plot whereby the metal uptake is plotted as a function of the final equilibrium concentrations of the two metals (Figures 49-51). The metal uptake term, q, may be the uptake of the two metals or both of them. The software, Sigma Plot, is capable of generating such surfaces by simply connecting the experimental data points using a 3-D mesh through interpolation. Figures 49, 50 and 51 are generated with experimental surfaces describing the lead uptake, copper uptake and total metal uptake respectively as a function of lead and copper equilibrium concentrations in binary metal (Pb+Cu) solution system.

An alternative approach is to fit a smooth surface to the data. However, an appropriate mathematical equation representing the surface and an appropriate computer program, e.g. Matlab, 4.0 (The MathWorks Inc., US), an interactive software package for scientific and engineering numeric computation, are required.

Figures 49 and 50 may be visualized as a series of equilibrium isotherms (q Vs Ce) of one metal at different equilibrium concentration of the second metal. As shown in Figures 49, 50 and 51, generating an isotherm surface by the interpolation approach has its drawbacks. There are lumps and irregularities appeared on the surfaces possibly caused by the experimental errors associated with those data points in space. Figures 49 and 50 show that the biosorption of lead decreased when copper is present and vice versa.

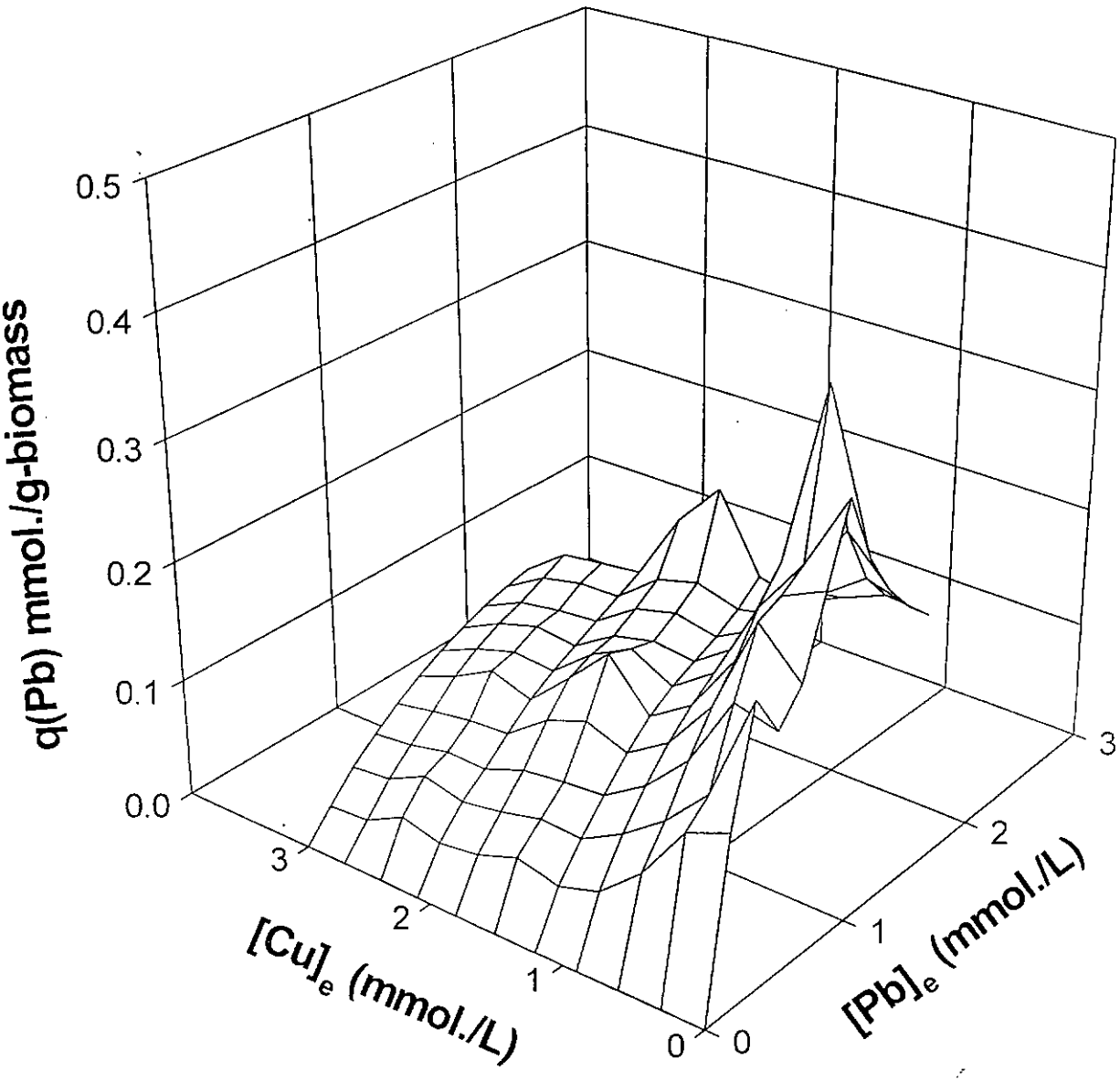

Figure 49. Interpolated isotherm surfaces for Pb^{2+} biosorption from (Pb^{2+} + Cu^{2+}) mixtures by *Mucor rouxii*

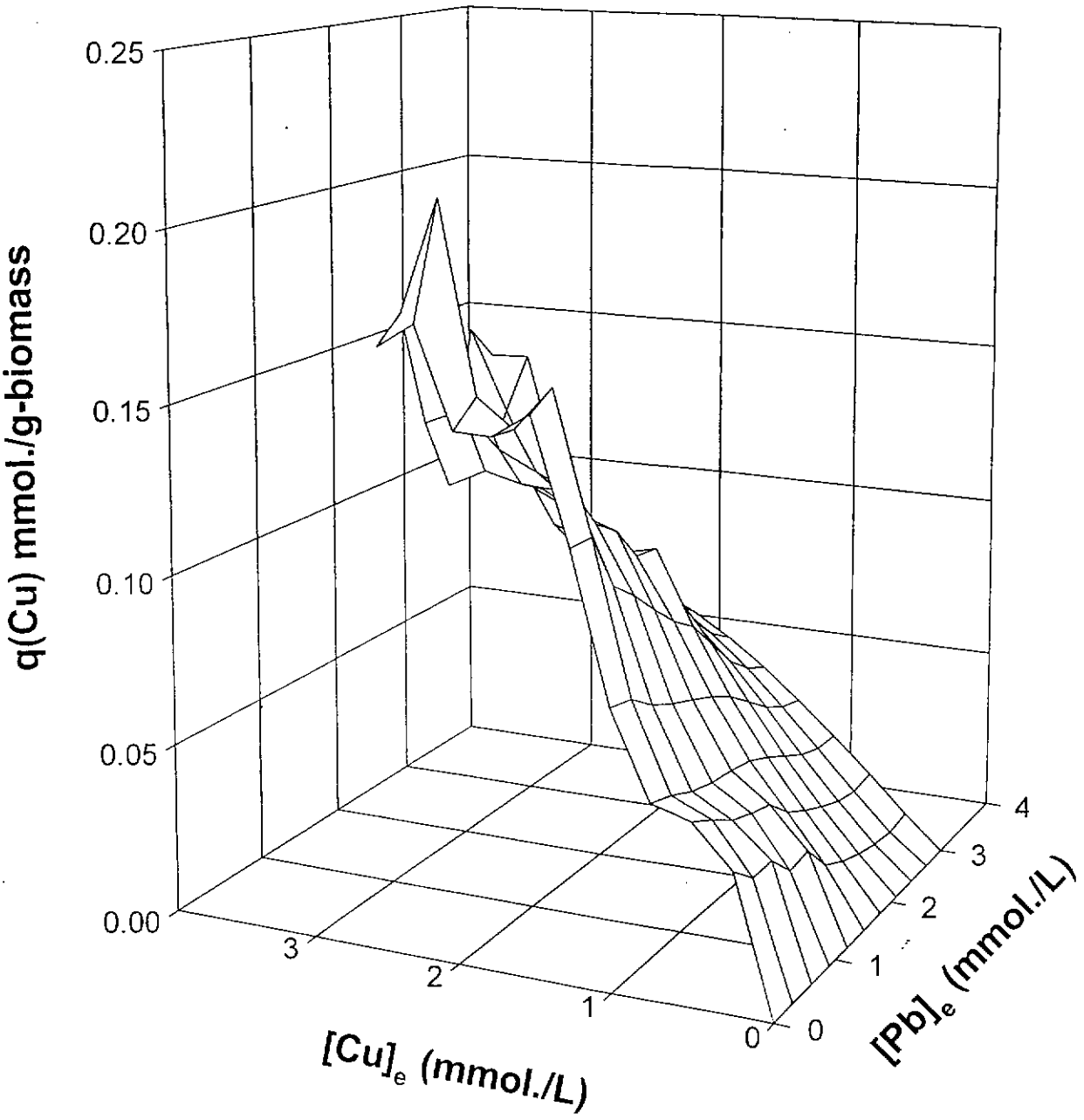

Figure 50. Interpolated isotherm surface for Cu^{2+} biosorption from (Pb^{2+} + Cu^{2+}) mixtures by *Mucor rouxii*

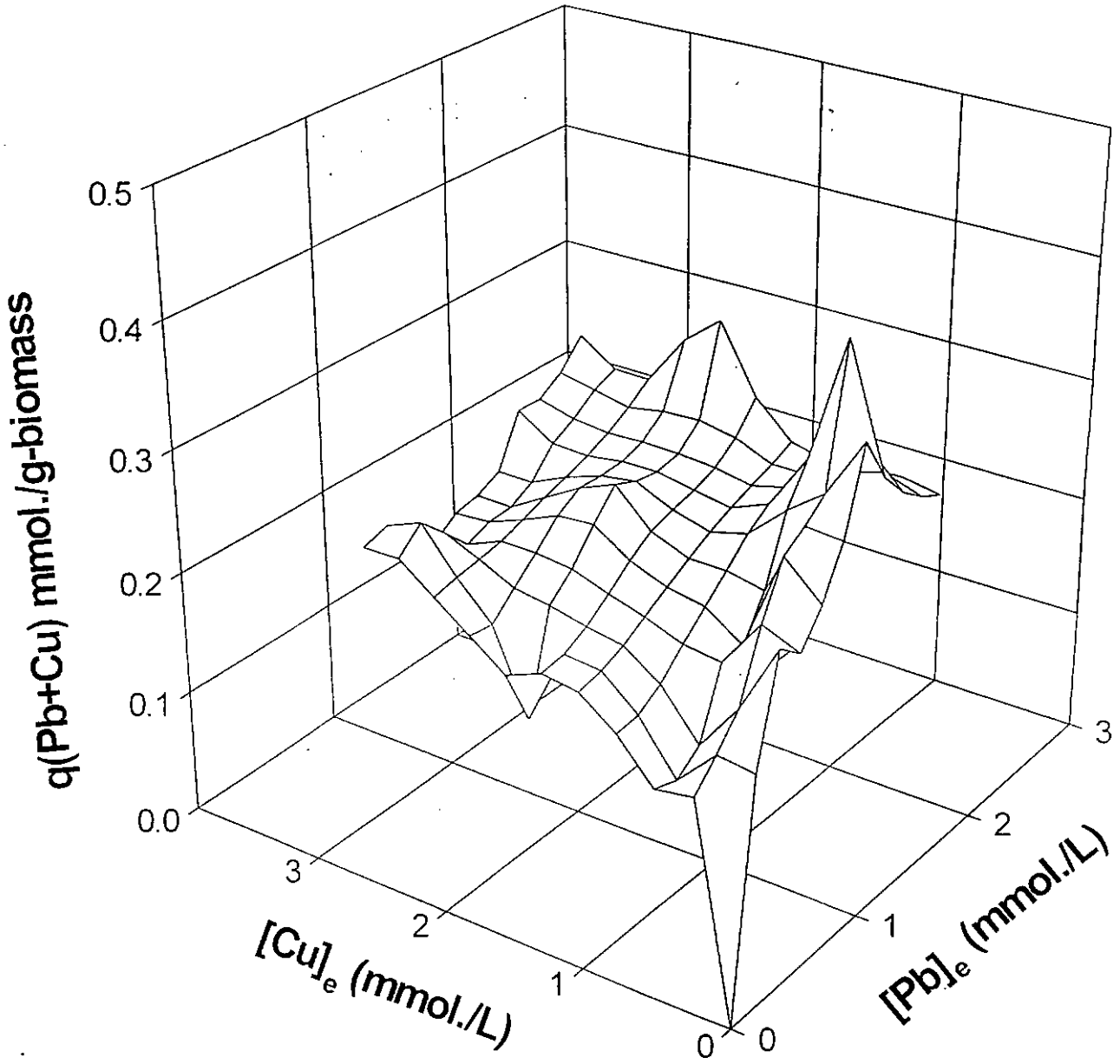

Figure 51. Interpolated isotherm surfaces for (Pb^{2+} + Cu^{2+}) biosorption from (Pb^{2+} + Cu^{2+}) mixtures by *Mucor rouxii*

4.7.3. Isotherm models for binary metal biosorption

In order to simulate the isotherm surfaces, three *Langmuir*-type models were evaluated. The mathematical biosorption model of the binary metal system may be used to estimate biosorption of one metal in the presence of another one. The following are description of each of the three models.

Model 1 - Competitive model

Consider the following equilibria :

$$X + M_1 \Leftrightarrow X - M_1 \qquad K_1 = \frac{k_1}{k_{-1}} = \frac{[X - M_1]}{[X][M_1]_e}$$

$$X + M_2 \Leftrightarrow X - M_2 \qquad K_2 = \frac{k_2}{k_{-2}} = \frac{[X - M_2]}{[X][M_2]_e}$$

where [X] is the number of binding sites on the biomass surface, $[M_1]$ and $[M_2]$ are the concentration of two different metals. This model assumes that the 2 metals are competing for the same type of binding sites, X on the biomass surface.

At equilibrium, there is no net change of $[X - M_1]$ and $[X - M_2]$ with respect to time.

Therefore, $\frac{d[X - M_1]}{dt} = 0$ and $\frac{d[X - M_2]}{dt} = 0$

The total number of mole of the binding sites on the biomass surface can be related to the free binding sites and the occupied sites by the following equation,

$$[X]_0 = [X] + [X - M_1] + [X - M_2]$$

$$[X - M_1] = \frac{K_1[M_1]_e[X_0]}{\{1 + K_1[M_1]_e + K_2[M_2]_e\}} \quad \text{(Eq. 4.1)}$$

We can define the term $[X - M_1]$ as the number of binding sites occupied by M_1 per gram of biomass. $[X_0]$ can be defined as the total number of binding sites per gram

of biomass. If both sides of Eq. 4.1 are multiplied with the unit "mmole M_1 per number of binding sites," we obtain

$$q(M_1) = \frac{q_{max} K_1 [M_1]_e}{1 + K_1 [M_1]_e + K_2 [M_2]_e} \qquad \text{(Eq. 4.2)}$$

Model 2 - Noncompetitive model (or Mixed model)

Consider the following equilibria :

$X + M_1 \Leftrightarrow X - M_1$ $\qquad K_1 = \frac{[X - M_1]}{[X][M_1]_e}$

$X + M_2 \Leftrightarrow X - M_2$ $\qquad K_2 = \frac{[X - M_2]}{[X][M_2]_e}$

$X - M_1 + M_2 \Leftrightarrow X - M_1 - M_2$ $\qquad K_{1,2} = \frac{[X - M_1 - M_2]}{[X - M_1][M_2]_e}$

$X - M_2 + M_1 \Leftrightarrow X - M_1 - M_2$ $\qquad K_{2,1} = \frac{[X - M_1 - M_2]}{[X - M_2][M_2]_e}$

$X + M_1 + M_2 \Leftrightarrow X - M_1 - M_2$ $\qquad K = \frac{[X - M_1 - M_2]}{[X][M_1]_e[M_2]_e}$

$$K = K_1 K_{1,2} = K_2 K_{2,1}$$

At equilibrium, there is no net change of $[X - M_1]$ and $[X - M_2]$ with respect to time.

Therefore, $\frac{d[X - M_1]}{dt} = 0$; $\frac{d[X - M_2]}{dt} = 0$ and $\frac{d[X - M_1 - M_2]}{dt} = 0$

The total number of mole of the binding sites on the biomass surface can be related to the free binding sites and the occupied sites by the following equation,

$[X_0] = [X] + [X - M_1] + [X - M_2] + [X - M_1 - M_2]$

The following equation can be derived,

$$[X - M_1] = \frac{[X_0][M_1]_e\{K_1 + K[M_2]_e\}}{1 + K_1[M_1]_e + K_2[M_2]_e + 2K[M_1]_e[M_2]_e\}} \quad \text{(Eq. 4.3)}$$

Eq. 4.3 can be rearranged as:

$$q(M_1) = \frac{q_{max}[M_1]_e\{K_1 + K[M_2]_e\}}{1 + K_1[M_1]_e + K_2[M_2]_e + 2K[M_1]_e[M_2]_e\}} \quad \text{(Eq. 4.4)}$$

Model 3 - Modified multicomponent model

This equation is based on the multicomponent sorption isotherm model which is originaly proposed by Yon and Turnoch (Liapis and Rippin, 1977) and has the following form :

$$q(M_1) = \frac{q_{max}K_1[M_1]}{1 + K_1[M_1]^{K_3} + K_2[M]^{K_4}} \quad \text{(Eq. 4.5)}$$

This model, derived from multicomponent isotherm model. is similar to the first model. Two more parameters K_3 and K_4 are incorporated as an exponent to the equilibrium concentration of the 2 metals in the denominator of Eq. 4.2.

4.7.4. Evaluation of the isotherm models

The first model is a competitive model with 3 parameters, the second model is a mixed or noncompetitive model with 4 parameters and the third model is a model derived from multicomponent sorption isotherm with 5 parameters. These three models were evaluated by minimizing the sum of square residuals (residual refers to the difference between experimental and the predicted value) using the model. The curve fitting function of Sigma Plot was employed for this purpose. The parameters determined for all the models are listed in Table 16. The *Langmuir* parameters for single-metal uptake by filamentous *Mucor rouxii* are listed in Table 17 for comparison.

Model 1 is a binary *Langmuir*-type equation which has been used in multicomponent equilibrium isotherm (Figures 52.a. - 52.c.). It resembles the equation used for describing competitive inhibition in enzyme kinetic studies. Higher values of K are associated with a higher ratio of the adsorption rate constant to the desorption rate constant. In single metal biosorption systems the binding affinity, K_2 (15.95±0.77 L/mmol.) determined for Cu^{2+} is larger than the binding affinity, K_1 (6.01±0.83 L/mmol.) for Pb^{2+}. However, in binary metal (Pb^{2+} + Cu^{2+}) system, the binding affinity for Pb^{2+}, K_1 is determined to be 9.48 L/mmol and for Cu^{2+} (K_2), 0.487 L/mmol. This indicates that the biomass has a higher affinity for Pb^{2+}.

Model 2 is similar to the first model except there are extra terms in the numerator and the denominator of the *Langmuir*-type equation (Figures 53.a. - 53.c.). It resembles the equation used for describing noncompetitive or mixed inhibition in enzyme kinetic studies. In Pb - Cu system, the lead binding affinity (K_1 = 22.8833 L/mmol.) is larger than the copper binding affinity (K_2 = 1.996 x 10^{-4} L/mmol). Therefore, the formation of X - Pb complex is preferred to that of X - Cu complex. The value of $K_{2,1}$ (0.086 L/mmol.) is much larger than the value of $K_{1,2}$ (7.464 x 10^{-7} L/mmol.). This indicates that the formation of X - Pb - Cu is more favourable from X - Cu than that from X - Pb complex. However, it can be observed that the value of K_1 is much larger than those of $K_{1,2}$ and $K_{2,1}$. This suggests that the formation of X - Pb complex is much more favourable when compared to the X - Pb - Cu complex. Therefore, the binding of 2 metals to the same binding site seems very unfavourable.

Model 3 (Figures 54.a. - c.) is derived from the multicomponent isotherm model. This model resembles the first model except that 2 parameters K_3 and K_4 are incorporated as an exponent to the residual concentrations of the 2 metals in the denominator. The values of K_3 and K_4 deviate much from unity which indicates that Model 3 is not very closed to Model 1.

In order to compare and evaluate the three models statistically, sum of square residue is calculated for each model. The sum of square residue is equal to:

$$\sum (q_{theoretical} - q_{experimental})^2$$

where $q_{theoretical}$ is the theoretical uptake capacity and $q_{experimental}$ is the experimental uptake capacity. The smaller the sum of square residue, the better the model fits the experimental data.

Among the three models studied, the third model shows the smallest sum of square residue which suggests that the third model fits all the experimental data statistically better than the other two models. The incorporation of two additional terms to the first model improves its predictability.

The second model (noncompetitive or mixed model) shows the highest sum of square residue among the three models but is only slightly higher than that obtained in the first model.

Table 16. Table summarized all the constants and sum of square residue calculated for the 3 models

Pb - Cu system	Degree of freedom	Sum of Square Residuals	Mean Square Residuals	Constants
Model 1	63	0.3559	0.0056	K_1 = 9.48 (L/mmol.) K_2 = 0.487 (L/mmol.) q_{max} = 0.3460 (mmol./g-biomass)
Model 2	63	0.3629	0.0058	K_1 = 22.88 (L/mmol.) K_2 = 1.996 x 10^{-4} (L/mmol.) K = 1.699 x 10^{-6} (L/mmol.) $K_{1,2}$ = 7.464 x 10^{-7} (L/mmol.) $K_{2,1}$ = 0.0856 (L/mmol.) q_{max} = 0.3155 (mmol./g-biomass)
Model 3	63	0.2374	0.0038	K_1 = 6.833 x 10^{11} (L/mmol.) K_2 = 6.667 x 10^{8} (L/mmol.) K_3 = 0.683 (dimensionless) K_4 = 2.420 (dimensionless) q_{max} = 0.3537 (mmol./g-biomass)

Table 17. Table summarized the biosorption parameters for single - metal uptake

Metal	*Langmuir* q_{max} (mmol./g-biomass)	*Langmuir* K (L/mmol.)
Pb	3.58 ± 0.19	6.01 ± 0.83
Cu	0.22 ± 0.03	15.95 ± 0.77

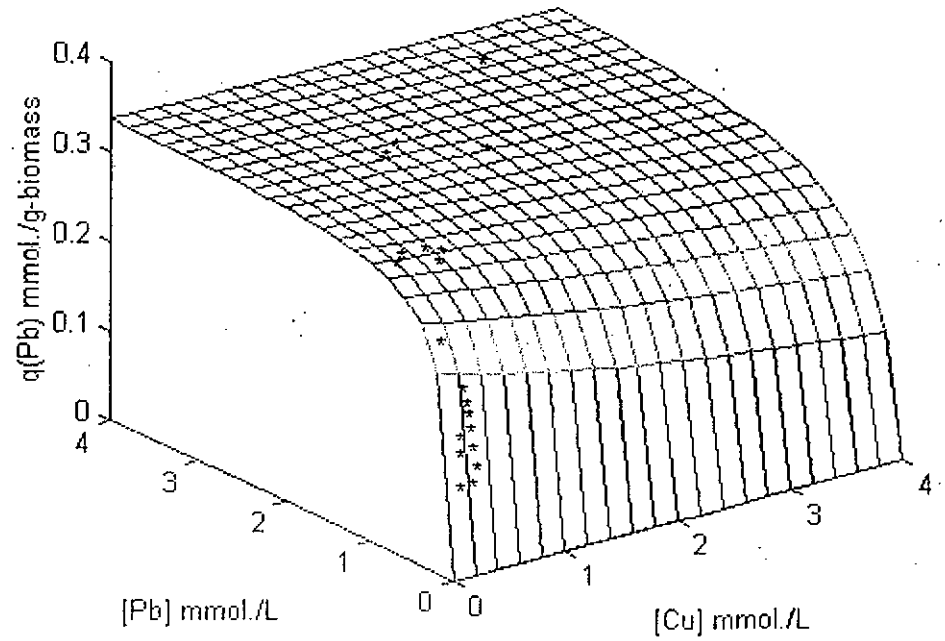

Figure 52.a. Model 1 simulation of Pb^{2+} biosorption isotherm surface for (Pb^{2+} + Cu^{2+}) binary system

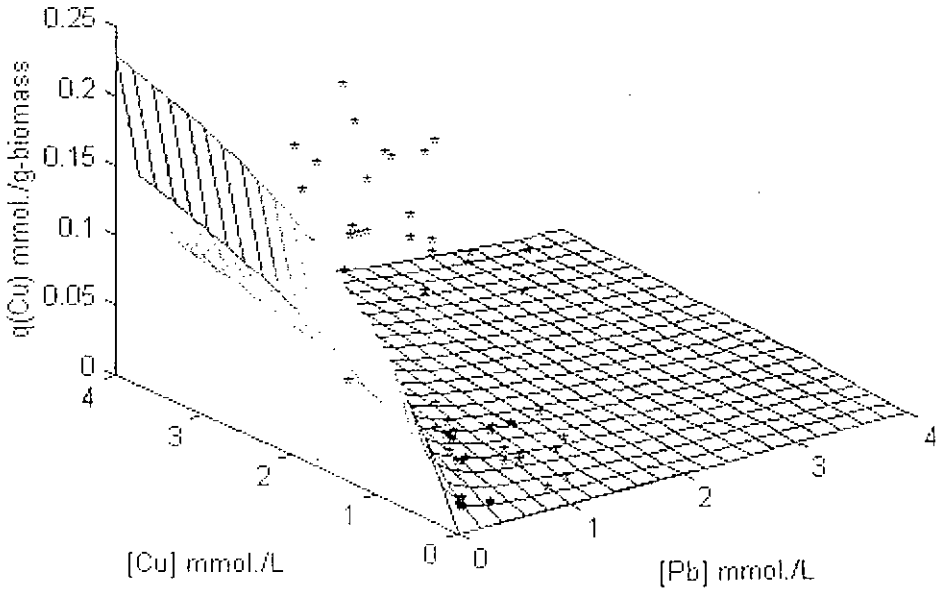

Figure 52.b. Model 1 simulation of Cu^{2+} biosorption isotherm surface for (Pb^{2+} + Cu^{2+}) binary system

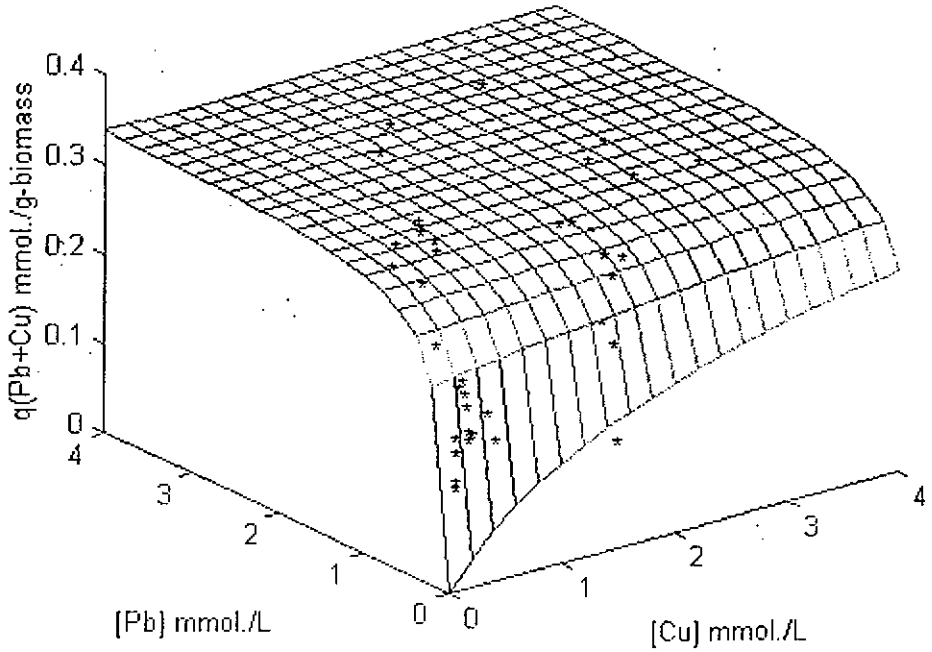

Figure 52.c. Model 1 simulation of (Pb^{2+} + Cu^{2+}) biosorption isotherm surface for (Pb^{2+} + Cu^{2+}) binary system

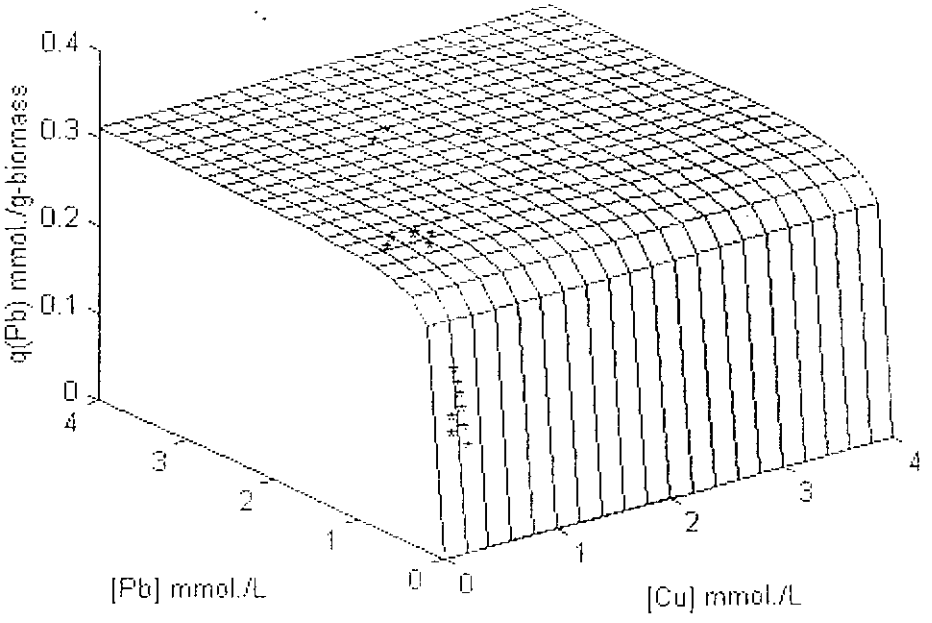

Figure 53.a. Model 2 simulation of Pb^{2+} biosorption isotherm surface for (Pb^{2+} + Cu^{2+}) binary system

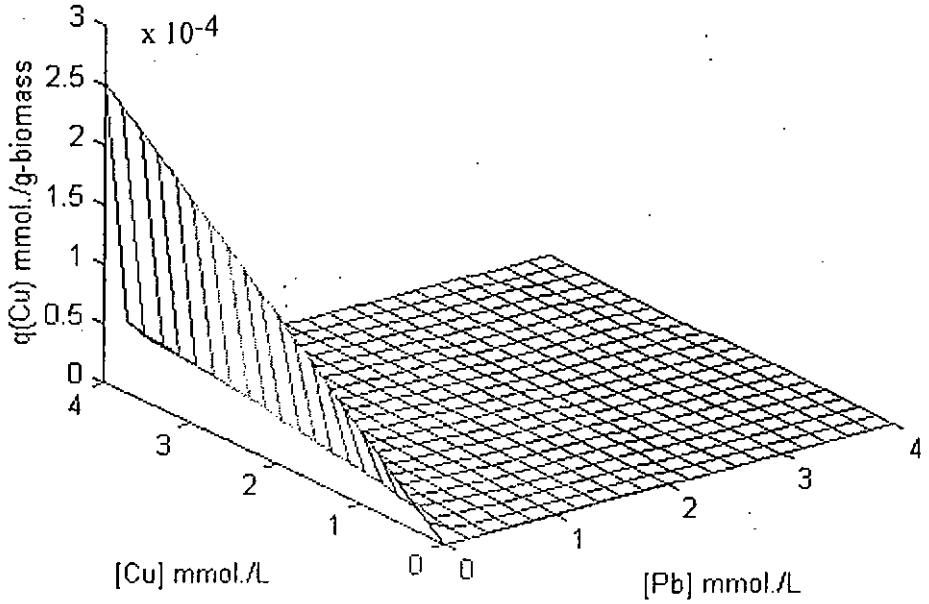

Figure 53.b. Model 2 simulation of Cu^{2+} biosorption isotherm surface for (Pb^{2+} + Cu^{2+}) binary system

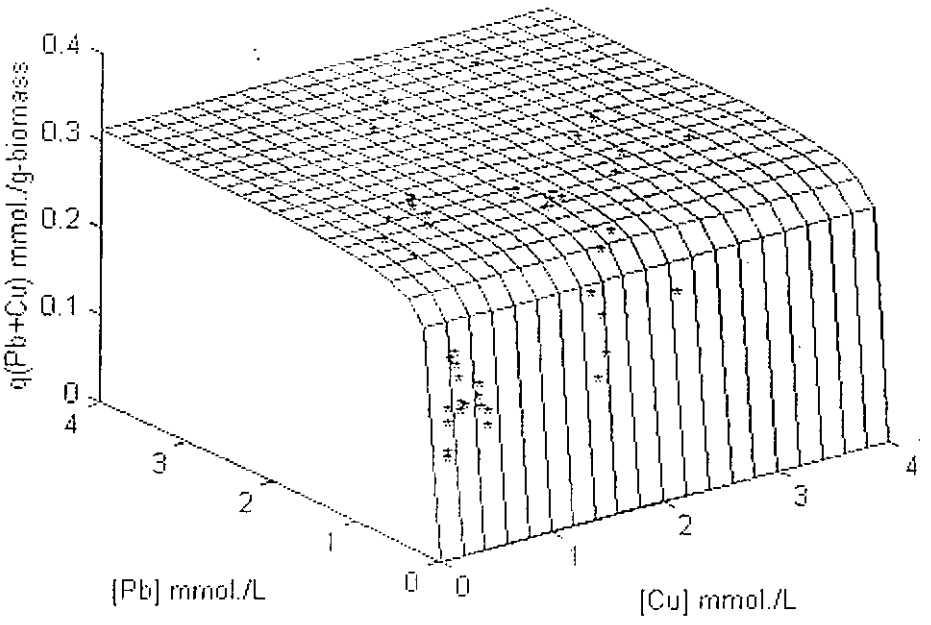

Figure 53.c. Model 2 simulation of (Pb^{2+} + Cu^{2+}) biosorption isotherm surface for (Pb^{2+} + Cu^{2+}) binary system

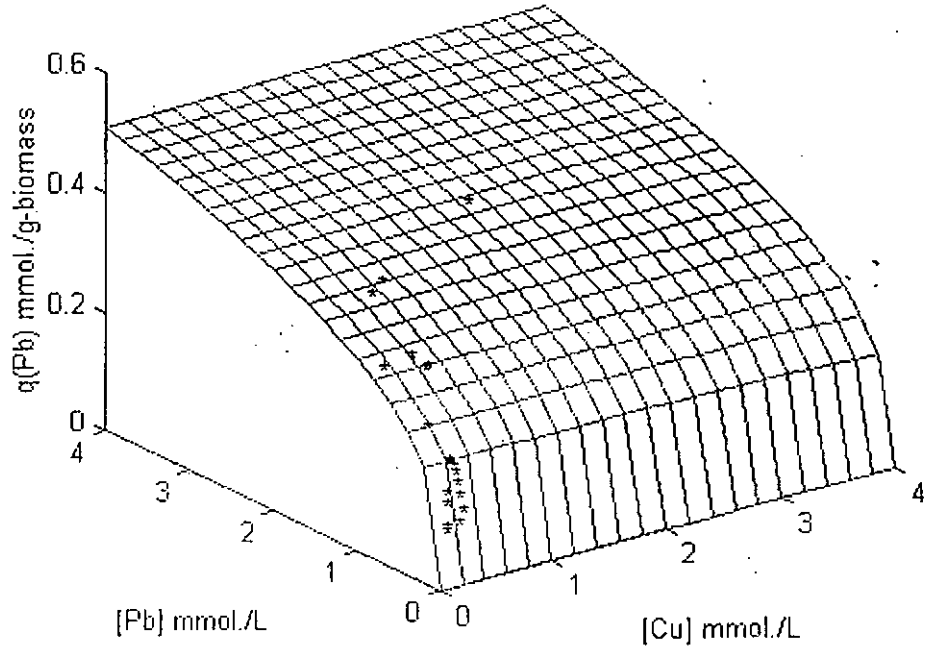

Figure 54.a. Model 3 simulation of Pb^{2+} biosorption isotherm surface for (Pb^{2+} + Cu^{2+}) binary system

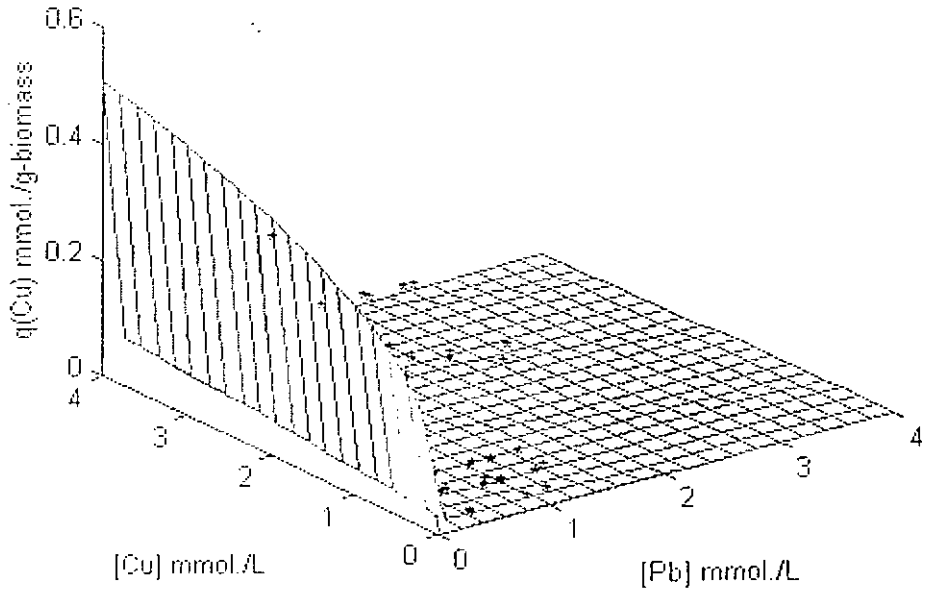

Figure 54.b. Model 3 simulation of Cu^{2+} biosorption isotherm surface for (Pb^{2+} + Cu^{2+}) binary system

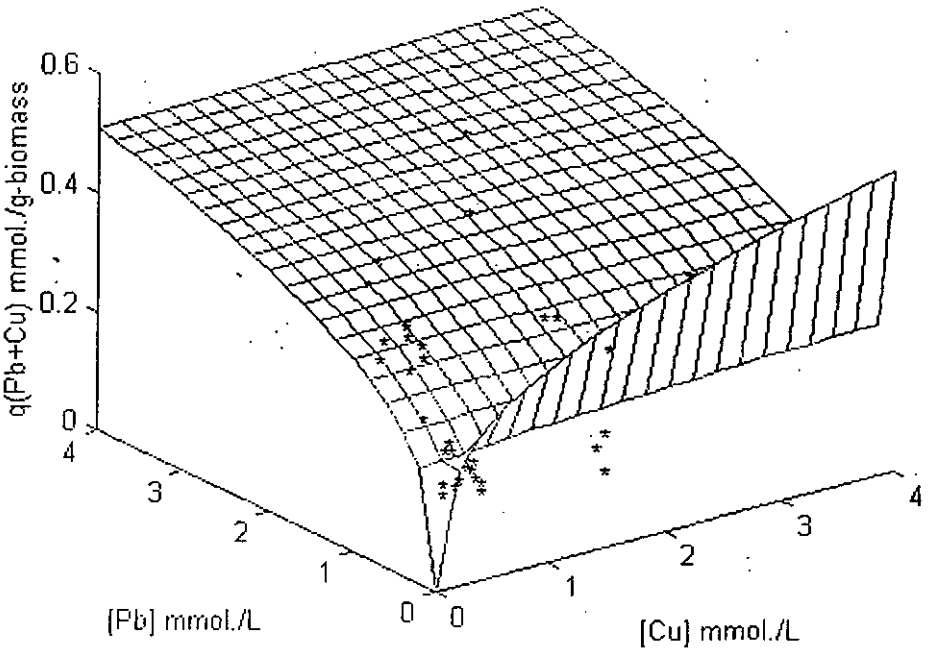

Figure 54.c. Model 3 simulation of (Pb^{2+} + Cu^{2+}) biosorption isotherm surface for (Pb^{2+} + Cu^{2-}) binary system

Chapter 5. Conclusions

The main focus of the proposed work is to develop an inexpensive and effective biosorption process for removing and recovering heavy metals from local industrial effluents using fungal-based biosorbents. The first phase of this research focused on screening a series of selected fungal strains for effective lead and copper removal at different metal and biomass concentrations. The second phase focused on studying the effects of different factors on metal biosorption of a fungal species selected based on the results of first phase. The following list summarizes the most significant results obtained during the course of this research:

1. *Aspergillus niger* and *Mucor rouxii* exhibited exceptionally high lead biosorption capacities, up to 50 % of the fungal biomass dry weight. This is higher than that reported for activated carbon and most other microorganisms. These two fungal strains may be applied to develop potentially cost-effective biosorbents for removing lead from effluents.

2. *Aspergillus nidulans, Mucor rouxii, Cladosporium cladosporioides and Phycomyces blakeleeanus* (+) exhibited moderate copper biosorption capacities (about 1-1.5% of the fungal biomass dry weight employed).

3. The pH was found to have significant effect on lead and copper biosorption. The *Mucor rouxii* biomass exhibited the highest removal efficiency at pH 6.0 for lead and at pH 5.0 for copper. For effective metal removal, the biosorption process must be operated at the optimum pH for metal biosorption.

4. NaOH treatment significantly increased copper biosorption capacity of *Mucor rouxii* by 100%. Consequently, the fungal biomass can be treated with NaOH to improve its copper biosorption.

5. *Mucor rouxii* was also found to adsorb a variety of different metal cations. At pH 5.0, the biosorption capacities for metals decreased in the following order: Pb^{2+} > Zn^{2+} > Mg^{2+} > Cr^{3+} > Cd^{2+} > Ag^{+} > Ni^{2+} > Cu^{2+} > Co^{2+} > Na^{+}. *Mucor rouxii* exhibited good zinc biosorption capacities (about 6-6.5% of the fungal biomass dry weight employed). Therefore the biomass may be used for removing zinc from industrial effluents.

6. Scatchard plots of lead biosorption at different initial copper concentrations strongly indicated the presence of multiple lead binding sites on the cell surfaces. Three-dimensional plotting of the biosorption isotherm surfaces can be used to evaluate graphically the performance of the binary metal biosorption system. The biosorption of lead decreased when copper was present. Three biosorption mathematical models (i.e. competitive, noncompetitive and modified multi-component models) were evaluated for their predictive ability of metal biosorption for the binary metal system. The modified multi-component model had the smallest sum of square residue which indicated a greater match with the experimental data. The mathematical model of the binary metal biosorption system can be used for quantitative estimation of one-metal biosorption in the presence of another metal. For evaluating and predicting the performance of multimetal biosorption systems, such a multiparameter mathematical approach may be taken.

Chapter 6. Suggestions for Further Studies

The following aspects of this project could be further studied:

1. To assess the full potential of biosorption, experimental data and theoretical analysis are needed on the performance of biosorbent systems with multimetal aqueous mixture. Most studies on biosorption have been limited to single metal. These studies of toxic metal biosorption should be extended to binary and tertiary metal systems. The effects of anions present in the effluents on metal biosorption should also be investigated.

2. Examination of the proposed solid-liquid biosorption system should also include dynamic continuous-flow biosorption studies in both fixed-bed column and stirred-tank reactors. Evaluation of equilibrium biosorption performance needs to be supplemented by process-oriented studies of its kinetics and eventually by dynamic continuous-flow tests. The rate of the metal biosorption, together with the hydrodynamic and mass transfer parameters determines the size of the reactor. Reaction engineering concepts and fundamentals can be applied for the experimental approach, leading to expression of the values of key process parameters used for performance prediction, process design, and scale-up purposes. At present, very little work has been done to develop quantitative methodologies and guidance for the scale-up and prediction of the biosorption column performance (Trujillo *et al.*, 1991). The multicomponent metal biosorption model for both continuous fixed-bed and stirred tank reactors should be developed. The kinetic and equilibrium parameters can be combined with the hydrodynamics and diffusion parameters as input into the models to simulate the performance of the continuous reactors. The model prediction should also be compared to the experimental biosorption performance of the reactor in detoxifying real process waste solution containing multimetals.

3. Methods for regenerating the fungal biomass for metal biosorption should be developed. In multiple cycles of biosorption and desorption, the decrease in metal uptake due to physical deterioration has to be evaluated.

References

1. Adamson, A. W., *Physical Chemistry of Surfaces*, 2nd edition, Interscience Publishers Inc., New York, 1967.

2. Andres, Y., MacCordick, H. J. and Hubert, J. C., 1993, Adsorption of several actinide (Th, U) and lanthanide (La, Eu, Yb) ions by *Mycobacterium smegmatis*, *Applied Microbiology and Biotechnology*, 39: 413-417.

3. Aronson, J. M. and Machlis, L., 1959, The chemical composition of the hyphal walls of the fungal allomyces, *American Journal of Botany*, 46 : 292-300.

4. Atkins, P. W., Processes at solid surfaces, In *Physical Chemistry*, fourth edition, Oxford University Press: 873-905.

5. Balakrishnan, M., Modak, J. M., Natarajan, K. A., and Naik, J. S. G., 1984, Biological uptake of precious and base metals from gold-process cyanide effluents, *Minerals and Metallurgical Processing*, 11: 197-202.

6. Bartnicki-Garcia, S. and Walter J. Nickerson, 1962a, Isolation, composition, and structure of cell walls of filamentous and yeast-like forms of *Mucor rouxii*, *Biochimica and Biophysica ACTA*: 102 - 119.

7. Bartnicki-Garcia, S. and Walter J. Nickerson, 1962b, Nutrition, Growth, and Morphogenesis of *Mucor rouxii*, *Journal of Bacteriology*, 84: 841 - 858.

8. Beveridge, T. J., and Murray, R. G. E., 1980, Sites of metal deposition in the cell walls of *Bacillus subtilis*, *Journal of Bacteriology*, 141: 876-887.

9. Blackwell, K. J., Singleton, I. And Tobin, J. M., 1995, Metal cation uptake by yeast: a review, Applied Microbiology and Biotechnology, 43: 579-584.

10. Blumenthal, H. J. and Roseman, S., 1957, Quantitative estimation of chitin in fungi, *Journal of Bacteriology*, 74: 222-224.

11. Brady, D., Stoll, A. and Ducan, J. R., 1994, Biosorption of heavy metal cations by non-viable yeast biomass, *Environmental Technology*, 15: 429-438.

12. Brady, D., and Ducan, J. R., 1994, Bioaccumulation of metal cations by *Saccharomyces cerevisiae*, *Applied and Microbiology Biotechnology*, 41: 429-438.

13. Byerley, J. J., Schareri, J. M., and Rioux, S., 1989, Reactions of precious metal complexes with biopolymer, *Journal American Chemical Society*, 60: 309-319.

14. Chong, K. H. and Volesky, B., 1995, Description of two-metal biosorption equilibria by *Langmuir*-type models, *Biotechnology and Bioengineering*, 47: Pp. 451-460.

15. Crist, R. H., Martin, J. R., Carr, D., Watson, J. R. and Clarke, H. J., 1994, Interaction of metals and protons with algae. 4. Ion exchange vs adsorption models and a reassessment of Scatchard plots; ion-exchange rates and equilibrium compared with calcium alginate, *Environmental Science and Technology*, 28: 1859-1866.

16. Cotton, F. A., and G. Wilkinson, 1996. *Advanced Inorganic Chemistry: A Comprehensive Text.* John Wiley & Sons, Inc., New York.

17. de Carvalho, R. P., Chong, K. H. and Volesky, B., 1994, Effects of leached alginate on metal biosorption, *Biotechnology Letter*, 46: 875-880.

18. de Rome, L. and Gadd, G. M., 1987, Copper adsorption by *Rhizopus arrhizus*, *Cladosporium resinae* and *Penicillium italicum*, *Applied Microbiology and Biotechnology*, 26: 84-90.

19. Doyle, R. J., Matthews, T. H., and Streips, U. N., 1980. Chemical basis for the selectivity of ions by the *Bacillus subtilis* cell wall, *Journal of Bacteriology*, 143: 471-480.

20. Farkas, V., 1979, Biosynthesis of cell walls of fungi, *Microbiological Review*, 43, 2: 117-144.

21. Fourest, E., and Roux, J. C., 1992, Heavy metal biosorption by fungal mycelial byproducts: mechanisms and influence of pH, *Applied Microbiology and Biotechnology*, 37: 399-403.

22. Freundlich, H., 1926, *Colloid and Capillary Chemistry*, Methuen. London.

23. Fris, N. and Keith, P. M., 1986, Biosorption of uranium and lead by *Streptomyces loognwoodensis*, *Biotechnology and Bioengineering*, 28: 21-28.

24. Galun, M., Keller, P. and Malki, D., 1983a, Removal of uranium (VI) from solution by fungal biomass and fungal wall related biopolymers, *Science*. 219: 285-286.

25. Galun, M., Keller, P., Feldstein, H. Galun, E., Siegel, S. and Siegel, B., 1983b, Recovery of uranim (VI) from solution using precultured *Penicillium* biomass, *Water, Air, and Soil Pollution*, 20: 221-232.

26. Galun, M., Galun, E., Siegel, B. Z., Keller, P., Lehr, H. and Siegel, S. M., 1987, Removal of metal ions from aqueous solutions by *Penicillium* biomass: Kinetic and uptake parameters, *Water Air and Soil Pollution*, 33: 359-371.

27. Gadd, G. M. and Mowll, H., 1985, Copper uptake by yeast like cell, hyphae and chlamydospores of *Aureobasidium pullulans*, *Experimental Mycology*, 9: 230-240.

28. Gadd, G. M., 1986, The uptake of heavy metals by fungi and yeasts: the chemistry and physiology of the process and applications for biotechnology, In *Immobilization of Ions by Biosorption*, ed. By H. H. Eccles and S., Hunt. Ellis Horwood, Chichester: 135-147.

29. Gadd, G. M., White, C. and Rome, L. de, 1988, Heavy metal and radionuclide uptake by fungi and yeasts, In *Biohydrometallurgy*, ed. by Norris, P. R. and Kew, D. P. Kelly, Antomy Rowe Ltd., Chippenham, Wittshire, Great Britain: 421-435.

30. Gadd, G. M., 1990, Fungi and yeasts for metal accumulation, In *Microbial Mineral Recovery*, ed. By Ehrlich, H. L. and Brierley, C. L., McGraw-Hill, New York: 249-274.

31. Garnham, G. W., Codd, G. A., and Gadd, G. M., 1993, Accumulation of zirconium by microalgae and cyanobacteria, *Applied Microbiology and Biotechnology*, 39: 666-672.

32. Giles, C. H., Macewan, T. H., Nakhwa, S. N. & Smith, D., 1960, Studies in adsorption. Part XI. A system of classification of solution adsorption isotherms, and its use in diagnosis of adsorption mechanisms and in measurement of a specific surface areas of solids, *Journal of the Chemical Society*, 3973-3993.

33. Guibal, E., Roulph, C. and Le Cloiree, P., 1992, Uranium biosorption by a filamentous fungus *Mucor miehei*: pH effect on the mechanisms and performances of uptake, *Water Research*, 26: 1139-1145.

34. Guven, K. C. and Akyuz, K., 1995, Selectivity of heavy metal binding by algal polysaccharides, *Toxicological and Environmental Chemistry*, 47: 65-70.

35. Harris, P. O., and Ramelow, G. J., 1990, Binding of metal ions by particulate biomass derived from *Chlorella Vulgaris* and *Scenedesmus Quadricauda*. *Environmental Science and Technology*, 24, 2: 220-228.

36. Hirs, C. H. W. & Timashelt, S. N., 1978, The meaning of Scatchard and Hill plots, in *Methods in Enzymology*, 48: 270-299.

37. Holan, Z. R., Volesky, B. and Prasetyo, I., 1993, Biosorption of cadmium by biomass of marine algae, *Biotechnology and Bioengineering*, 41: 819 - 825.

38. Huang, C, P., Dean Westman, Kenneth Quirk and Huang, J. P., 1988a, The removal of cadmium (II) from dilute aqueous solutions by fungal adsorbent, *Water Science and Technology*, 20: 369-376.

39. Huang, C. P., Westman, D., Quirk, K. and Huang, J. P., 1988b, Removal of cadmium (II) from dilute solutions by fungal biomass, *Particulate Science and Technology*, 6: 405-419.

40. Huang, C. P., and Morehart, A. L., 1990, The removal of Cu (II) from diluted aqueous solutions by *Saccharomyces cerevisiae*, *Water Research*, 24: 433-439.

41. Huang, C., Huang, C. P. & Morehart, A. L., 1991, Proton competition in Cu (II) adsorption by fungal mycelia, *Water research*, 25: 1365-1375.

42. Jang, L. K., Nguyen, D. and Geesey, G. G., 1995, Selectivity of alginate gel for Cu Vs Co, *Water research*, 29, 1: 307-313.

43. Jorge L., Gardea-Torresdey, Irene Cano-Augilera, Robert Webb, Kirk J. Tiemann, and Felix Gutierrez-Corona, 1996, Copper adsorption by inactivated cells of *Mucor rouxii* : Effect of esterification of carboxyl groups, *Journal of Hazardous Materials*, 48: 171-180.

44. Kapoor, A. and Viraraghavan, T, 1995, Fungal biosorption - an alternative treatment option for heavy metal bearing wastewaters: A review, *Bioresource Technology*, 53: 195-206.

45. Kiff, R. J. and Little, D. R., 1986, Biosorption of heavy metals by immobilized fungal biomass. In *Immobilization of Ions by Biosorption*, ed. by H. H. Eccles and S. Hunt. Ellis Horwood, Chichester, 71-80.

46. Kuyucak, N and Volesky, B., 1988, Recovery of cobalt by a new biosorbent, *Canadian Institute of Mining and Metallurgy Bulletin*, 8: 95-99.

47. Kuyucak, N. and Volesky, B., 1988, Biosorbent for recovery of metals from industrial solutions. *Biotechnology Letters*, 10, 2: 137-142.

48. Kuyucak, N. and Volesky, B., 1989a, Accumulation of cobalt by marine alga, *Biotechnology and Bioengineering*, 33: 809-814.

49. Kuyucak. N. and Volesky, B., 1989b, Accumulation of gold by algal biosorbent. *Biorecovery*, 1: 189-204.

50. Leusch, A., Holan, Z. R. and Volesky, B., 1995, Biosorption of heavy metals (Cd, Cu. Ni, Pb, Zn) by chemically-reinforced biomass of marine algae, *Journal of Chemical Technology and Biotechnology*, 62: 279-288.

51. Lewis, D. and Kiff, R.J., 1988, The removal of heavy metals from aqueous effluents by immobilized fungal biomass, *Environmental Technology Letters*, 9: 991-998.

52. Lu, Y. and Wilkins, E., 1996, Heavy metal removal by caustic-treated yeast immobilized in alginate, *Journal of Hazardous Materials*, 49: 165-179.

53. Luef E., Prey, T., and Kubicek, C. P., 1991, Biosorption of zinc by fungal mycelial wastes, *Applied Microbiology and Biotechnology*, 34: 688-692.

54. Margaret E., Treen-Sears, Volesky, B. and Ronald J. Neufeld, 1984, Ion exchange/complexation of uranyl ion by *Rhizopus* biosorbent, *Biotechnology and Bioengineering*, 26: 1323-1329.

55. Modak, J. M. and Natarajan, K. A., 1995 Biosorption of metals using nonliving biomass - A review, *Minerals and Metallurgical processing*, 12: 189 - 196.

56. Muraleedharan, L. Iyengar and C. Venkobachar, 1991, Biosorption: an attractive alternative for metal removal and recovery, *Current Science*, 61: 379-385.

57. Muraleedharan, T. R. and Venkobachar, C., 1990, Mechanism of biosorption of copper (II) by *Ganoderma lucidium*, *Biotechnology and Bioengineering*, 35: 320-325.

58. Muraleedharan, T. R., Lyengar, L. & Venkkobachar, C., 1994, Further insight into the mechanism of biosorption of heavy metals by *Ganoderma lucidum*, *Environmental Technology*, 15: 1015-1027.

59. Muraleedharan, T. R., Lyengar, L. and Venkobachar, C., 1991. Biosorption: An attractive alternative for metal removal and recovery, *Current Science*, 610: 379-385.

60. Muzzarelli R. A. and Sipos, L., 1971, Chitosan for collection from seawater of naturally occurring zinc, cadmium, lead and copper, *Talanta*, 18: 853-858.

61. Muzzarelli, R. A. A., 1972, *Chitin*, Pergamon Press, London.

62. Muzzarelli, R. A. A., 1980, Chelating, film - forming, and coagulating ability of the chitosan-glucan complex from *Aspergillus niger* industrial wastes, *Biotechnology and Bioengineering*, 22: 885-896.

63. Muzzarelli, R. A. A., Tanfani, F., Scarpini, G. and Tucci, E.. 1980, Removal and Recovery of cupric and mercuric ions from solutions using chitosan-glucan from *Aspergillus niger*, *Journal of Applied Biochemistry*, 2: 54-59.

64. Muzzarelli, R. A. A., Tanfani, F. and Emanuelli, M., 1981, The chelating ability of chitinous materials from streptomyces, *Mucor rouxii*, *Phycomyces blakeleeanus*, and *Choanephora cucurbitarum*, *Journal of Applied Biochemistry*, 3: 322-327.

65. Muzzarelli, R. A., and Tanfani, F., 1982, The chelating ability of chitinous materials from *Aspergillus niger*, *Streptomyces*, *Mucor rouxii*, *Phycomyces blakleeanus* and *Choanephora curcurbitum*, In *Chitin and Chitosan*, ed. by S. Mirano and S. Tokura, Japanese Society of Chitin and Chitosan: 183-186.

66. Niu Hui, Xue Shu Xu, and Jian Hua Wang, 1993, Romoval of lead from aqueous solutions by *Penicillium* biomass, *Biotechnology and Bioengineering*, 42: 785-787.

67. Olson, G. J. and Brinckman, F. E., 1987, Review and discussion - algal sorbents for selective metal ion recovery, In *Metal speciation, Separation, and Recovery*, ed. by J. W., Patterson and R., Passino, Lewis Publishers, Inc., Chelsea, 333-338.

68. Panchanadikar, V. V. and Das, R. P., 1994, Biosorption process for removing lead (II) ions from aqueous effluents using *Pseudomonas* sp., *Internal Journal of Environmental Studies*, 46: 243-250.

69. Perkin-Elmer technical manual, 0303-0152, *Analytical Methods for Atomic Absorption Spectroscopy*, Perkin-Elmer Corporation, 1994.

70. Pons, M. P., and Fuste, C. M.. 1993, Uranium uptake by immobilized cells of *Pseudomonas* strain EPS 5028, *Applied Microbiology and Biotechnology*, 39: 661-665.

71. Ross, I. S. and Townsley, C. C.. 1986, The uptake of heavy metals by filamentous fungi, in *Immobilization of Ions by Biosorption*, ed. by H. Eccles and S. Hunt. Ellis Horwood, Chichester: 49-57.

72. Rose, R. K., 1996. Competitive binding of calcium, magnesium and zinc to *Streptococcus sanguis* and purified *S. sanguis* cell walls, *Caries Rearch*, 30: 71-75.

73. Sag, Y. and Kutsal. T., 1995, Biosorption of heavy metals by *Zoogloea ramigera*: use of adsorption isotherms and a comparison of biosorption characteristics, *The Chemical Engineering Journal*, 60: 181-188.

74. Sag, Y. and Kutsal. T., 1996, Fully competitive biosorption of chromium (VI) and iron (III) ions from binary metal mixtures by *R. arrhizus*: use of the competitive *Langmuir* model. *Process Biochemistry*, 31: 573-585.

75. Siegel, S. M., Margalith, G., Paulina K., Siegel, B. Z. and Esra G., 1986a. Fungal biosorption: A comparative study of metal uptake by *Penicillium* and *Cladosporium*,

Proceedings of the International Symposium on Metals Speciation, Separation and Recovery, Illinois, July 27-August 1, 1986, ed. by W. Patterson: 339-361.

76. Siegel, S., Keller, P., Galun, M., Lehr, H., Siegel, B. and Galun, E., 1986b, Biosorption of lead and chromium by *Penicillium* preparations, *Water Air and Soil Pollution*, 27: 69-75.

77. Stegel, S. M., Galun, M., Siegel, B. Z., 1990, Filamentous fungi as metal biosorbents: A review, *Water, Air and soil Pollution*, 53: 335-344.

78. Snoeyink, V. L., 1990, Adsorption of organic compounds, In *Water Quality and Treatment*, A Handbook of Community Water Supplies, American Water Works Association, ed. by F. W. Pontius, fourth edition, McGraw-Hill, Inc., New York: 781-785.

79. Spiro, T. G., 1980, *Copper Protein*. John Wiley and Sons, New York.

80. Strandberg, G. W., Shumate II, S. E. and Parrott, J. R., Microbial cells as biosorbents for heavy metals: Accumulations of uranium by *Saccharomyces cerevisiae* and *Pseudomonas aeruginosa*, *Applied and Environmental Microbiology*, 41: 237-245.

81. Tobin, J. M., Cooper D. G. and Neufeld, R. J., 1984, Uptake of metal ions by *Rhizopus arrhizus* biomass, *Applied and Environmental Microbiology*, 47: 821-824.

82. Tobin, J. M., Cooper D. G. and Neufeld, R. J., 1987, Influence of anions on metal adsorption by *Rhizopus arrhizus* biomass, *Biotechnology and Bioengineering*, 30: 882-886.

83. Tobin, J. M., L'homme, B. and Roux, J. C., 1993, Immobilization protocols and effects on cadmium uptake by *Rhizopus arrhizus* biosorbents, *Biotechnology Techniques*, 7: 739-744.

84. Townsley, C. C. and Rose, I. S., 1985, Copper uptake by *Penicillium spinulosum*, *Microbios*, 44: 125-132.

85. Townsley, C. C. and Rose, I. S., 1986a, Copper uptake in *Aspergillus niger* during batch growth and in non-growing mycelial suspensions, *Experimental Mycology*, 10: 281-288.

86. Townsley, C. C., Ross. I. S. and Atkins, A. S., 1986b, Biorecovery of metallic residues from various industrial effluents using filamentous fungi. In *Fundamental and Applied Biohydrometallurgy*, ed. Lawrence, R. W., Branion, R. M. R. and Enner, H. G., Elsevier, Amsterdam: 279-289.

87. Townsley, C. C., Ross, I. S. and Atkins, A. S., 1986c, Copper removal from a simulated leach effluent using the filamentous fungus *Trichoderma viride*, In Immobilization of Ions by Biosorption, ed. by H. Eccles and S. Hunt. Ellis Horwood, Chichester: 159-170

88. Treen-Sears, M. E., Martin, S. M. and Volesky, B., 1984a, Propagation of *Rhizopus javanicus* biosorbent, *Applied and Environemntal Microbiology*, 48: 137 - 141.

89. Treen-Sears, M. E., Volesky, B. and Neufeld, R. J., 1984b, Ion exchange/complexation of uranyl ion by *Rhizopus* biosorbent, *Biotechnology and Bioengineering*, 26: 1323-1329.

90. Tsezos, M. and Volesky, B., 1981, Biosorption of uranium and thorium, *Biotechnology and Bioengineering*, 23: 583-604.

91. Teszos, M. and Volesky, B., 1982a, The mechanism of uranium biosorption by *Rhizopus arrhizus*, *Biotechnology and Bioengineering*, 24: 385-401.

92. Teszos, M. and Volesky, B., 1982b, The mechanism of thorium biosorption by *Rhizopus arrhizus*, *Biotechnology and Bioengineering*, 24: 955-969.

93. Tsezos, M. and Keller, D. M., 1983a, Adsorption of radium-226 by biological origin adsorbents, *Biotechnology and Bioengineering*, 24: 201-215.

94. Tsezos, M., 1983b, The role of chitin in uranium adsorption by *Rhizopus arrhizus*, *Biotechnology and Bioengineering*, 25: 2025-2040.

95. Tsezos, M. & Deutschmann, A. A., 1990, An investigation of engineering parameters for the use of immobilized biomass particles in biosorption, *Journal of Chemical Techmology and Biotechnology*, 48: 29-39.

96. Volesky, B., 1987, Biosorbents for metal recovery, *Trends in Biotechnology*, 5: 96-101.

97. Volesky, B., 1990, The cell wall and metal binding, In *Biosorption of Heavy Metals*, CRC Press, Boca Raton: 83-92.

98. Volesky, B., 1994, Advances in biosorption of metals: Selection of biomass types, *FEMS Microbiology Reviews* 14: 291-302.

99. Volesky, B. and Holan Z. R., 1995, Biosorption of heavy metals, *Biotechnology Progress*, 11: 235-250.

100. Wales, D. S. and Sagar, B. F., 1990, Recovery of metal ions by microfungal filters, *Journal of Chemical Technology and Biotechnology*, 49: 345-355.

101.Weber, JR. and Walter, J., 1972, Adsorption, In *Physiochemical Processes for Water Quality Control*, ed. by Weber, JR., John Wiley and Sons, Inc., New York, 199-259.

102.White, C. and Gadd, M., 1990, Biosorption of radionuclides by fungal biomass, *Journal of Chemical Technology and Biotechnology*, 49: 331-343.

103.Yakubu, N. A. and Dudeney, A. W. L., 1986, Biosorption of uranium with *Aspergillus niger*, In *Immobilization of Ions by Biosorption*, ed. by H. H. Eccles and S. Hunt. Ellis Horwood, Chichester, 183-200.

104.Zhou, J. L., and Kiff, R. J., 1991, The uptake of copper from aqueous solution by immobilized fungal biomass, *Journal of Chemical Technology and Biotechnology*, 52: 317-340.

Appendix

Model 1 - Competitive model
For [Pb]

```
x=0; y=0;
for i=1:21
   for j=1:21
      z(i,j)=(0.3460/0.1055*x)/(1+x/0.1055+y/2.0548);
      y=y+0.2;
   end
   y=0;
   x=x+0.2;
end
t=0:0.2:4;
[x,y]=meshgrid(t,t);
mesh(x,y,z);
title('Model 1');xlabel('[Cu] mmol./L');ylabel('[Pb] mmol./L');zlabel('q(Pb) mmol./g-biomass');
load Pbdata1a.dat;
PbM1=Pbdata1a;
          for i=1:63;
             text(PbM1(i,1),PbM1(i,2),PbM1(i,3),'*');
          end
whitebg
```

Model 1 - Competitive model
For [Cu]

```
x=0; y=0;
for i=1:21
   for j=1:21
      z(i,j)=(0.3460/2.0548*x)/(1+x/2.0548+y/0.1055);
      y=y+0.2;
   end
   y=0;
   x=x+0.2;
end
t=0:0.2:4;
[x,y]=meshgrid(t,t);
mesh(x,y,z);
title('Model 1');xlabel('[Pb] mmol./L');ylabel('[Cu] mmol./L');zlabel('q(Cu) mmol./g-biomass');
load cudata1a.dat;
CuM1=cudata1a;
          for i=1:63;
             text(CuM1(i,1),CuM1(i,2),CuM1(i,3),'*');
          end
whitebg
colormap(jet)
```

Model 1 - Competitive model
For [Pb+Cu]

```
x=0; y=0;
for i=1:21
   for j=1:21
      z(i,j)=(0.3460/0.1055*x)/(1+x/0.1055+y/2.0548)+(0.3460/2.0548*y)/(1+y/2.0548+x/0.1055);
      y=y+0.2;
```

```
   end
   y=0;
   x=x+0.2;
end
t=0:0.2:4;
[x,y]=meshgrid(t,t);
mesh(x,y,z);
title('Model 1');xlabel('[Cu] mmol./L');ylabel('[Pb] mmol./L');zlabel('q(Pb+Cu) mmol./g-biomass');
load tmdata1a.dat;
PbCuM1=tmdata1a;
          for i=1:63
             text(PbCuM1(i,1),PbCuM1(i,2),PbCuM1(i,3),'*');
          end
```

Model 2 - Mixed or noncompetitive model
For [Pb]

```
x=0; y=0;
for i=1:21
   for j=1:21

z(i,j)=0.3155*x*(1+0.0437/58551.565*y)/(0.0437+x+0.0437/5011.2795*y+2*0.0437/58551.5650*x*y
);
      y=y+0.2;
   end
   y=0;
   x=x+0.2;
end
t=0:0.2:4;
[x,y]=meshgrid(t,t);
mesh(x,y,z);
title('Model 2');xlabel('[Cu] mmol./L');ylabel('[Pb] mmol./L');zlabel('q(Pb) mmol./g-biomass');
load Pbdata1a.dat;
PbM1=Pbdata1a;
          for i=1:63;
             text(PbM1(i,1),PbM1(i,2),PbM1(i,3),'*');
          end
```

Model 2 - Mixed or noncompetitive model
For [Cu]

```
x=0; y=0;
for i=1:21
   for j=1:21

z(i,j)=0.3155*x*(1+5011.2795/58551.5650*y)/(5011.2795+x+5011.2795/0.0437*y+2*5011.2795/585
51.5650*x*y);
      y=y+0.2;
   end
   y=0;
   x=x+0.2;
end
t=0:0.2:4;
[x,y]=meshgrid(t,t);
mesh(x,y,z);
title('Model 2');xlabel('[Pb] mmol./L');ylabel('[Cu] mmol./L');zlabel('q(Cu) mmol./g-biomass');
load cudata1a.dat;
CuM1=cudata1a;
```

```
        for i=1:63;
          text(CuM1(i,1),CuM1(i,2),CuM1(i,3),'*');
        end
```

Model 2 - Mixed or noncompetitive model
For |Pb+Cu|

```
x=0; y=0;
for i=1:21
  for j=1:21

z(i,j)=0.3155*x*(1+0.0437/58551.5650*y)/(0.0437+x+0.0437/5011.2795*y+2*0.0437/58551.5650*x*
y)+0.3155*y*(1+5011.2795/58551.5650*x)/(5011.2795+y+5011.2795/0.0437*x+2*5011.2795/58551.
5650*x*y);
    y=y+0.2;
  end
  y=0;
  x=x+0.2;
end
t=0:0.2:4;
[x,y]=meshgrid(t,t);
mesh(x,y,z);
title('Model 2');xlabel('[Cu] mmol./L');ylabel('[Pb] mmol./L');zlabel('q(Pb+Cu) mmol./g-biomass');
load tmdata1a.dat;
PbCuM1=tmdata1a;
        for i=1:63
          text(PbCuM1(i,1),PbCuM1(i,2),PbCuM1(i,3),'*');
        end
```

Model 3 - Modqified Multicomponent model
For |Pb|

```
x=0; y=0;
for i=1:21
  for j=1:21
    z(i,j)=(0.3275/1.4634e-12*x)/(1+1/1.4634e-12*(x)^0.6828+1/1.5540e-9*(y)^2.4193);
    y=y+0.2;
  end
  y=0;
  x=x+0.2;
end
t=0:0.2:4;
[x,y]=meshgrid(t,t);
mesh(x,y,z);
title('Model 3');xlabel('[Cu] mmol./L');ylabel('[Pb] mmol./L');zlabel('q(Pb) mmol./g-biomass');
load Pbdata1a.dat;
PbM1=Pbdata1a;
        for i=1:63;
          text(PbM1(i,1),PbM1(i,2),PbM1(i,3),'*');
        end
```

Model 3 - Modified Multicomponent model
For |Cu|

```
x=0; y=0;
for i=1:21
  for j=1:21
    z(i,j)=(0.3275/1.5540e-9*x)/(1+1/1.5540e-9*(x)^0.6828+1/1.4634e-12*(y)^2.4193);
```

```
    y=y+0.2;
  end
  y=0;
  x=x+0.2;
end
t=0:0.2:4;
[x,y]=meshgrid(t,t);
mesh(x,y,z);
title('Model 3');xlabel('[Pb] mmol./L');ylabel('[Cu] mmol./L');zlabel('q(Cu) mmol./g-biomass');
load cudata1a.dat;
CuM1=cudata1a;
        for i=1:63;
          text(CuM1(i,1),CuM1(i,2),CuM1(i,3),'*');
        end
```

Model 3 - Modified Multicomponent model
For |Pb+Cu|

```
x=0; y=0;
for i=1:21
  for j=1:21
    z(i,j)=(0.3275/1.4634e-12*x)/(1+1/1.4634e-12*(x)^0.6828+1/1.5540e-
9*(y)^2.4193)+(0.3275/1.5540e-9*y)/(1+1/1.5540e-9*(y)^0.6828+1/1.4634e-12*(x)^2.4193);
    y=y+0.2;
  end
  y=0;
  x=x+0.2;
end
t=0:0.2:4;
[x,y]=meshgrid(t,t);
mesh(x,y,z);
title('Model 3');xlabel('[Cu] mmol./L');ylabel('[Pb] mmol./L');zlabel('q(Pb+Cu) mmol./g-biomass');
load tmdata1a.dat;
PbCuM1=tmdata1a;
        for i=1:63
          text(PbCuM1(i,1),PbCuM1(i,2),PbCuM1(i,3),'*');
        end
```